Supporting Information

Multi-Responsive Polymers with Degradable Side-Chain Functionality for Controlled Hydrolysis and Tunable Thermal Transition

Maryam Behzad Khoshgoee,[1,‡] Mithun Kumar Debnath,[1,‡] Griffin Pardo,[1] Yichun Yuan,[1] Muhammad Zeeshan,[2,3] Erqian Mao,[1] Thomas Gray,[1] Burcu Gurkan,[2] Matthew J. Bertin,[1] and Metin Karayilan[1,*]

‡ These authors contributed equally to this work.
[1] Department of Chemistry, Case Western Reserve University, 10900 Euclid Ave., Cleveland, Ohio 44106, USA
[2] Department of Chemical and Biomolecular Engineering, Case Western Reserve University, Cleveland, Ohio 44106, United States
[3] Department of Mechanical Engineering, Massachusetts Institute of Technology, Cambridge, MA 02139, USA
* Corresponding author: metin.karayilan@case.edu

Table of Contents

Materials and Equipment

Materials

Oligo(ethylene glycol) methyl ether methacrylate (OEGMA, M_n = 500 g/mol, Sigma-Aldrich) and di(ethylene glycol) methyl ether methacrylate (DEGMA 95%, Sigma-Aldrich) were passed through a neutral alumina column to remove inhibitors. DL-Panolactone (TCl, 95%), methacryloyl chloride (MCCl, Sigma-Aldrich, 97%), triethylamine (TEA, TCl, 99%), 4-(hydroxymethyl)-1,3-dioxolan-2-one (Thermoscientific, 90%), 4-cyano-4-(((dodecylthio)carbonothioyl)thio) pentanoic acid (CTA, Boron Molecular, 99%), dichloromethane (DCM, Fisher Scientific, ACS grade), toluene (Fisher Scientific, ACS grade) were used as recevied. *N*-Isopropylacrylamide (NIPAM, TCl, ≥98%) and 2,2′-azobis(2-methylpropionitrile) (AIBN, Sigma-Aldrich, 98%) was recrystallized from methanol. For hydrolysis test, DI water, PBS pH 7.4 ($CaCl_2$, $MgCl_2$, Gibco co.), sodium hydroxide (NaOH, Thermoscientific, pellets), and hydrochloric acid (HCl, Thermoscientific) were used as received. For injectability tests, Agarose (Thermoscientific) and neon green (Rit Dye) were used as received. For dye release test, Rhodamine B (≥95% Sigma-Aldrich) and dialysis tubing (Spectrum Labs Spectra/Por 3, regenerated cellulose, 3.5 kDa MWCO, Fisher Scientific) were used.

Equipment

^{1}H NMR measurements were carried out on a 500 MHz Bruker Ascend NMR Spectrometer. The molecular weight and dispersity were measured by Agilent Technologies gel permeation chromatography (GPC) with HPLC DMF containing 0.05 M LiBr as the mobile phase at a flow rate of 0.6 mL/min. PMMA was used as the standard. The GPC was equipped with a Wyatt Optilab T-rEX refractive index detector and a Wyatt Dawn Heleos II 18-angle light scattering detector. The refractive index and light scattering detectors operated at an optical wavelength of 658 nm. The dn/dc measurements of the synthesized polymers are included in the Supporting Information. To prepare GPC samples, 6 mg of polymer was dissolved in 2 mL of DMF and passed through a 0.2 μm filter before analysis. Thermogravimetric analysis (TGA) was conducted using a TGA 500-TA Instrument with a platinum pan, heating from 30 °C to 600 °C at a 10 °C/min heating rate. Differential scanning calorimetry (DSC) was performed using a DSC 250 Discovery-TA Instruments at a heating rate of 10 °C/min over a temperature range of -50 °C to 120 °C in a single cycle. Each sample was sealed in a hermetic pan, and heat flow was measured relative to an empty reference pan. The cloud point temperature (T_{cp}) for all the terpolymers was obtained with 1 wt% solution in distilled water and PBS. An Agilent Cary 3500 Peltier UV–Vis spectrometer was used to record absorption and transmittance spectra for the hydrolysis study. The temperature was increased at a ramp rate of 0.5 °C/min at 600 nm, and the cloud point temperature was determined at 90% transmission. The cloud point temperature (T_{cp}) of the copolymer was assessed using a 1 wt% solution in distilled water. A Pike Technologies Peltier-Controlled cuvette holder provided precise temperature regulation, while a 632.8 nm laser diode was utilized for voltage measurement. Custom inhouse software, developed with an Arduino microcontroller, monitored the laser intensity as a function of time and temperature. The temperature was gradually increased at a ramp rate of 0.5 °C/min, and the cloud point temperature was recorded at 90% of the voltage. Rheological studies were conducted using an HR 20 rheometer (TA Instruments) with a gap of 200 μm. Rheology samples were prepared at varying concentrations in DI water. All hydrolysis samples were lyophilized using a Labconco Refrigerated CentriVap Centrifugal Vacuum Concentrator (Labconco Corporation), coupled with an Edwards nXDS6i Dry Scroll Pump (Edwards Vacuum). Lyophilization was carried out at a sample chamber temperature of 25 °C for 565 minutes, with the chiller set to –105 °C. For

the hydrolysis study under accelerated conditions (1 M HCl and 1 M NaOH), samples were neutralized before lyophilization. Lyophilization samples were prepared by dissolving 100 mg of each polymer in 5 mL of deionized water (2 wt%). The solutions were placed on a hot plate at 50 °C for 7 days. For injectability analysis, a Fisherbrand 18L Low Temp Incubator (Thermoscientific) was to incubate the gel at 37 °C. Fourier Transform Infrared Spectrometer (FTIR) analysis was conducted using JASCO FT/IR-4600. A Fisherbrand accumet basic AB315 benchtop laboratory pH/mV meter was used to conduct pH measurements

1. Synthesis of Hydrolyzable Monomers

1.1. Synthesis of Lactone Monomer (LMA)

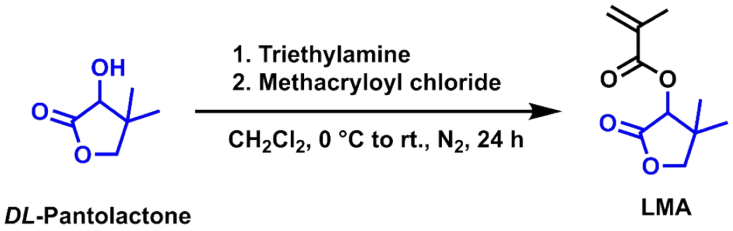

Scheme S1. Synthesis of methacrylate monomer having lactone unit (LMA)

Methacrylate monomer with a hydrolyzable lactone moiety (LMA) was synthesized using the following procedure: A 50 mL Schlenk flask equipped with a magnetic stir bar was charged with *DL*-pantolactone (511 mg, 3.93 mmol), triethylamine (2.15 mL, 15.36 mmol), and dichloromethane (26.0 mL). The mixture was cooled to 0 °C and stirred under N_2 for 10 minutes, and then methacryloyl chloride (0.75 mL, 7.68 mmol) was added dropwise, and the reaction mixture was allowed to warm up to room temperature. The reaction mixture was subsequently stirred for 24 hours under N_2 at room temperature. After the completion of the reaction, the solvents were removed under reduced pressure using a rotary evaporator. Ethyl acetate (EtOAc) was added to the obtained crude mixture, which resulted in the precipitation of salt. The precipitate was then filtered out, and the filtrate was dried under reduced pressure to obtain the crude mixture. The crude was purified by silica gel column chromatography using a mixture of hexanes and ethyl acetate as the eluent (10:1 by volume). Finally, the solvents were removed under reduced pressure to yield the LMA (711 mg, 3.59 mmol, 91% yield) as a colorless oil. The monomer LMA was characterized by ^{1}H, ^{13}C, and DEPT-135 spectroscopy techniques.

1.2. Synthesis of Cyclic Carbonate Monomer (C^2MA)

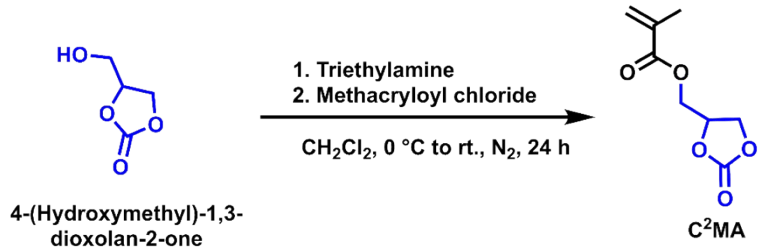

Scheme S2. Synthesis of methacrylate monomer having cyclic carbonate unit (C^2MA)

Vinyl monomer, such as methacrylate monomer that has hydrolyzable carbonate (C^2MA), was synthesized using the following procedure: A 150 mL Schlenk flask equipped with a magnetic stir bar was charged with 90% pure 4-(Hydroxymethyl)-1,3-dioxolan-2-one (1.45 mL, 15.47 mmol), triethylamine (8.6 mL, 61.70

mmol), and dichloromethane (120.0 mL). The mixture was cooled to 0 °C and stirred under N_2 for 10 mins, and then methacryloyl chloride (3.0 mL, 30.71 mmol) was added, and the reaction mixture was allowed to warm at room temperature. The reaction mixture was subsequently stirred for 24 h under N_2. After the completion of the reaction, the solvents were removed by applying reduced pressure. EtOAc was added to the obtained crude product, which resulted in the precipitation of salt. The solid salt residue was then separated by filtration, and the filtrate was evaporated under reduced pressure to obtain the crude product. This crude product was purified by silica gel column chromatography using a 1:1 (*v/v*) mixture of hexane and EtOAc as the eluent. Finally, the solvents were removed under reduced pressure to provide C^2MA (2.65 g, 14.23 mmol, 92% yield) as a colorless oil. The monomer C^2MA was characterized by ^{1}H NMR, ^{13}C NMR, and DEPT-135 NMR spectroscopy.

2. Synthesis of Homopolymers of LMA and C^2MA via RAFT Polymerization

2.1. Synthesis of homopolymer PLMA via RAFT polymerization

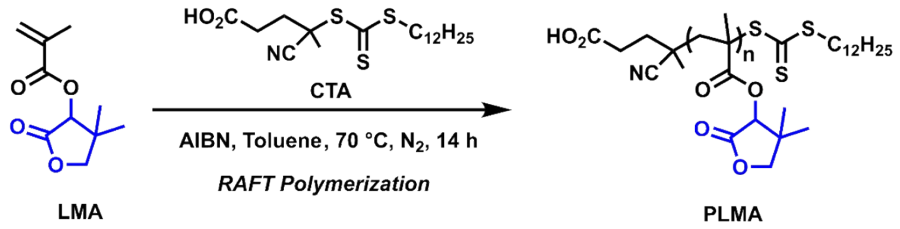

Scheme S3. Synthesis of PLMA via RAFT polymerization

The monomer **LMA** (0.50 g, 2.52 mmol), CTA (10 mg, 0.0252 mmol), AIBN (4 mg, 0.0243 mmol), and toluene (1.0 mL) were added to a 10 mL Schlenk flask equipped with a magnetic stir bar. The reaction mixture was degassed by purging with N_2. Polymerization was carried out in a constant temperature oil bath at 70 °C for 14 h, after which the reaction was quenched by allowing the reaction mixture to cool in the open air under the fume hood. The resulting polymer was purified by precipitating in methanol. The obtained polymer **PLMA** was obtained and dried under vacuum to give a pale-yellow solid (398 mg, 80% isolated).

2.2. Synthesis of homopolymer PC²MA via RAFT polymerization

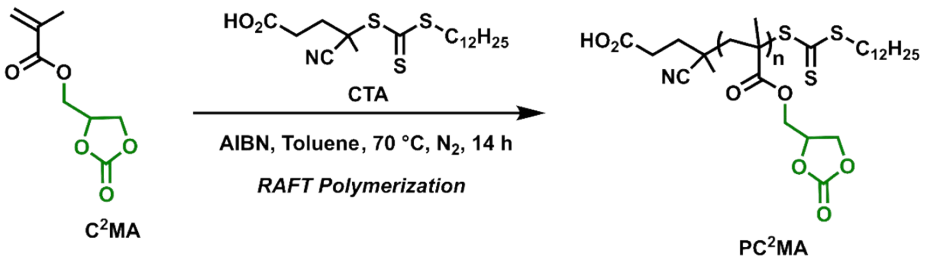

Scheme S4. Synthesis of PC^2MA homopolymer via RAFT polymerization

The monomer C^2MA (0.50 g, 2.69 mmol), CTA (11 mg, 0.0269 mmol), AIBN (4 mg, 0.0243 mmol), and toluene (1.0 mL) were added to a 10 mL Schlenk flask equipped with a magnetic stir bar. The reaction

mixture was degassed by purging N_2. Polymerization was carried out in a constant temperature oil bath at 70 °C for 14 h, after which the reaction was quenched by allowing the reaction mixture in the open air under the fume hood. The resulting polymer was purified by precipitating in methanol. The obtained polymer PC²MA was obtained and dried under vacuum to give a pale-yellow solid (425 mg, 85% isolated yield). The polymer PC²MA was characterized by ^{1}H NMR spectroscopy.

3. Synthesis of Copolymers via RAFT Polymerization

3.1. Synthesis of copolymer P(OEGMA$_{90}$-co-LMA$_{10}$) via RAFT polymerization

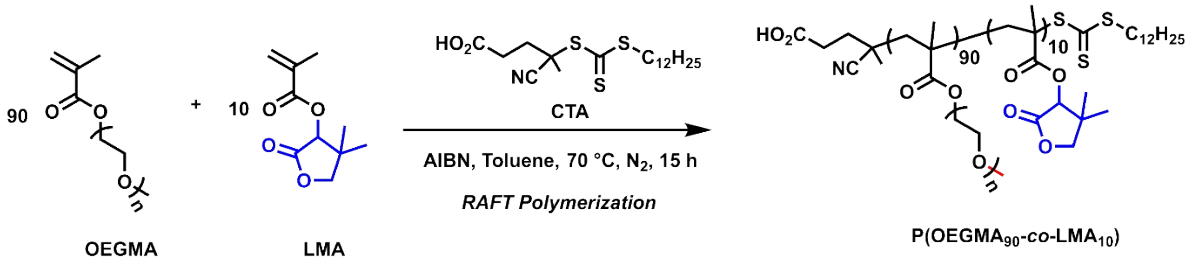

Scheme S5. Synthesis of P(OEGMA$_{90}$-co-LMA$_{10}$) via RAFT polymerization

In a 10 mL Schlenk flask equipped with a magnetic stir bar, LMA (46 mg, 0.232 mmol), OEGMA (970 mg, 1.94 mmol), CTA (10 mg, 0.0247 mmol), AIBN (5 mg, 0.0304 mmol), and toluene (2.0 mL) were added. The reaction mixture was sparged with nitrogen and stirred for 15 h at 70 °C. The polymerization reaction was quenched by stirring the mixture in an open-air under the hood. The resulting polymer was purified by precipitating in hexanes. The overall monomer conversion and the isolated yield was >90%. The purified polymers were characterized by ^{1}H NMR spectroscopy.

3.2. Synthesis of copolymer P(OEGMA$_{70}$-co-LMA$_{30}$) via RAFT polymerization

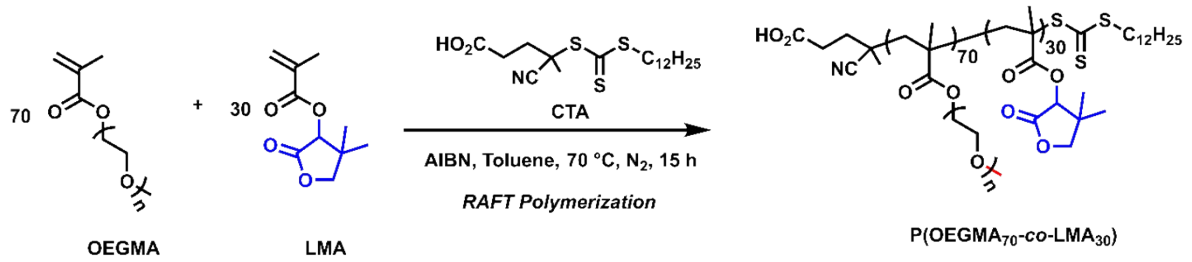

Scheme S6. Synthesis of P(OEGMA$_{70}$-*co*-LMA$_{30}$) via RAFT polymerization

In a 10 mL Schlenk flask equipped with a magnetic stir bar, LMA (145 mg, 0.7315 mmol), OEGMA (860 mg, 1.72 mmol), CTA (10 mg, 0.0247 mmol), AIBN (5 mg, 0.0304 mmol), and toluene (2.0 mL) were added. The reaction mixture was sparged with nitrogen and stirred for 15 h at 70 °C. The polymerization reaction was quenched by stirring the mixture in an open-air under the hood. The resulting polymer was purified by precipitating in hexanes. The overall monomer conversion and the isolated yield was >90%. The purified polymers were characterized by ^{1}H NMR.

3.3. Synthesis of copolymer P(OEGMA$_{50}$-co-LMA$_{50}$) via RAFT polymerization

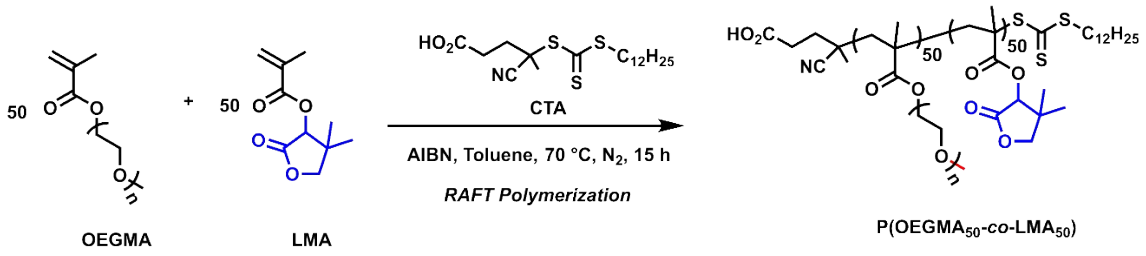

Scheme S7. Synthesis of P(OEGMA$_{50}$-co-LMA$_{50}$) via RAFT polymerization

In a 10 mL Schlenk flask equipped with a magnetic stir bar, LMA (285 mg, 1.44 mmol), OEGMA (717 mg, 1.43 mmol), CTA (12 mg, 0.0297 mmol), AIBN (5 mg, 0.0304 mmol), and toluene (2.0 mL) were added. The reaction mixture was sparged with nitrogen and stirred for 15 h at 70 °C. The polymerization reaction was quenched by stirring the mixture in an open-air under the hood. The resulting polymer was purified by precipitating in hexanes. The overall monomer conversion and the isolated yield was >90%. The purified polymers were characterized by ^{1}H NMR.

3.4. Synthesis of copolymer P(OEGMA$_{30}$-co-LMA$_{70}$) via RAFT polymerization

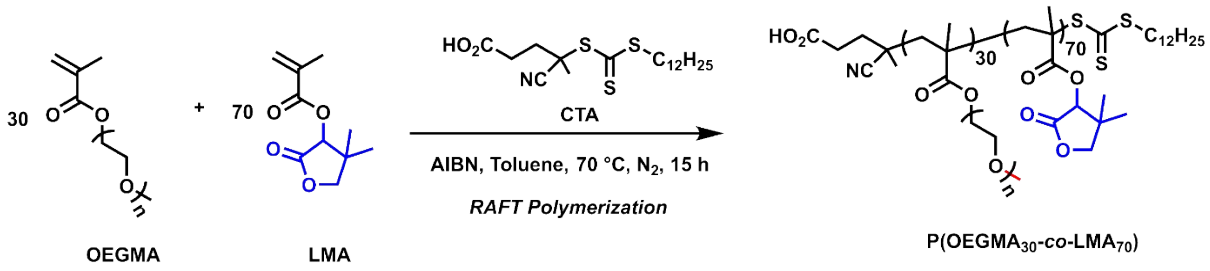

Scheme S8. Synthesis of P(OEGMA$_{30}$-co-LMA$_{70}$) via RAFT polymerization

In a 10 mL Schlenk flask equipped with a magnetic stir bar, LMA (480 mg, 2.42 mmol), OEGMA (519 mg, 1.04 mmol), CTA (14 mg, 0.035 mmol), AIBN (6 mg, 0.037 mmol), and toluene (2.0 mL) were added. The reaction mixture was sparged with nitrogen and stirred for 15 h at 70 °C. The polymerization reaction was quenched by stirring the mixture in an open-air under the hood. The resulting polymer was purified by precipitating in hexanes. The overall monomer conversion and the isolated yield was >90%. The purified polymers were characterized by ^{1}H NMR.

Table S1. Determination of the molar composition.

Polymer	OEGMA:LMA (mol%)	Feed ratio of LMA (mol%)	Composition of LMA (mol%)
P (OEGMA$_{90}$-*co*-LMA$_{10}$)	90:10	10	16
P (OEGMA$_{70}$-*co*-LMA$_{30}$)	70:30	30	36
P (OEGMA$_{50}$-*co*-LMA$_{50}$)	50:50	50	54
P (OEGMA$_{30}$-*co*-LMA$_{70}$)	30:70	70	72

3.5. Synthesis of copolymer P(OEGMA$_{70}$-co-C^{2}MA$_{30}$) via RAFT polymerization

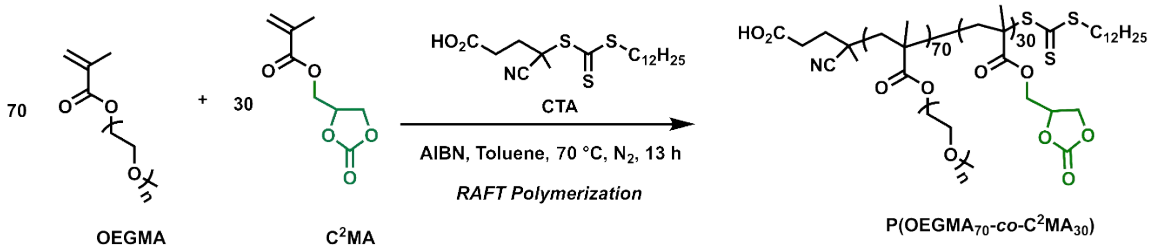

Scheme S9. Synthesis of P(OEGMA$_{70}$-co-C^{2}MA$_{30}$) via RAFT polymerization

In a 10 mL Schlenk flask equipped with a magnetic stir bar, C^{2}MA (70 mg, 0.376 mmol), OEGMA (432 mg, 0.864 mmol), CTA (5 mg, 0.0124 mmol), AIBN (3 mg, 0.0183 mmol) , and toluene were added. The reaction mixture was sparged with nitrogen and stirred for 13 h at 70 °C. The polymerization reaction was quenched by stirring the mixture in an open-air under the hood. The resulting polymer was purified by precipitating in hexanes. The overall monomer conversion and the isolated yield was >90%.

3.6. Synthesis of copolymers of P(NIPAM$_{70}$-co-C^{2}MA$_{30}$) via RAFT polymerization

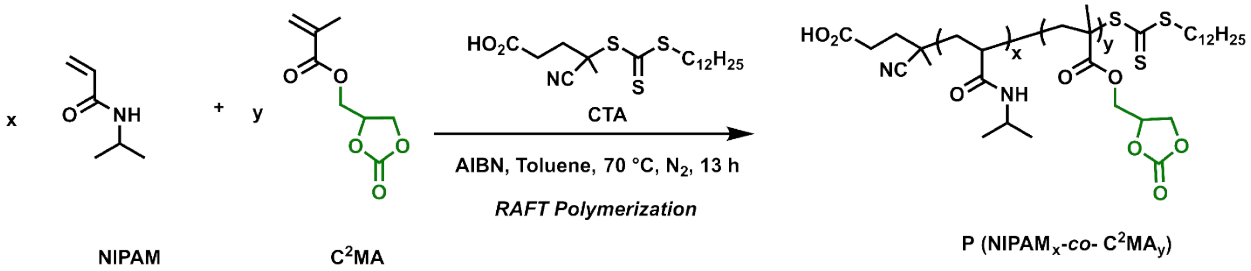

Scheme S10. Synthesis of P(NIPAM$_{70}$-*co*-C^{2}MA$_{30}$) via RAFT polymerization

In a 10 mL Schlenk flask equipped with a magnetic stir bar, C^{2}MA (207 mg 1.107 mmol), NIPAM (296 mg, 2.616 mmol), CTA (14 mg, 0.0347 mmol), AIBN (7 mg, 0.0426 mmol), and toluene (1 mL) were added. The reaction mixture was sparged with nitrogen and stirred for 13 h at 70 °C. The polymerization reaction was quenched by stirring the mixture in an open-air under the hood. The resulting polymer was purified by precipitating in hexanes. The overall monomer conversion and the isolated yield was >90%.

3.7. Synthesis of copolymer P(DEGMA$_{70}$-co-C^{2}MA$_{30}$) via RAFT polymerization

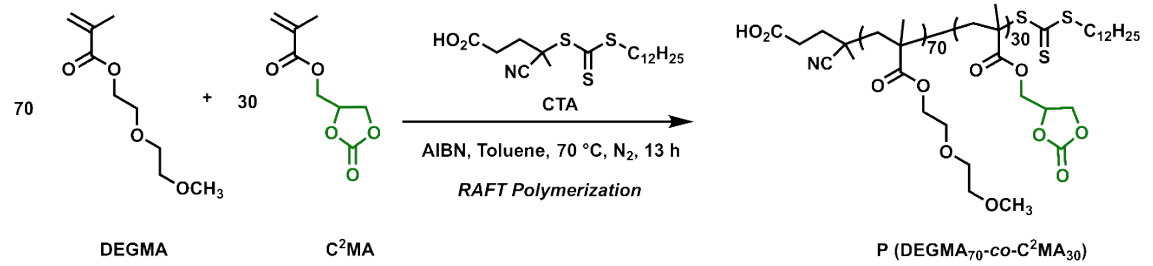

Scheme S11. Synthesis of P(DEGMA$_{70}$-*co*-C^{2}MA$_{30}$) via RAFT polymerization

In a 10 mL Schlenk flask equipped with a magnetic stir bar, C^{2}MA (148 mg, 0.795 mmol), DEGMA (351 mg, 1.866 mmol), CTA (10 mg, 0.0248 AIBN (5 mg, 0.0304 mmol), and toluene (1.0 mL) were added. The reaction mixture was sparged with nitrogen and stirred for 13 h at 70 °C. The polymerization reaction was quenched by stirring the mixture in an open-air under the hood. The resulting polymer was purified by precipitating in hexanes. The overall monomer conversion and the isolated yield was >90%.

4. Synthesis of Terpolymers via RAFT Polymerization

4.1. Synthesis of terpolymer P(DEGMA$_{80}$-co-OEGMA$_{10}$-co-LMA$_{10}$) via RAFT polymerization

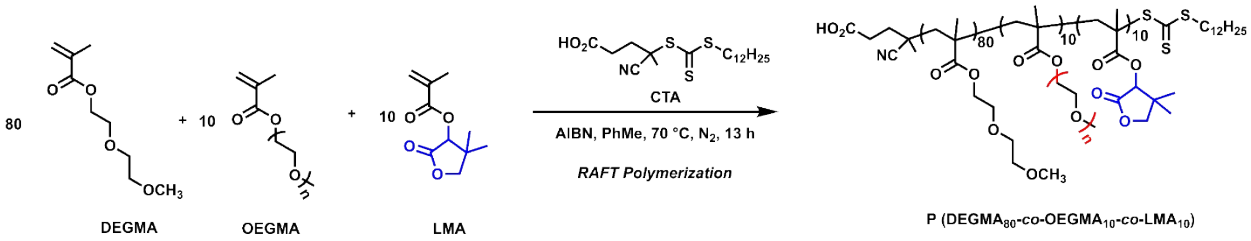

Scheme S12. Synthesis of P(DEGMA$_{80}$-*co*-OEGMA$_{10}$-*co*-LMA$_{10}$) via RAFT Polymerization

In a 10 mL Schlenk flask equipped with a magnetic stir bar, LMA (90 mg, 0.454 mmol), OEGMA (224 mg, 0.448 mmol), DEGMA (690 mg, 3.67 mmol), CTA (19 mg, 0.047 mmol), AIBN (8 mg, 0.048 mmol) and toluene (2 mL) were added. The reaction mixture was sparged with nitrogen and stirred for 13 h at 70 °C. The polymerization reaction was quenched by stirring the mixture in an open-air under the hood. The resulting polymer was purified by precipitating in hexanes. The overall monomer conversion and the isolated yield was >90%.

4.2. Synthesis of terpolymer P(DEGMA$_{60}$-co-OEGMA$_{10}$-co-LMA$_{30}$) via RAFT polymerization

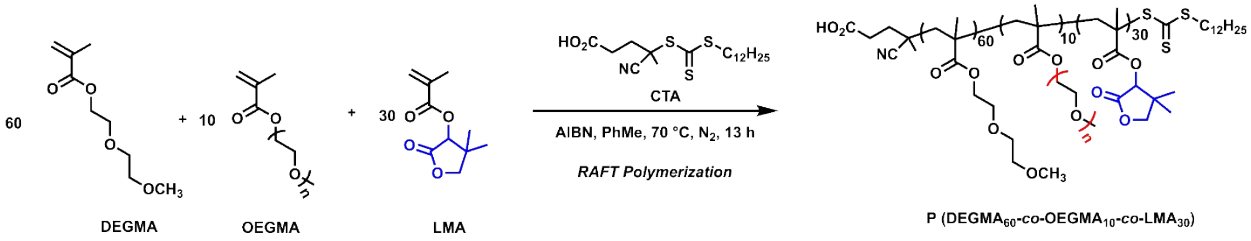

Scheme S13. Synthesis of P(DEGMA$_{60}$-*co*-OEGMA$_{10}$-*co*-LMA$_{30}$) via RAFT Polymerization

In a 10 mL Schlenk flask equipped with a magnetic stir bar, LMA (266 mg, 1.347 mmol), OEGMA (224 mg, 0.448 mmol), DEGMA (510 mg, 2.709 mmol), CTA (19 mg, 0.047 mmol), AIBN (8 mg, 0.048 mmol) and toluene (2 mL) were added. The reaction mixture was sparged with nitrogen and stirred for 13 h at 70 °C. The polymerization reaction was quenched by stirring the mixture in an open-air under the hood. The resulting polymer was purified by precipitating in hexanes. The overall monomer conversion and the isolated yield was >90%.

4.3. Synthesis of terpolymer P(DEGMA$_{80}$-co-OEGMA$_{10}$-co-C^{2}MA$_{10}$) via RAFT polymerization

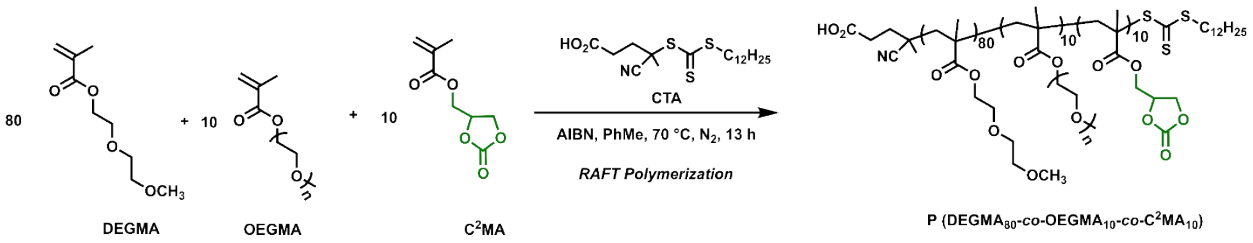

Scheme S14. Synthesis of P(DEGMA$_{80}$-co-OEGMA$_{10}$-co-C^{2}MA$_{10}$) via RAFT polymerization

In a 10 mL Schlenk flask equipped with a magnetic stir bar, C^{2}MA (85 mg, 0.456 mmol), OEGMA (228 mg, 0.456 mmol), DEGMA (685 mg, 3.639 mmol), CTA (19 mg, 0.047 mmol), AIBN (8 mg, 0.048 mmol), and toluene (2 mL) were added. The reaction mixture was sparged with nitrogen and stirred for 13 h at 70 °C. The polymerization reaction was quenched by stirring the mixture in an open-air under the hood. The resulting polymer was purified by precipitating in hexanes. The overall monomer conversion and the isolated yield was >90%.

4.4. Synthesis of terpolymer P(DEGMA$_{60}$-co-OEGMA$_{10}$-co-C^{2}MA$_{30}$) via RAFT polymerization

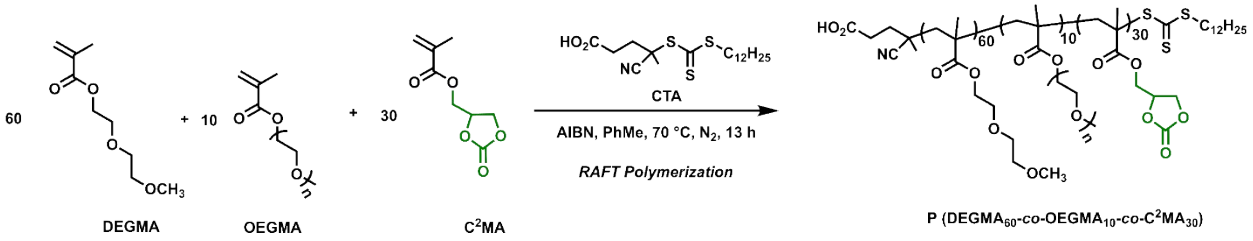

Scheme S15. Synthesis of P(DEGMA$_{60}$-co-OEGMA$_{10}$-co-C^{2}MA$_{30}$) via RAFT polymerization

In a 10 mL Schlenk flask equipped with a magnetic stir bar, C^{2}MA (255 mg, 1.371 mmol), OEGMA (228 mg, 0.456 mmol), DEGMA (516 mg, 2.74 mmol), CTA (19 mg, 0.047 mmol), AIBN (8 mg, 0.048 mmol), and toluene (2 mL) were added. The reaction mixture was sparged with nitrogen and stirred for 13 h at 70 °C. The polymerization reaction was quenched by stirring the mixture in an open-air under the hood. The resulting polymer was purified by precipitating in hexanes. The overall monomer conversion and the isolated yield was >90%.

5. Determination of the Molar Composition of the Polymers using ^{1}H NMR Spectra Analysis

The molar compositions of **LMA** within the copolymers were determined using ^{1}H NMR spectroscopy.

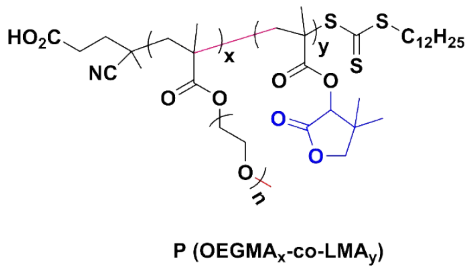

Scheme S16. Structure of P(OEGMA$_x$-*co*-LMA$_y$)

6. Cloud Point Temperature (T_{cp}) Measurements

The cloud point temperatures (T_{cp}) of the copolymers were determined by preparing 1 wt% aqueous solutions and measuring turbidity as a function of temperature using a turbidimeter with a ramp rate of 0.5 °C min^{-1}.

Table S2. Cloud point temperature measurements for polymers (#: not measured)

Polymer	Physical Sate	Water solubility	T_{cp} (°C) in DI H_2O	T_{cp} (°C) in PBS
PLMA	Solid	No	NA	#
P(OEGMA$_{90}$-*co*-LMA$_{10}$)	Liquid	Yes	79.9	#
P(OEGMA$_{70}$-*co*-LMA$_{30}$)	Liquid	Yes	64.2	#
P(OEGMA$_{50}$-*co*-LMA$_{50}$)	Liquid	Yes	53.1	#
P(OEGMA$_{30}$-*co*-LMA$_{70}$)	Semi-solid	Partially soluble	NA	#
P(DEGMA$_{80}$-*co*-LMA$_{10}$-*co*-OEGMA$_{10}$)	Liquid	Yes	28.2-29.2	33.45
P(DEGMA$_{60}$-*co*-LMA$_{30}$-*co*-OEGMA$_{10}$)	Semi-solid	Partially soluble	25.8-28.3	29
PC^{2}MA	Solid	No	NA	#
P(OEGMA$_{70}$-*co*-C^{2}MA$_{30}$)	Liquid	Partially soluble	NA	#
P(DEGMA$_{70}$-*co*-C^{2}MA$_{30}$)	Semi-solid	Partially soluble	Na	#
P(NIPAM$_{70}$-*co*-C^{2}MA$_{30}$)	Solid	No	NA	#
P(NIPAM$_{95}$-*co*-C^{2}MA$_5$)	Solid	Yes	26.9	#
P(DEGMA$_{80}$-*co*-C^{2}MA$_{10}$-*co*-OEGMA$_{10}$)	Liquid	Yes	28.1-34.2	32.29
P(DEGMA$_{60}$-*co*-C^{2}MA$_{30}$-*co*-OEGMA$_{10}$)	Semi-solid	Partially soluble	30.9-32.6	30.79

6.1. The effect of ramp rate on the cloud point temperature

Table S3. Effect of ramp temperature on the cloud point measurement

Polymer	Ramp rate (ºC/min)	Cloud point (ºC)[a,b]
P(DEGMA$_{60}$-*co*-OEGMA$_{10}$-*co*-C^{2}MA$_{30}$)	0.25	34.0
P(DEGMA$_{60}$-*co*-OEGMA$_{10}$-*co*-C^{2}MA$_{30}$)	0.50	34.2
P(DEGMA$_{60}$-*co*-OEGMA$_{10}$-*co*-C^{2}MA$_{30}$)	1.0	34.4
P(DEGMA$_{60}$-*co*-OEGMA$_{10}$-*co*-C^{2}MA$_{30}$)	2.0	34.44
P(DEGMA$_{60}$-*co*-OEGMA$_{10}$-*co*-C^{2}MA$_{30}$)	4.0	35.09

[a] Determined when the transmittance dropped to 90% from its initial value.
[b] The concentration is 1 wt%.

6.2. The effect of concentration on the cloud point temperature

Table S4. Effect of concentration on the cloud point

Polymer	Concentration (wt%)	Cloud Point (ºC)[a]
P(DEGMA$_{80}$-*co*-OEGMA$_{10}$-*co*-C^{2}MA$_{10}$)	0.5	30.95
P(DEGMA$_{80}$-*co*-OEGMA$_{10}$-*co*-C^{2}MA$_{10}$)	1.0	28.10
P(DEGMA$_{80}$-*co*-OEGMA$_{10}$-*co*-C^{2}MA$_{10}$)	2.0	25.87
P(DEGMA$_{80}$-*co*-OEGMA$_{10}$-*co*-C^{2}MA$_{10}$)	4.0	24.82
P(DEGMA$_{80}$-*co*-OEGMA$_{10}$-*co*-C^{2}MA$_{10}$)	6.0	25.06
P(DEGMA$_{80}$-*co*-OEGMA$_{10}$-*co*-C^{2}MA$_{10}$)	8.0	28.24

[a] Determined when the transmittance dropped to 90% from its initial value.

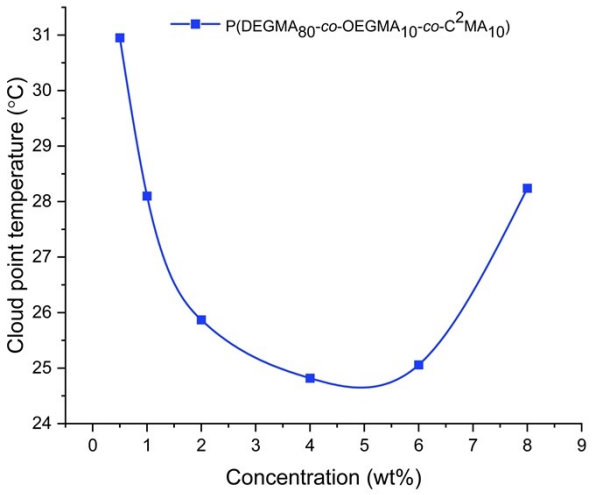

Figure S1. LCST curve for P(DEGMA$_{80}$-*co*-OEGMA$_{10}$-*co*-C^{2}MA$_{10}$)

7. Hydrolysis Study of Terpolymers

Samples for the hydrolysis study were prepared by dissolving 50 mg of each polymer in 5 mL (1 wt%) of deionized water or PBS. The solutions were placed on a hot plate at 50 °C for 7 days. After 7 days, the samples were transferred to a freeze-dryer for lyophilization, followed by characterization using ^{1}H NMR spectroscopy. The ^{1}H NMR spectra showed no significant differences compared to the reference spectra, indicating that hydrolysis proceeds slowly under these conditions. To accelerate hydrolysis, the procedure was repeated using 1 M HCl and 1 M NaOH solutions instead of deionized water or PBS.

7.1. Cloud point temperature analysis of hydrolyzed terpolymers

Cloud point samples for the hydrolysis study were prepared in both DI water and PBS with a 1 wt% concentration for all mediums. For accelerated conditions, samples were taken after neutralizing and prior to lyophilization. Samples were analyzed for temperature-dependent transmittance at 600 nm using an Agilent Cary 3500 Peltier UV-Vis spectrophotometer, with a temperature ramp rate of 0.5 °C.

8. Kinetics study

To compare the hydrolysis rates of the LMA and C^2MA side chains under milder conditions, a separate study was conducted in 0.5 M NaOH at 25 °C. Samples were neutralized after 1 h, 4 h, 8 h, and 1 day and placed in the freeze-dryer instrument. ^1H NMR spectrum of each sample was analyzed to confirm the hydrolysis over time and compare the hydrolysis rate between L30 and C30 polymers.

9. Radiofrequency Treatment of Terpolymers

RF-assisted heating experiments of samples were performed using a custom-built experimental setup. The setup consists of two copper strips on a Teflon block, with one copper strip connected to the inner conductor and the other to outer conductor of a coaxial cable. A RIGOL DSG836 model signal generator (9 kHz-3 GHz) was used to generate the RF signals, and the corresponding signal was amplified to achieve the desired input power by an RF Amplifier 50W1000D model. RF signals were delivered to the copper strips applicator via 50 Ω coaxial cable. Thermal imaging and heating rate data during RF-assisted heating experiments were recorded by FLIR A655sc High-Resolution Science Grade LWIR Camera, and data analysis was performed using FLIR® ResearchIR Recording and Analysis software. To perform heating experiments, 30 µL of solution was added to a quartz glass test tube touching the copper strips in non-contact applicator configuration **(Figure S2a)**, whereas in direct-contact configuration **(Figure S2b)**, 30 µL of solution was placed directly on the applicator between the copper strips.

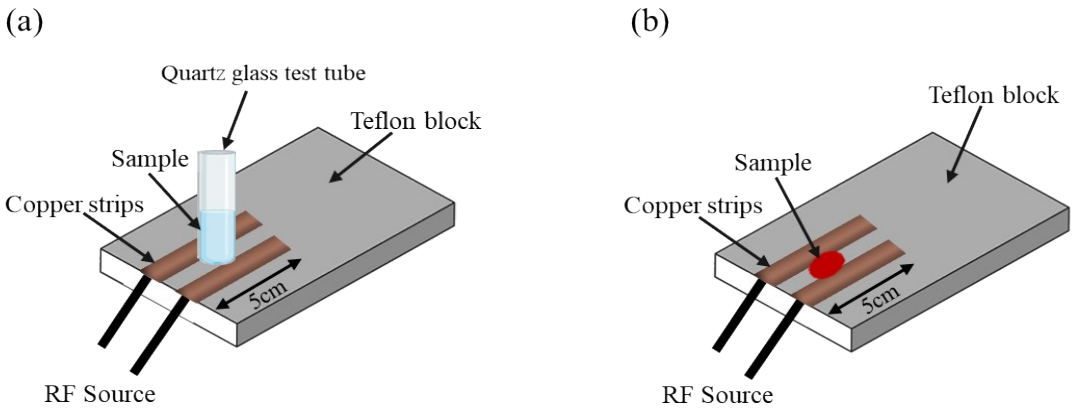

- Length and width of copper strips: 5 cm × 0.5 cm
- Space between two copper strips: 0.5 cm

Figure S2. Illustration of the experimental setup of RF assisted heating setup: (a) non-contact and (b) direct-contact applicator configuration

10. Rheology of Terpolymers

Rheological measurements were conducted on a stress-controlled rheometer (TA Instruments or Anton Paar, model as appropriate) equipped with a parallel plate geometry. Two terpolymers, P($DEGMA_{60}$-*co*-$OEGMA_{10}$-*co*-LMA_{30}) and P($DEGMA_{60}$-*co*-$OEGMA_{10}$-*co*-C^2MA_{30}), were selected for analysis. Polymer solutions were prepared by dissolving the requisite amount of polymer in deionized water, followed by thorough equilibration to ensure complete hydration and homogeneity. Samples were carefully loaded onto the lower plate to achieve uniform coverage while minimizing air entrapment and excess spillover. Prior to

measurement, samples were equilibrated under the measurement gap for several minutes to relax residual stress. Complex viscosity (η) was measured as a function of angular frequency (ω). To determine the gelation temperature (T_{gel}), temperature sweeps (20–40 °C at 1 °C/min) were performed at multiple angular frequencies (0.2, 1, 5, 10, 20, and 50 rad/s), and tanδ was plotted versus temperature; the crossover point indicated T_{gel}. The strain amplitude was maintained at 0.1%, confirmed to lie within the linear viscoelastic regime (LVR) by preliminary amplitude sweeps.

11. Injectability Test of Terpolymers

The pronounced differences in complex viscosity between the terpolymers have important implications for their injectability. The C30 terpolymer exhibited a lower viscosity (1.1 Pa·s) compared to the L30 terpolymer (7.25 Pa·s), suggesting that C30 can be more easily injected through a fine-gauge needle. This lower viscosity reduces the required injection force and minimizes the risk of shear-induced damage to encapsulated bioactive agents or surrounding tissues. Despite these differences, both terpolymers demonstrated favorable injectability.

To further evaluate their injectability and potential for controlled release, we selected two representative terpolymers: L30 and C30. Aqueous solutions (10 wt%) of each polymer were injected into a 0.3 wt% agarose gel matrix, pre-formed and incubated at 37 °C to simulate physiological conditions. This tissue-mimicking setup enabled assessment of the polymers' ability to flow through soft matrices and their subsequent behavior over time. As a control, a neon green dye solution was first injected alone into the agarose gel, which rapidly diffused throughout the matrix. In contrast, when the dye was premixed with terpolymer solution, diffusion was markedly slower. This reduced dispersion is attributed to the polymer networks entrapping the dye molecules and modulating their release.

Only the dye system exhibited the most streamlined and easy injectability, with the dye entering cleanly; however, diffusing symmetrically upward and accumulating at the top. Over time, a clear diffusion front formed, and by 7 hours, the dye was dispersed only in the upper portion of the vial. In contrast, the L30+dye system demonstrated relatively harder injectability through 22 G needle, with the dye-polymer system initially appearing as clumped aggregates, suggesting a more viscous or semi-solid nature. The diffusion was slower although slightly irregular, with streaking and less vertical movement during the 7-hour period. This behavior points to a formulation that resists dispersion and may be suited for localized or depot-based delivery applications. The C30+dye system displayed intermediate characteristics: while some clumping was observed during injection, the dye dispersed more uniformly than in the L30+dye system. Over time, the dye formed a broader but slightly uneven gradient, reflecting moderate viscosity and improved diffusion compared to the L30+dye system, probably due to the faster hydrolysis behavior. Overall, while the L30+dye system suggested a more viscous and localized release profile, the C30+dye system offered a balance between injectability and controlled release. These results confirm that both terpolymers are readily injectable and can sustain the release of encapsulated small molecules, highlighting their potential as injectable scaffolds for controlled delivery in biomedical applications.

11.1. Preparation of 0.3 wt% agarose gel in DI water

A 0.3 wt% agarose gel was prepared by dissolving 60 mg of agarose in 20 mL of deionized water. The heterogeneous mixture was heated to 90–95 °C under gentle stirring until a clear, homogeneous solution

was obtained, indicating complete dissolution of agarose. The solution was then allowed to cool to room temperature to facilitate gelation, followed by incubation at 37 °C.

Figure S3. 0.3 wt% agarose gel in DI water

11.2. Preparation of 10 wt% terpolymer and neon green dye solution

100 mg of P(DEGMA$_{60}$-*co*-OEGMA$_{10}$-*co*-LMA$_{30}$) was dissolved in a 1-dram vial containing a 1:1 (v/v) mixture of H_2O/Neon green and a neon green dye solution to obtain a 10 wt% polymer–dye solution. Similarly, P(DEGMA$_{60}$-*co*-OEGMA$_{10}$-*co*-C^{2}MA$_{30}$) (100 mg) was dissolved under identical conditions to prepare a 10 wt% polymer–dye solution. Prior to injection, all the prepared agarose gel vial were incubated at 37 °C for 2 h to ensure homogeneity. For injection into the agarose gel matrix, a 1 mL syringe equipped with a 22G needle was employed. In each experiment, 60 µL of the prepared solution was precisely injected into the gel for subsequent analysis.

12. Characterizations

12.1. NMR spectroscopy

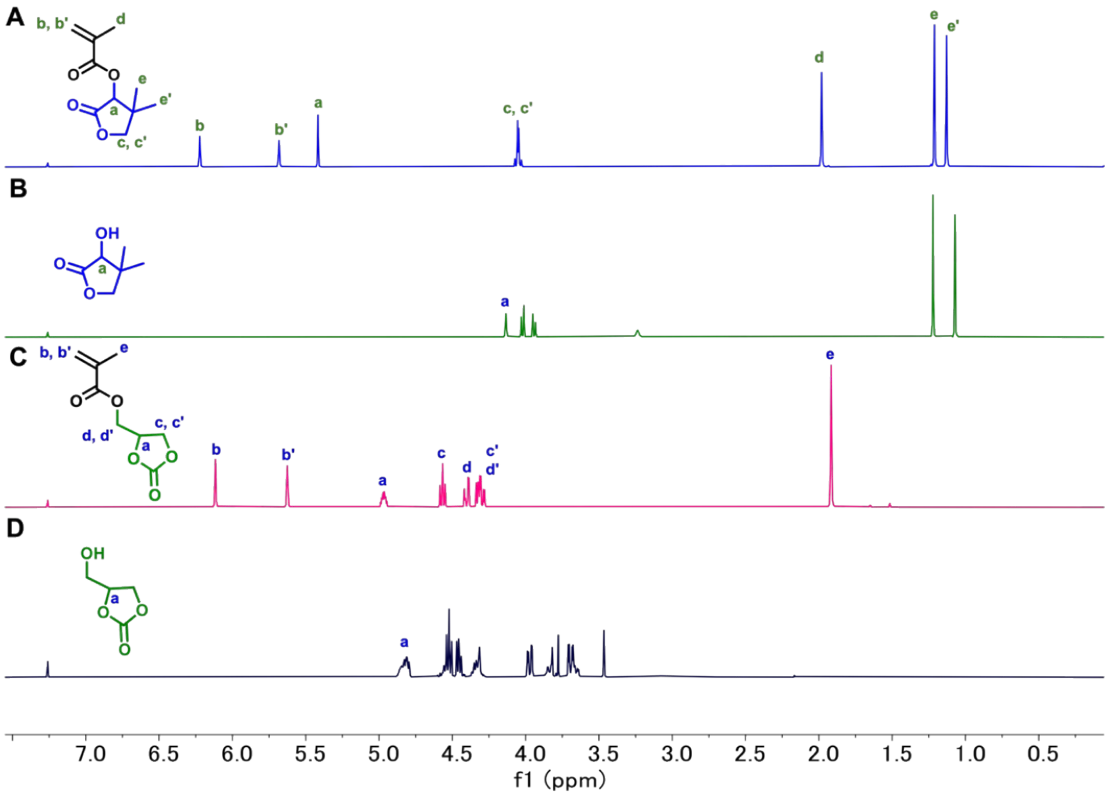

Figure S4. ^{1}H NMR spectra of **(A)** LMA monomer, **(B)** DL-Pantolactone, **(C)** C^{2}MA monomer, and **(D)** 4-(hydroxymethyl)-1,3-dioxolan-2-one in $CDCl_3$

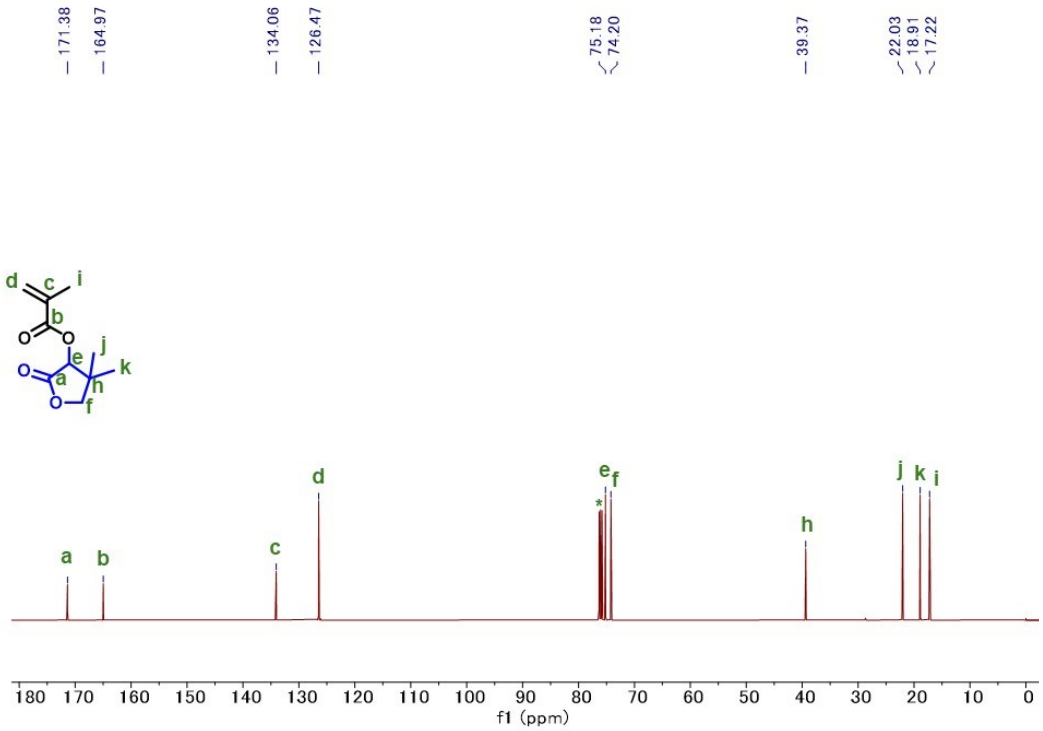

Figure S5. ^{13}C NMR spectrum of LMA in $CDCl_3$

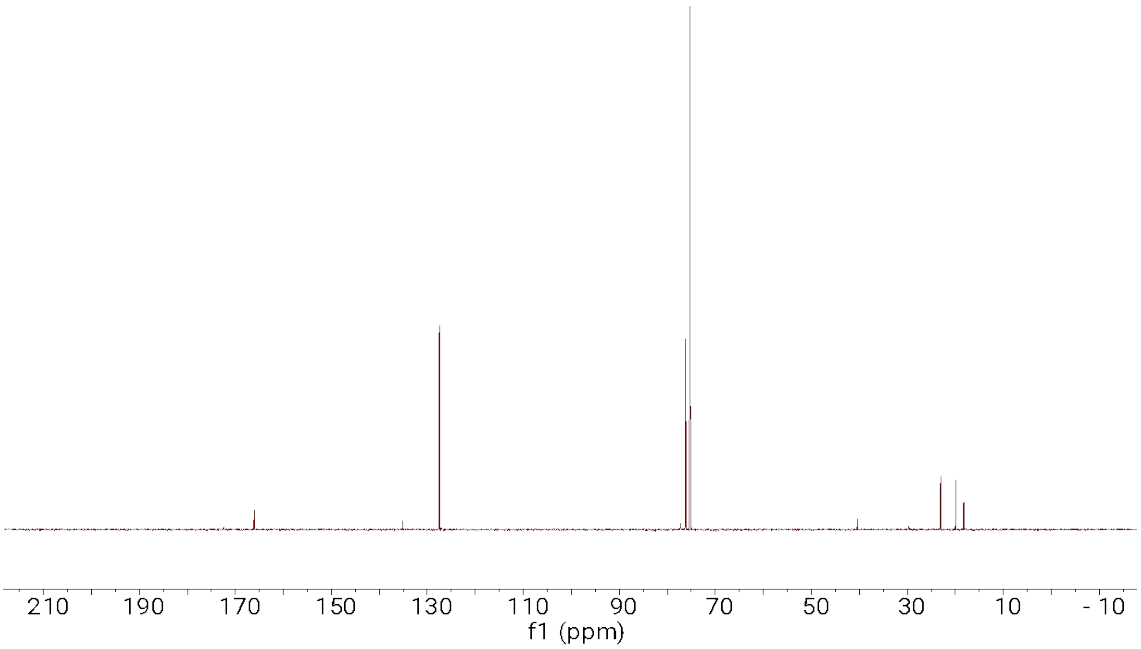

Figure S6. DEPT-90 NMR spectrum of LMA in $CDCl_3$

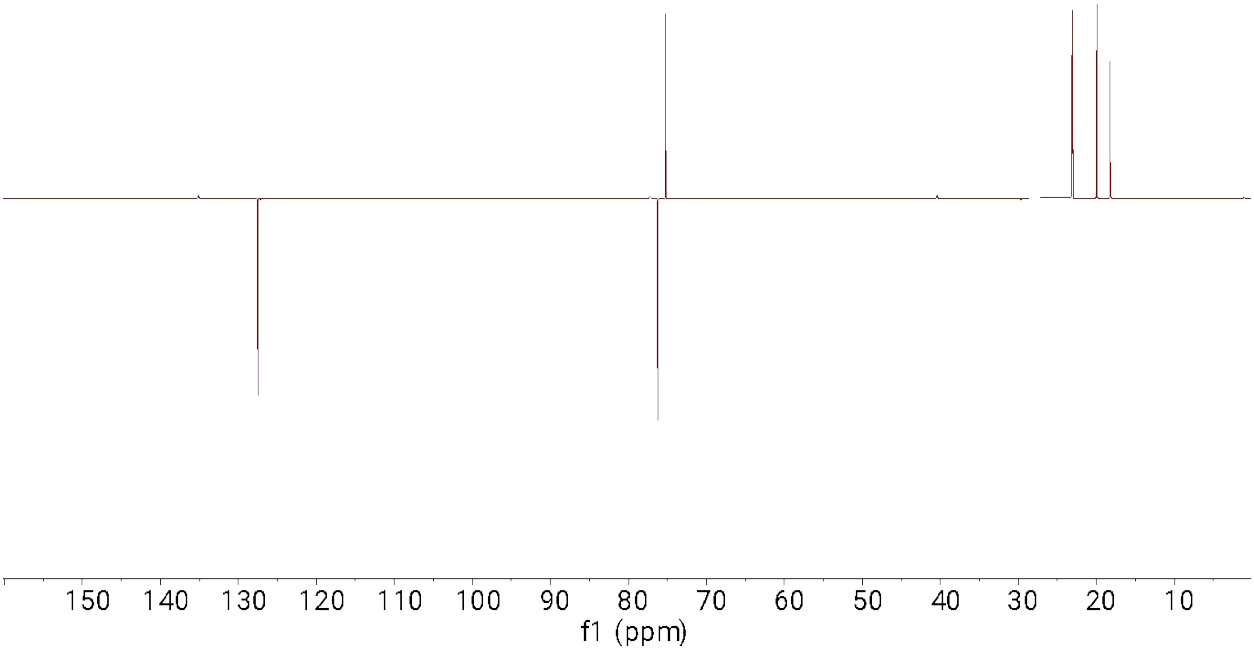

Figure S7. DEPT-135 NMR spectrum of LMA in $CDCl_3$

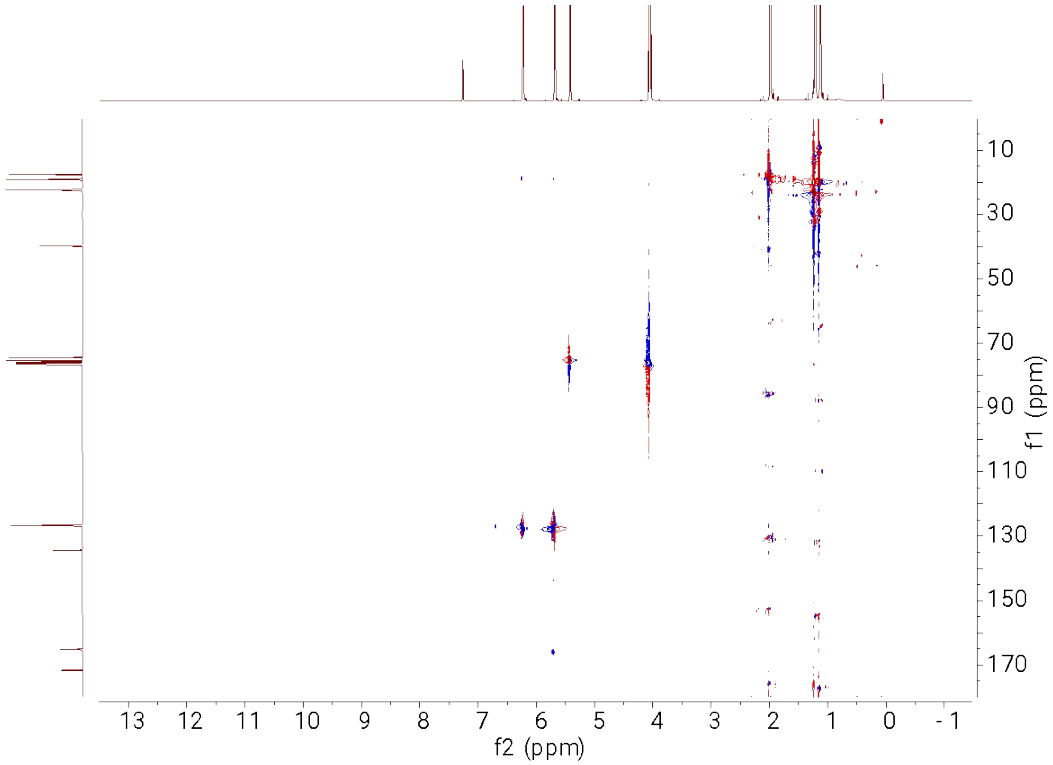

Figure S8. HSQC NMR spectrum of LMA in $CDCl_3$

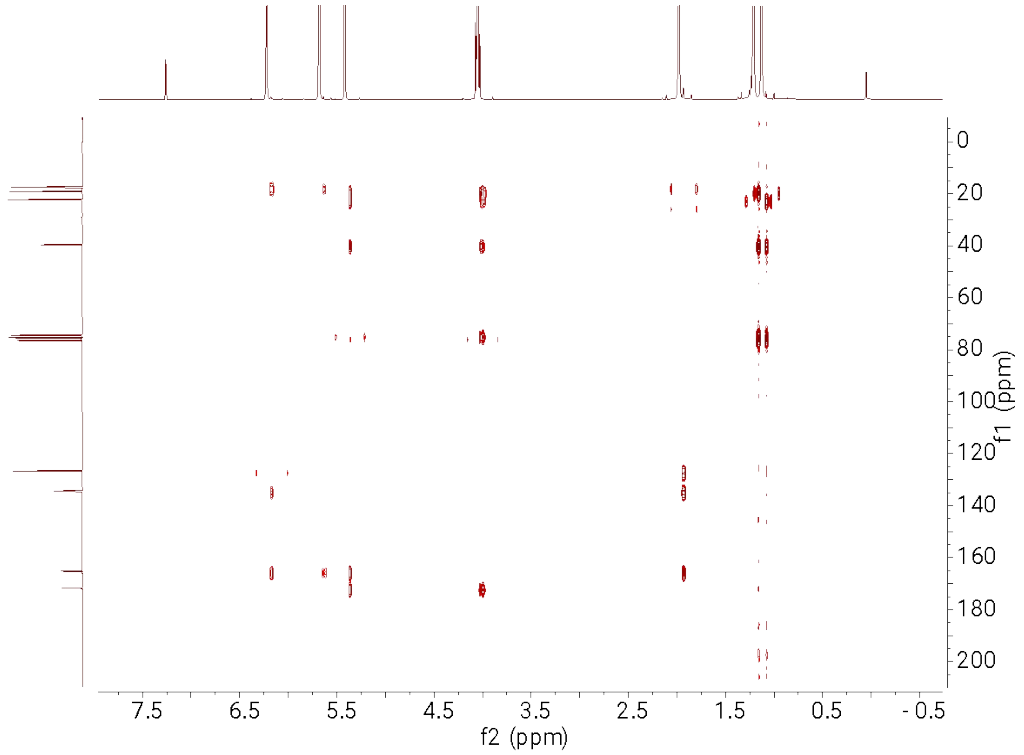

Figure S9. HMBC NMR spectrum of LMA in $CDCl_3$

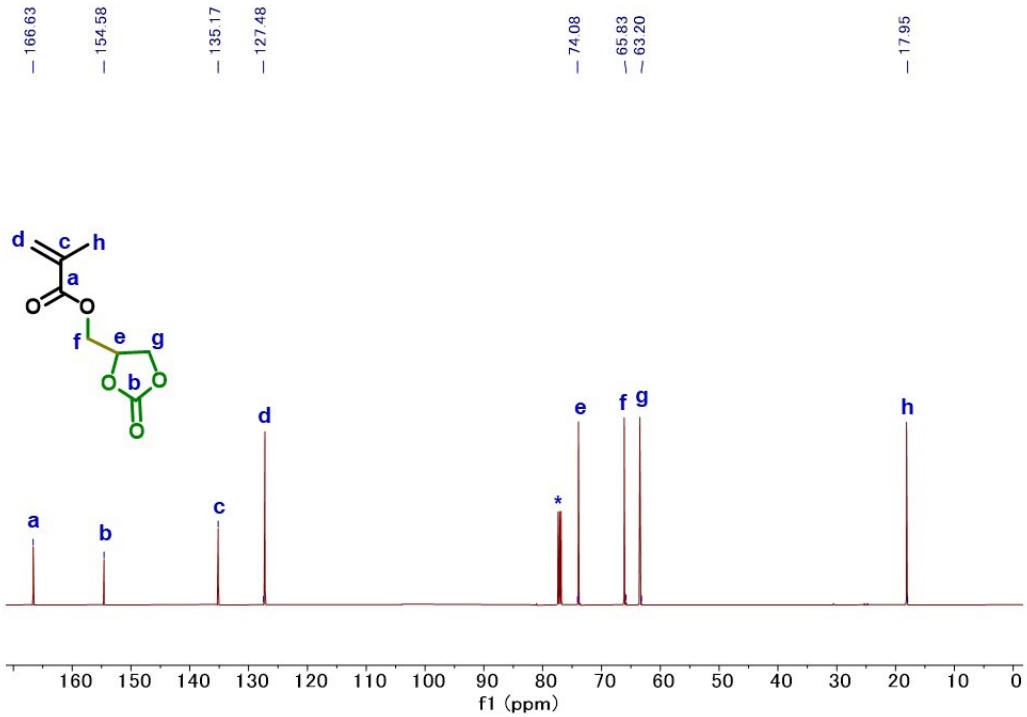

Figure S10. ^{13}C NMR spectrum of C^2MA in $CDCl_3$

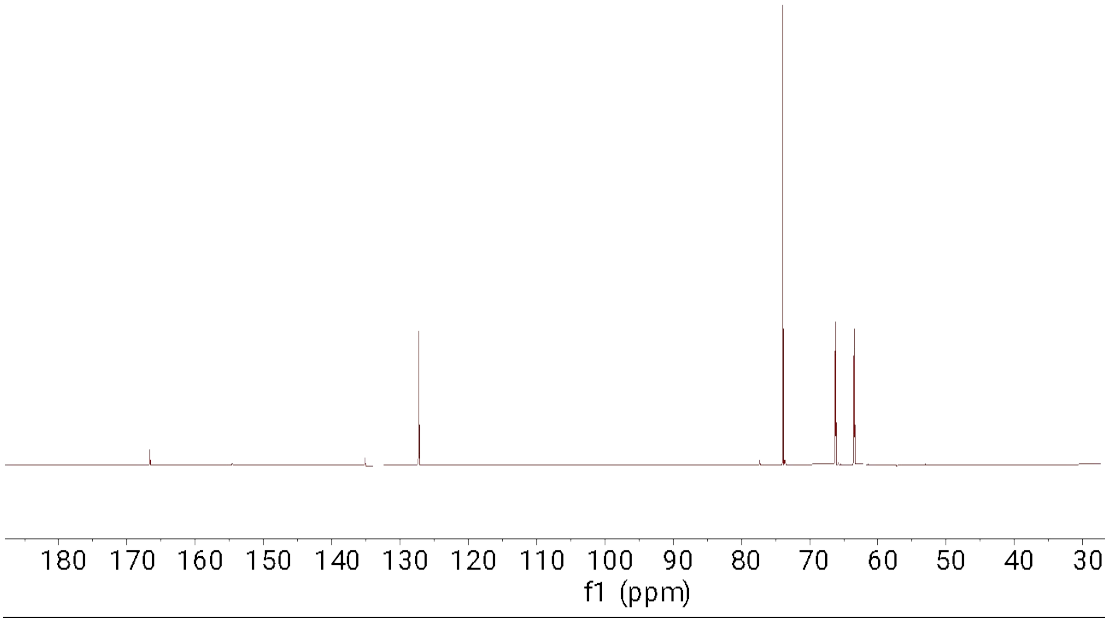

Figure S11. DEPT-90 NMR spectrum of C^2MA in $CDCl_3$

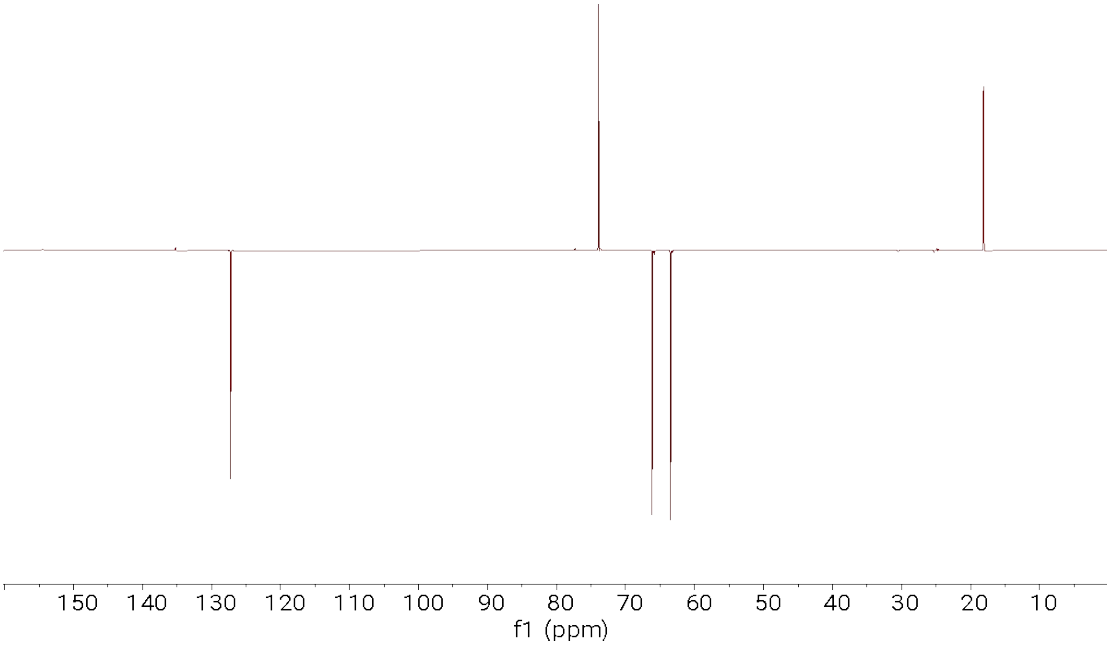

Figure S12. DEPT-135 NMR spectrum of C^2MA in $CDCl_3$

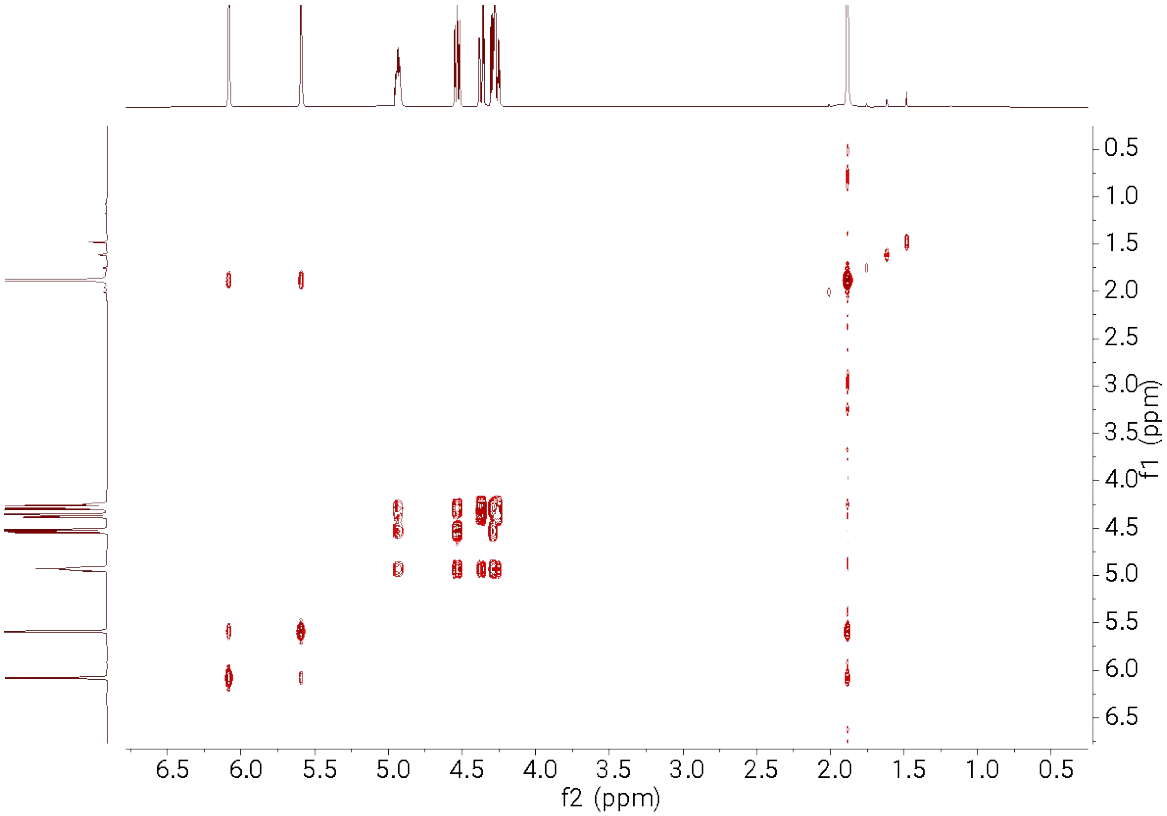

Figure S13. COSY NMR spectrum of C^2MA in $CDCl_3$

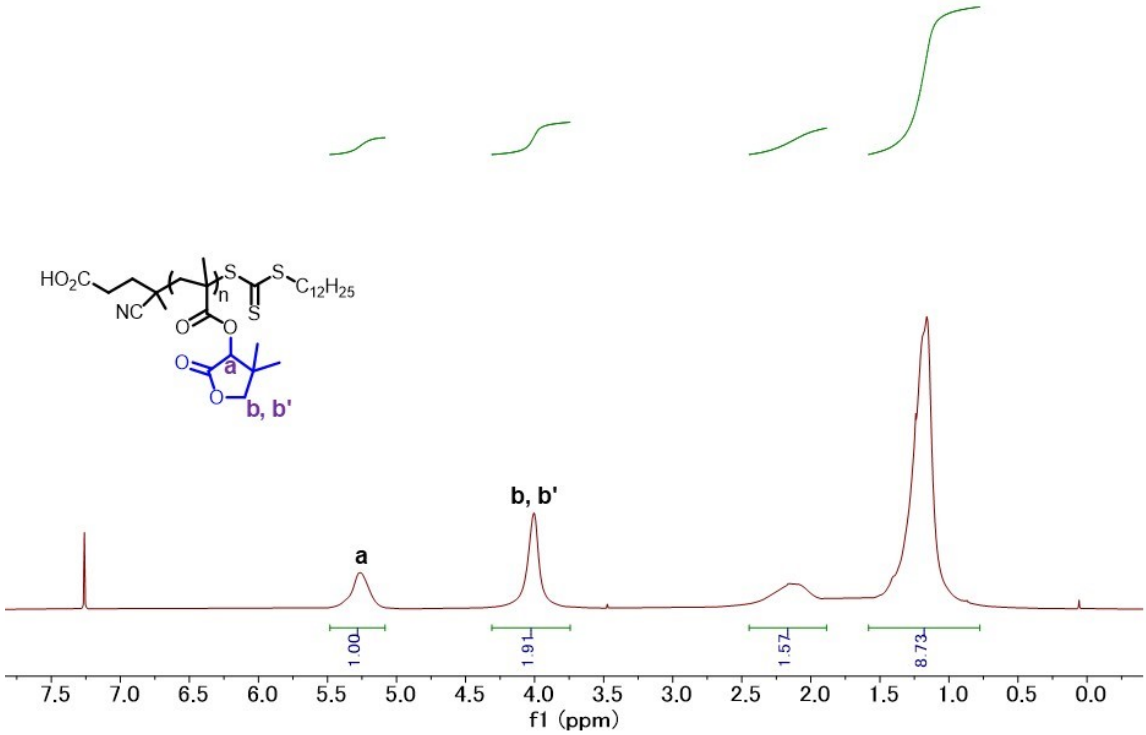

Figure S14. ^1H NMR spectrum of PLMA in $CDCl_3$

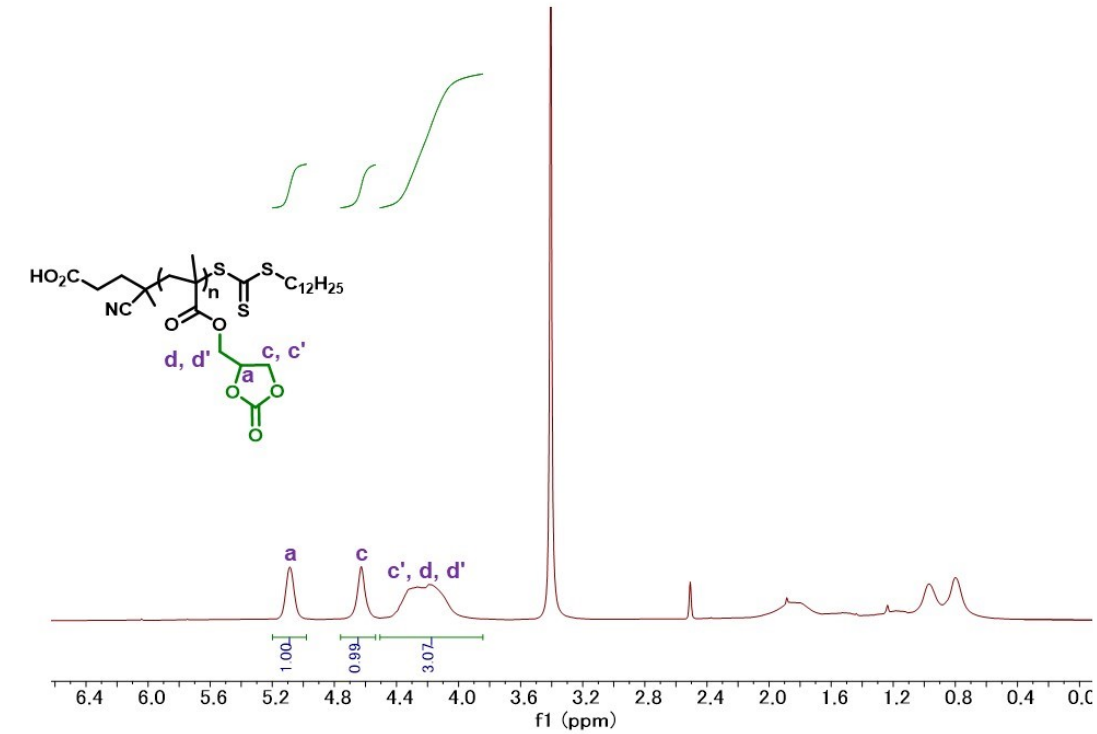

Figure S15. ^{1}H NMR spectrum of PC^{2}MA in DMSO-d6

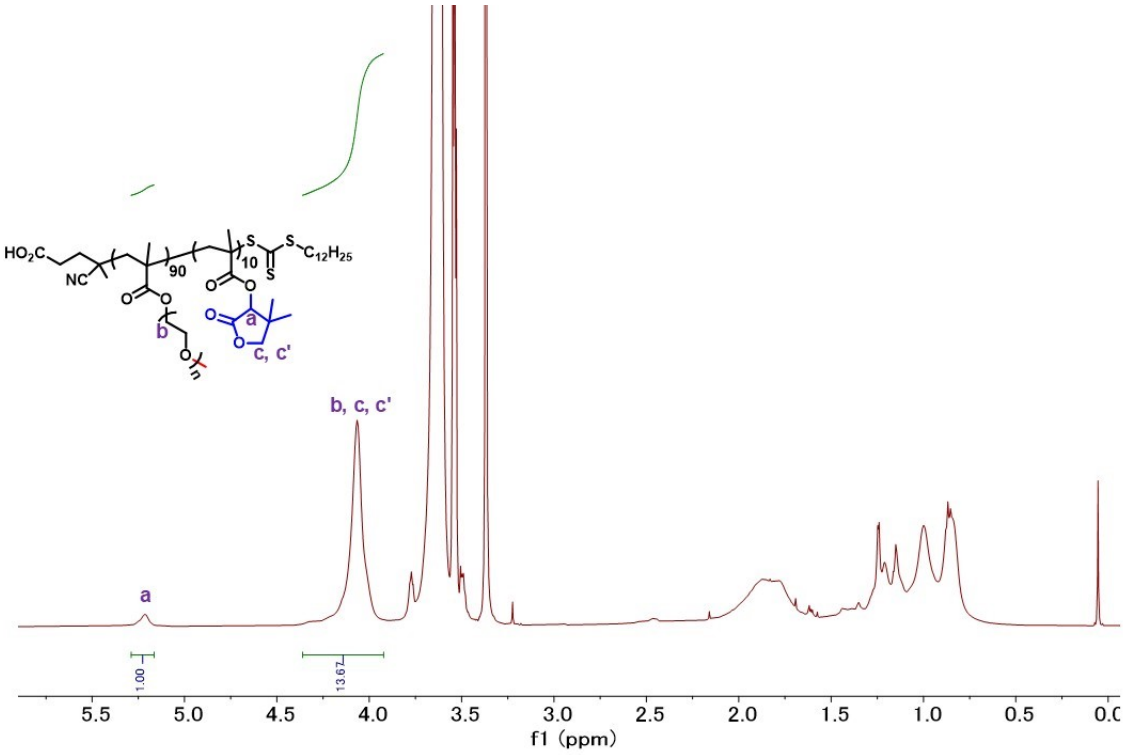

Figure S16. ^{1}H NMR spectrum of P(OEGMA$_{90}$-*co*-LMA$_{10}$)

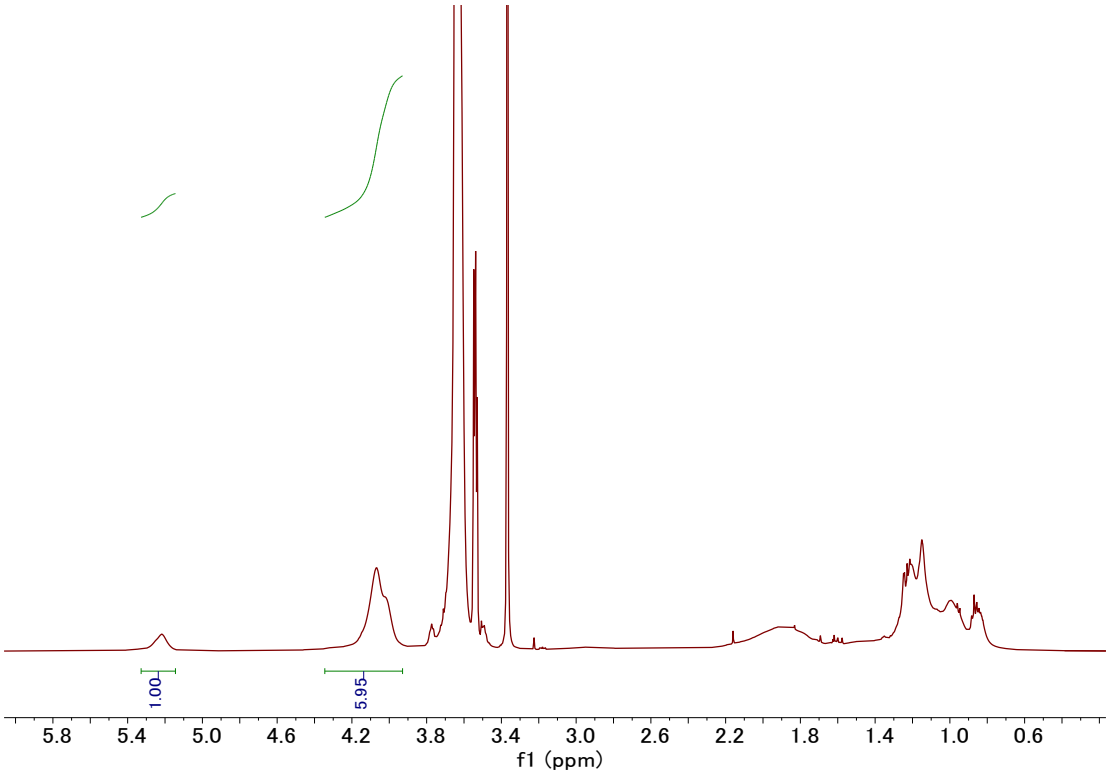

Figure S17. ^{1}H NMR spectrum of P(OEGMA$_{70}$-*co*-LMA$_{30}$)

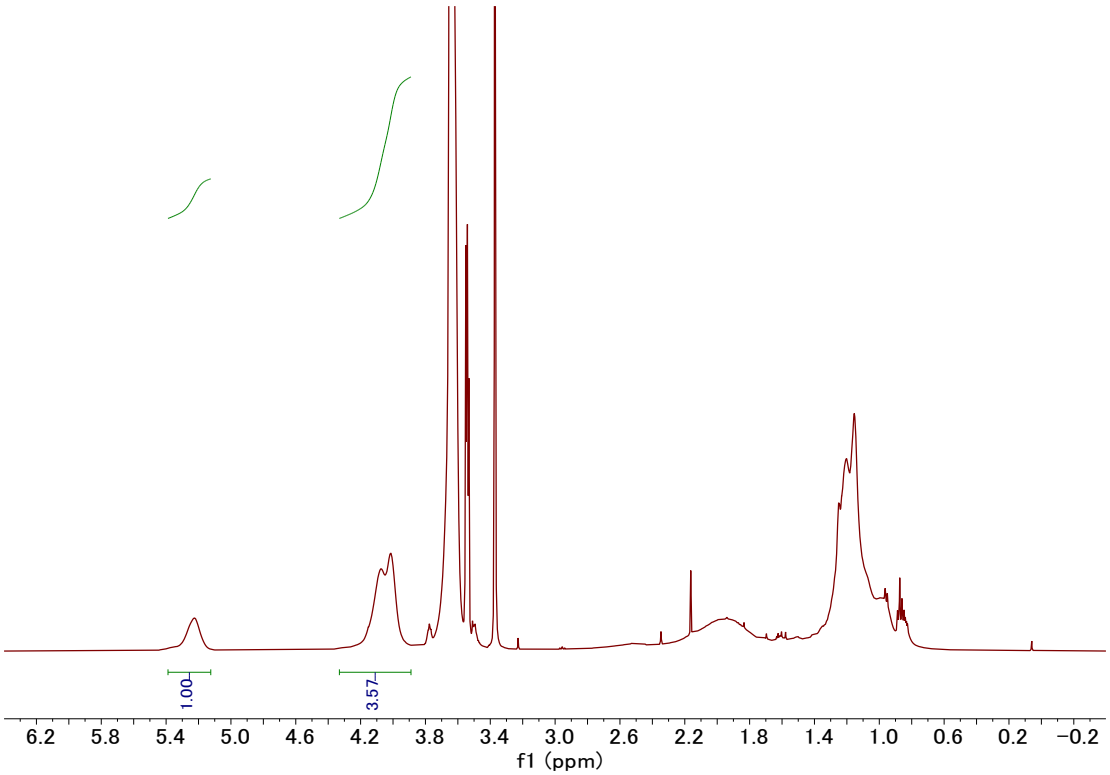

Figure S18. ^{1}H NMR spectrum of P(OEGMA$_{50}$-*co*-LMA$_{50}$)

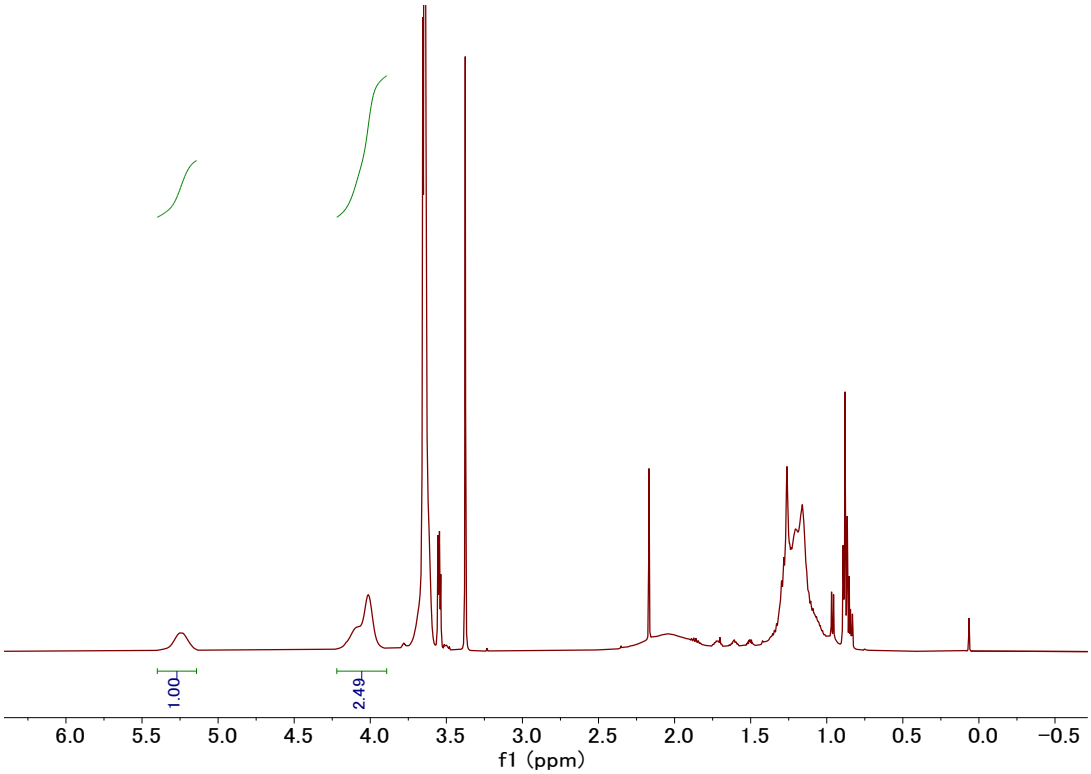

Figure S19. ^{1}H NMR spectrum of P(OEGMA$_{30}$-*co*-LMA$_{70}$)

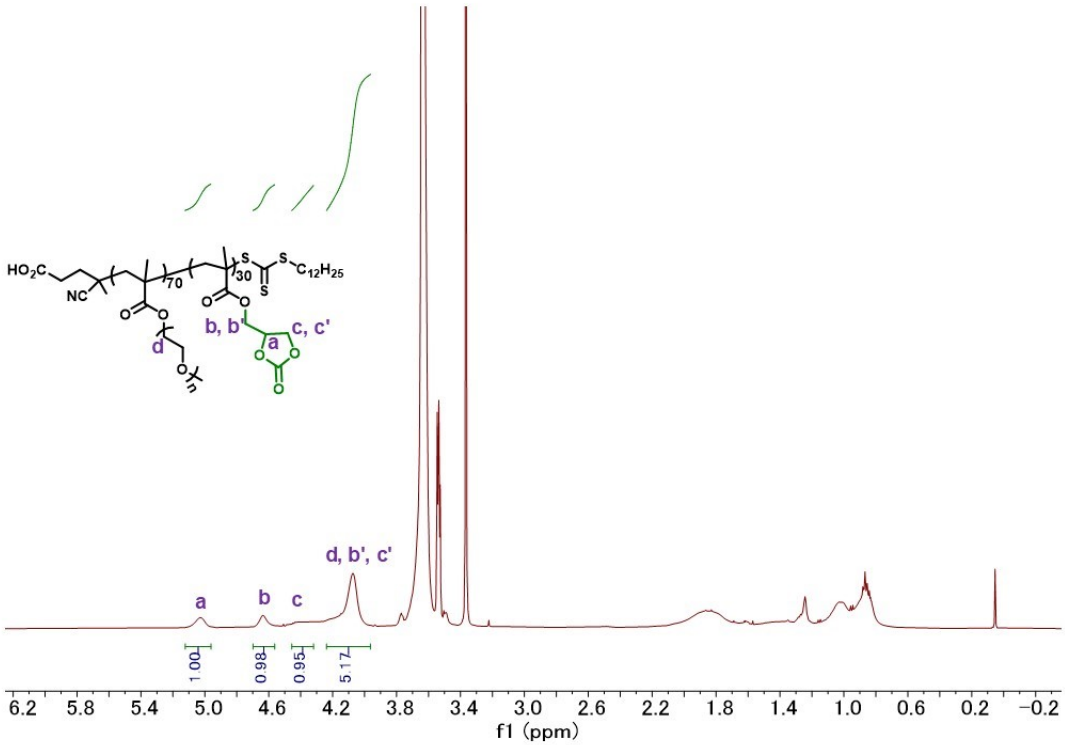

Figure S20. ^{1}H NMR spectrum of P(OEGMA$_{70}$-*co*-C^{2}MA$_{30}$)

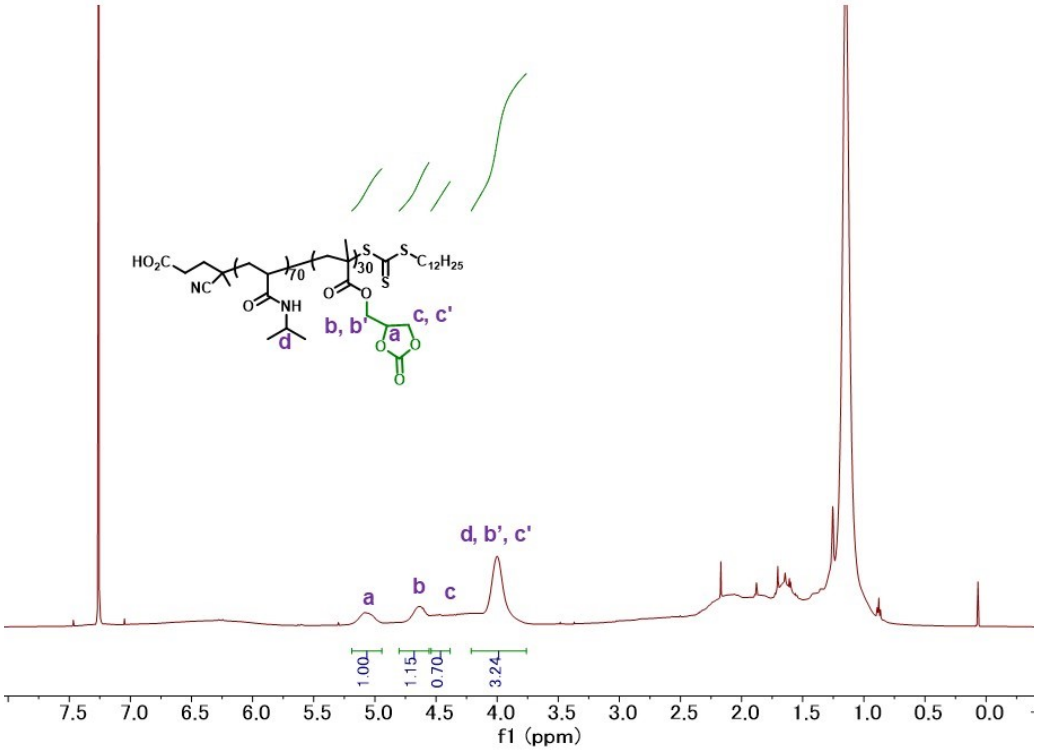

Figure S21. ^{1}H NMR spectrum of P(NIPAM$_{70}$-*co*-C^{2}MA$_{30}$) in CDCl3

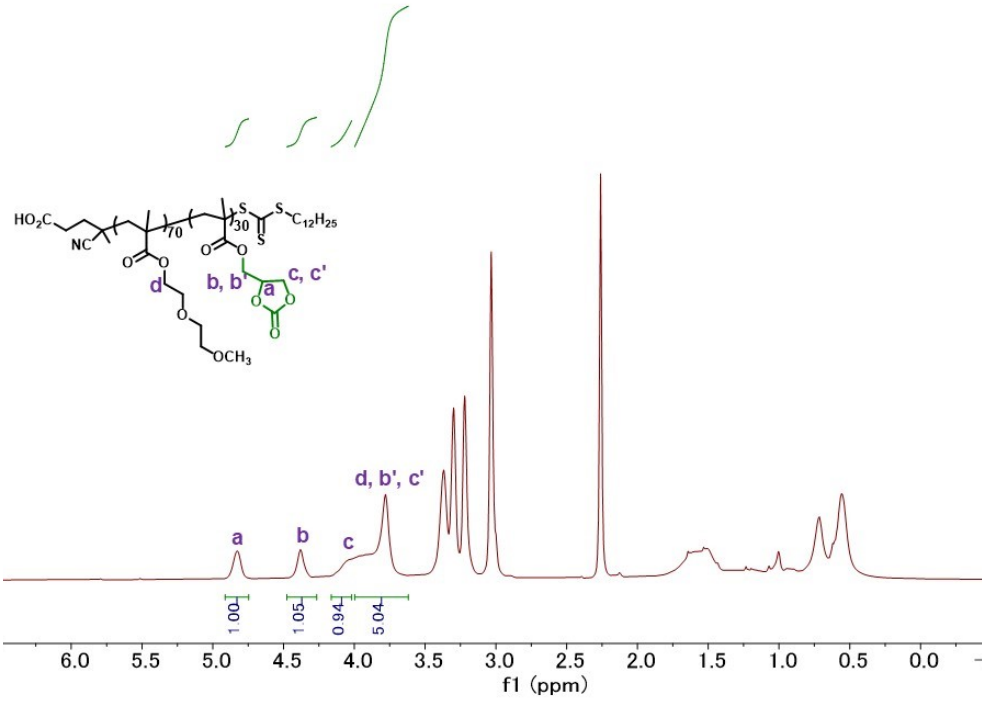

Figure S22. ^{1}H NMR spectrum of P(DEGMA$_{70}$-*co*-C^{2}MA$_{30}$) in DMSO-d6

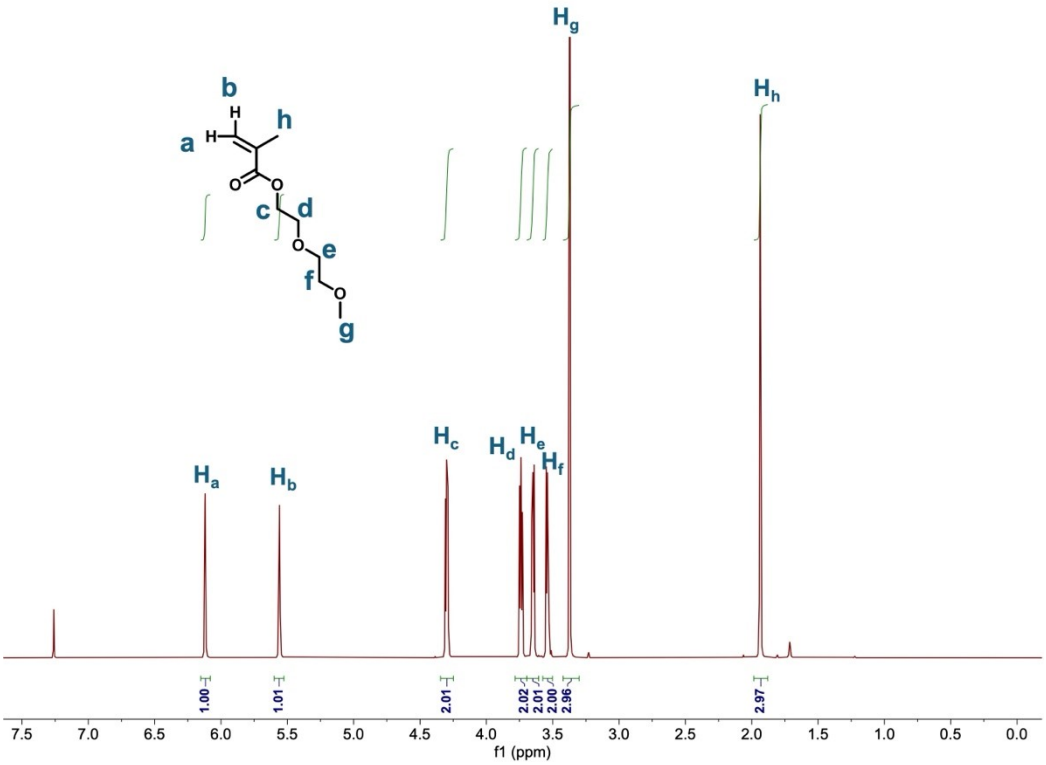

Figure S23. ^{1}H NMR spectrum of DEGMA in $CDCl_3$

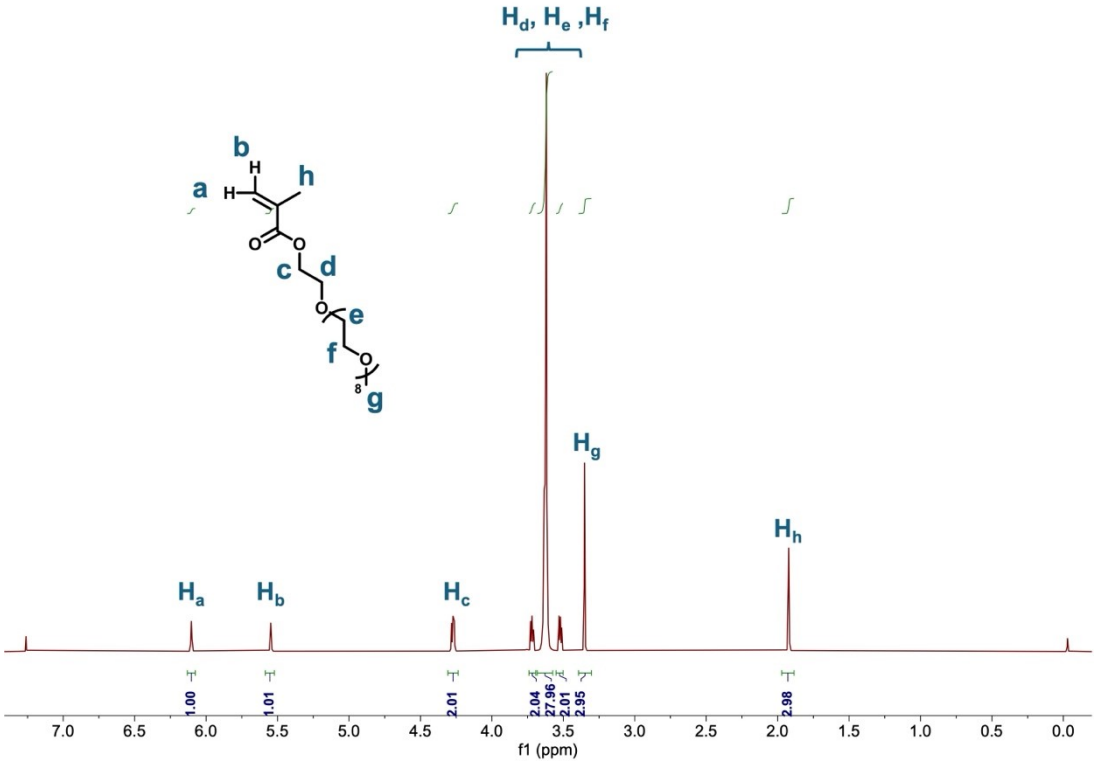

Figure S24. ^{1}H NMR spectrum of OEGMA in $CDCl_3$

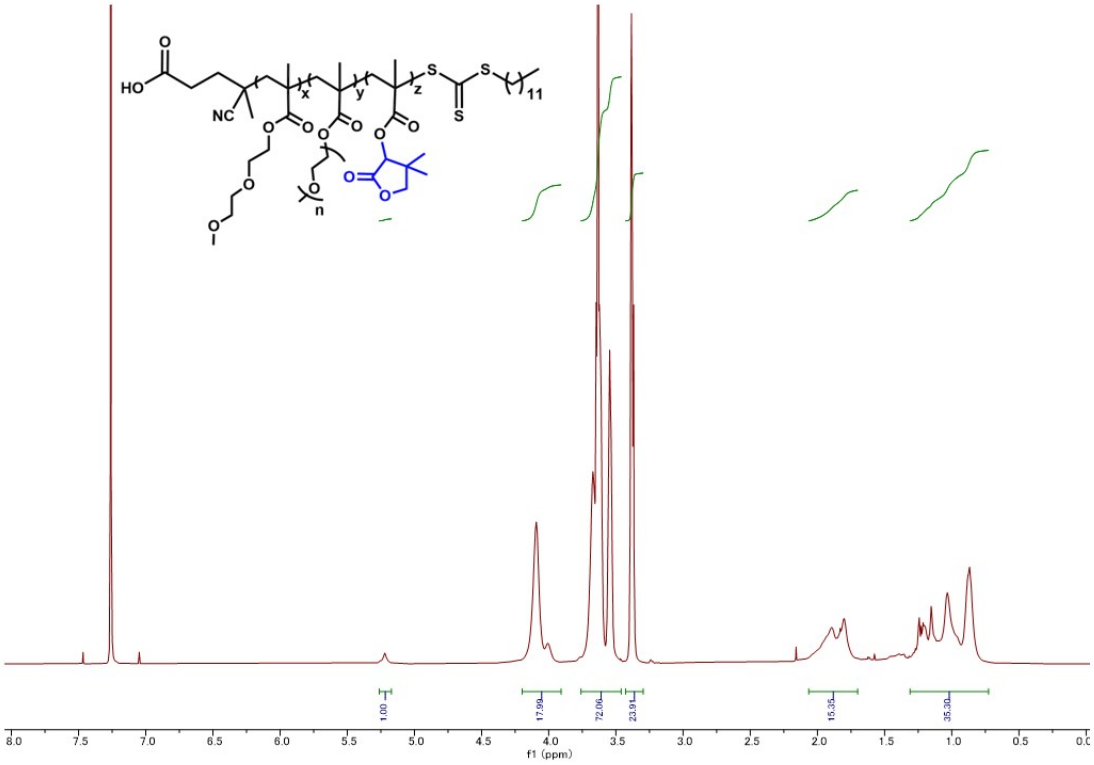

Figure S25. ^{1}H NMR of P(DEGMA$_{80}$-*co*-OEGMA$_{10}$-*co*-LMA$_{10}$) in $CDCl_3$

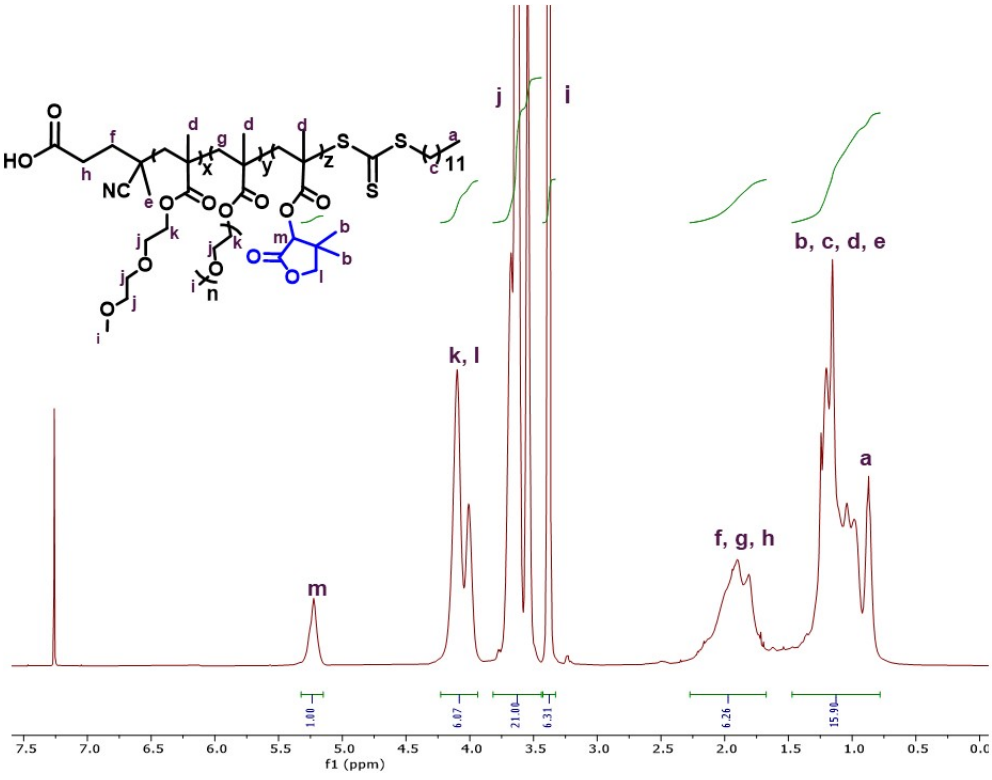

Figure S26. ^{1}H NMR spectrum of P(DEGMA$_{60}$-*co*-OEGMA$_{10}$-*co*-LMA$_{30}$) in $CDCl_3$

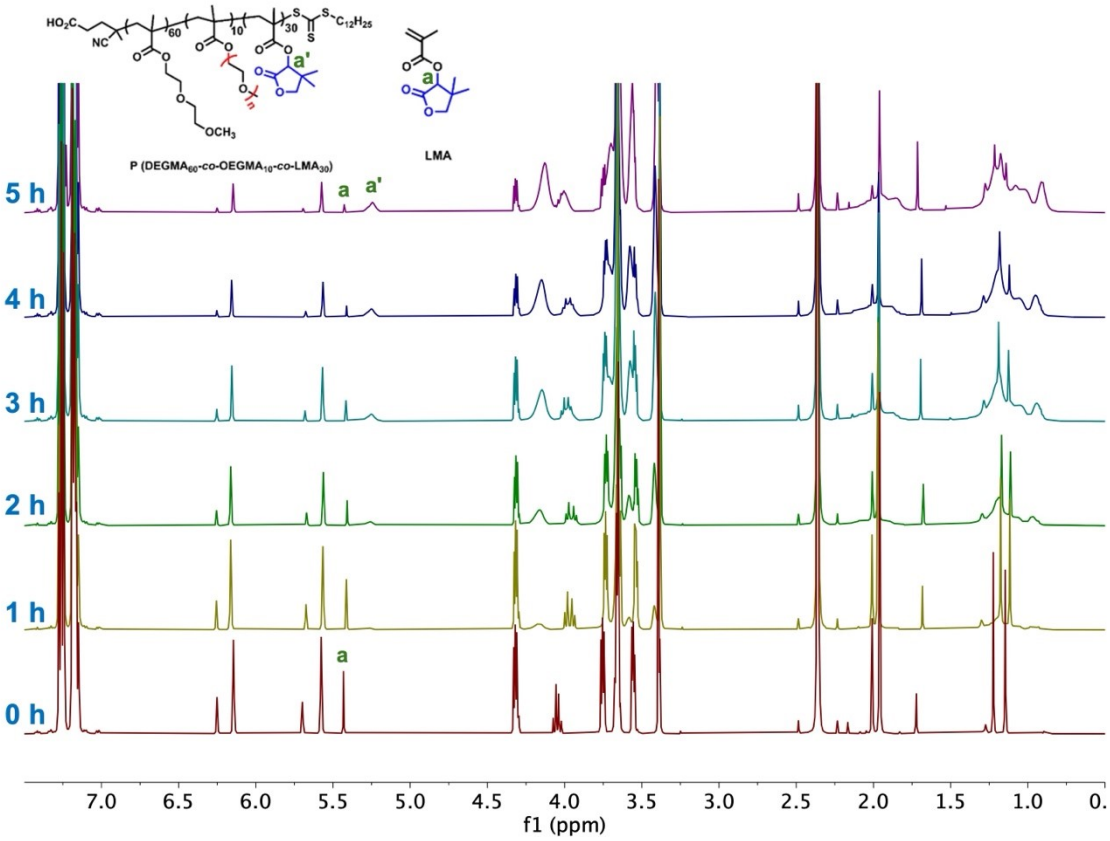

Figure S27. Overlayed ^{1}H NMR spectra of P(DEGMA$_{60}$-*co*-OEGMA$_{10}$-*co*-LMA$_{30}$) in $CDCl_3$ showing monomer conversion as a function of time

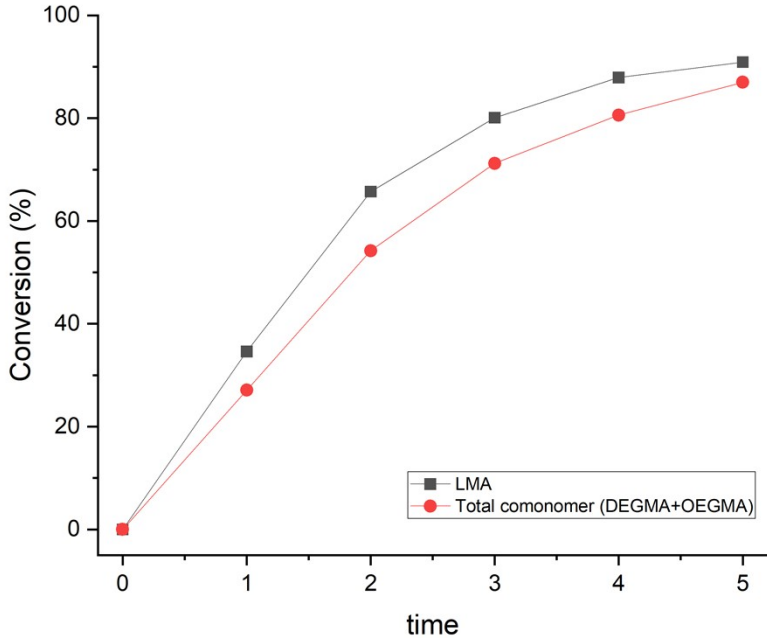

Figure S28. LMA conversion vs total DEGMA+OEGMA comonomer conversion as a function of time for P(DEGMA$_{60}$-co-OEGMA$_{10}$-co-LMA$_{30}$)

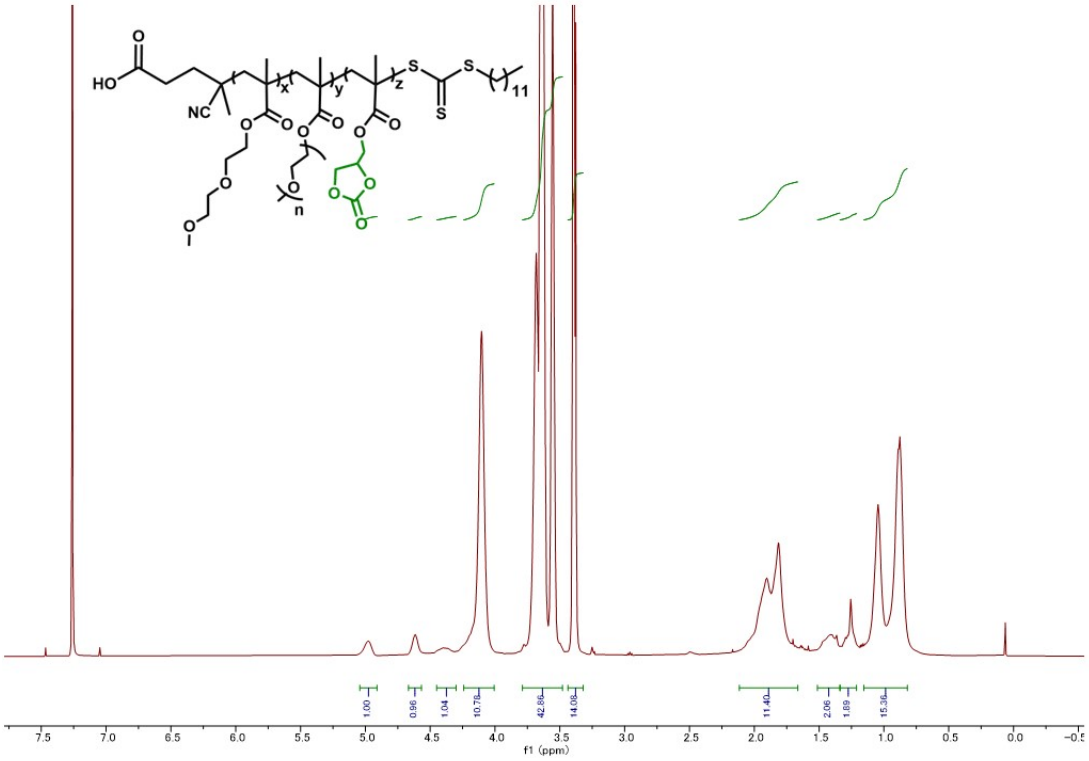

Figure S29. ^{1}H NMR spectrum of P(DEGMA$_{80}$-*co*-OEGMA$_{10}$-*co*-C^{2}MA$_{10}$) in $CDCl_3$

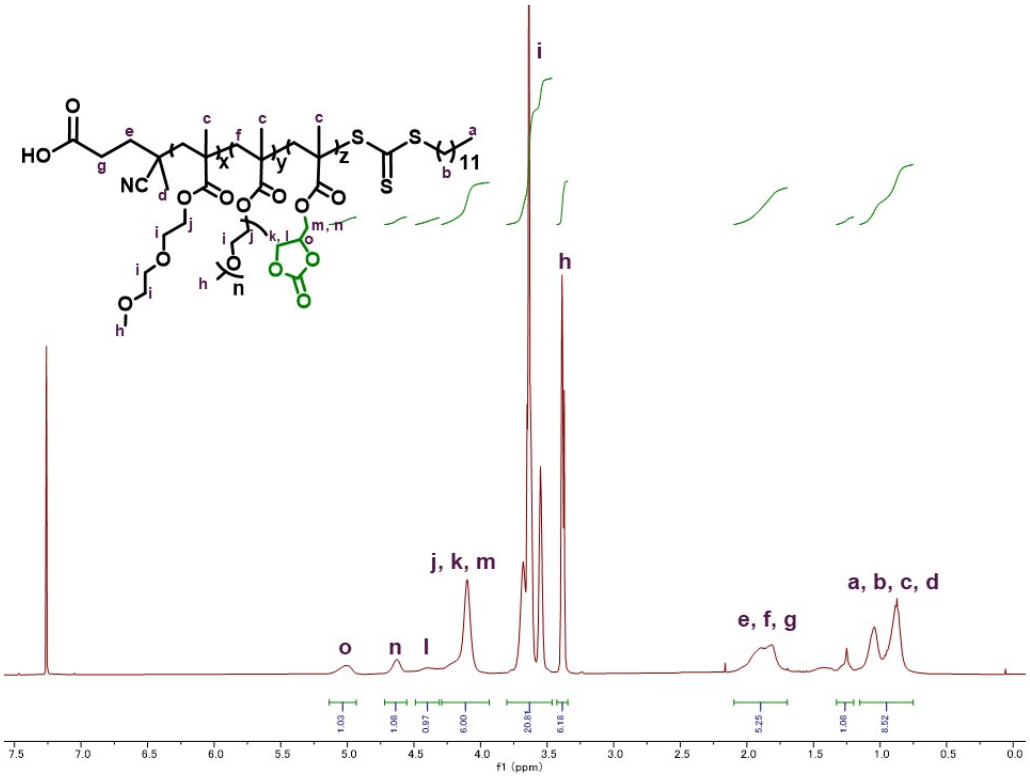

Figure S30. ^{1}H NMR spectrum of P(DEGMA$_{60}$-*co*-OEGMA$_{10}$-*co*-C^{2}MA$_{30}$) in $CDCl_3$

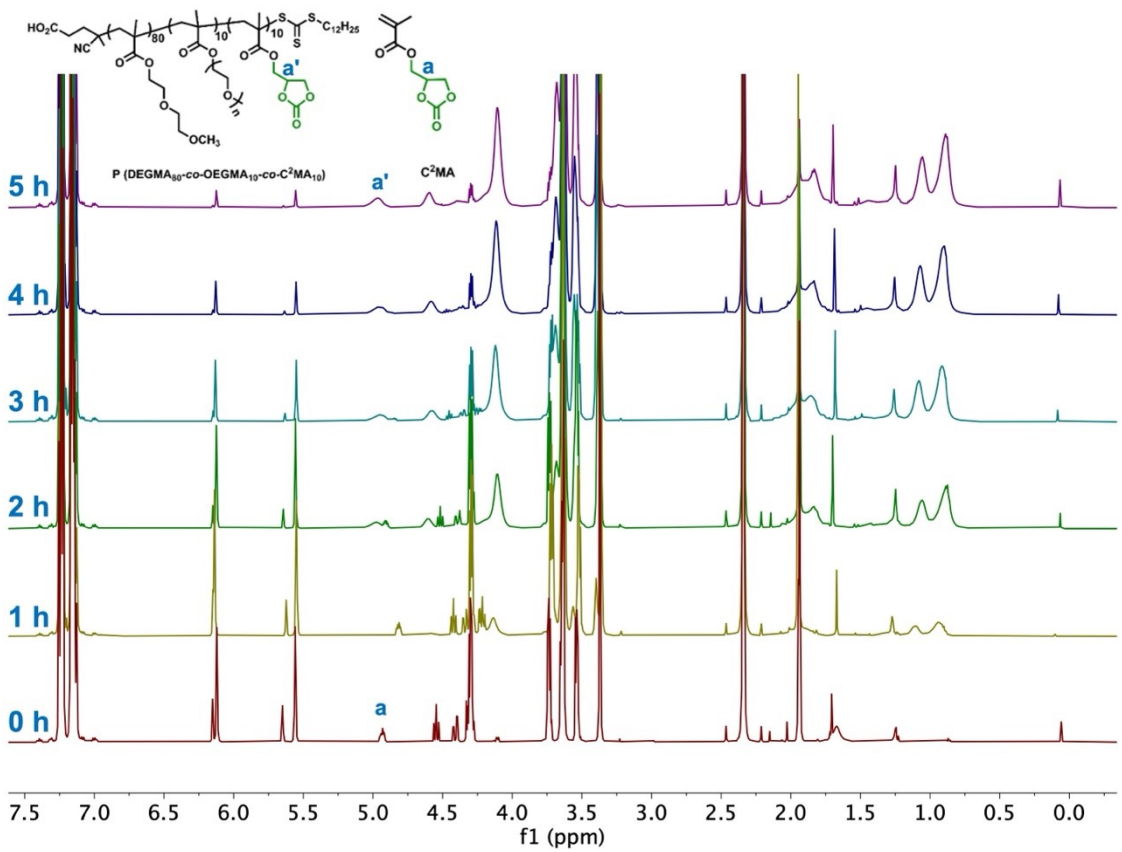

Figure S31. Overlayed ^{1}H NMR spectra of P(DEGMA$_{60}$-*co*-OEGMA$_{10}$-*co*-C^{2}MA$_{30}$) in $CDCl_3$ showing monomer conversion as a function of time

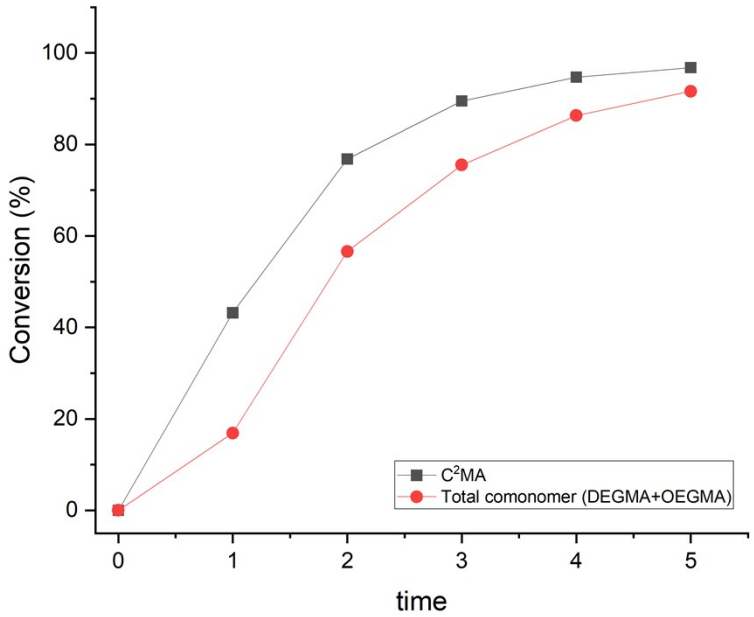

Figure S32. C^{2}MA conversion vs total DEGMA+OEGMA comonomer conversion as a function of time for P(DEGMA$_{60}$-*co*-OEGMA$_{10}$-*co*-C^{2}MA$_{30}$)

Table S5. Time-dependent conversion (%) for all monomers during polymerization.

Time	LMA:(total comonomer)	Unreacted LMA mol%	LMA %conversion	Total comonomer %conversion
0	0.33	25	-	-
1 h	0.289	22.4	34.6	27.1
2 h	0.234	18.9	65.7	54.2
3 h	0.198	16.5	80.1	71.2
4 h	0.19	15.9	87.9	80.6
5 h	0.205	17	90.9	87
Time	**C^2MA:(total comonomer)**	**Unreacted C^2MA mol%**	**C^2MA %conversion**	**Total comonomer %conversion**
0	0.382	27.6	-	-
1 h	0.261	20.7	43.2	16.9
2 h	0.204	16.9	76.8	56.6
3 h	0.164	14.1	89.5	75.5
4 h	0.147	12.8	94.7	86.3
5 h	0.143	12.5	96.8	91.6

12.2. Hydrolysis study using ^1H NMR spectroscopy

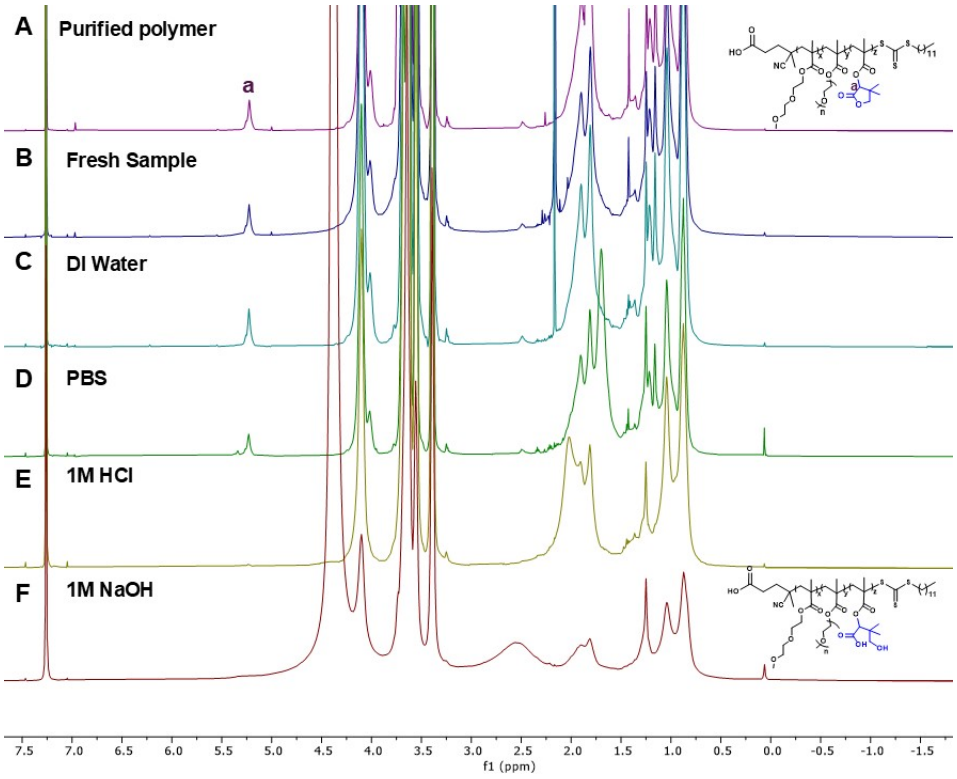

Figure S33. ^1H NMR spectra of P(DEGMA$_{80}$-*co*-OEGMA$_{10}$-*co*-LMA$_{10}$); A) purified polymer, B) fresh sample (the polymer was dissolved in DI water (1wt%) and lyophilized immediately, C) after 7 days in DI water at 50 °C, D) after 7 days in PBS at 50 °C, E) after 7 days in 1 M HCl at 50 °C, F) after being 7 days in 1 M NaOH at 50 °C.

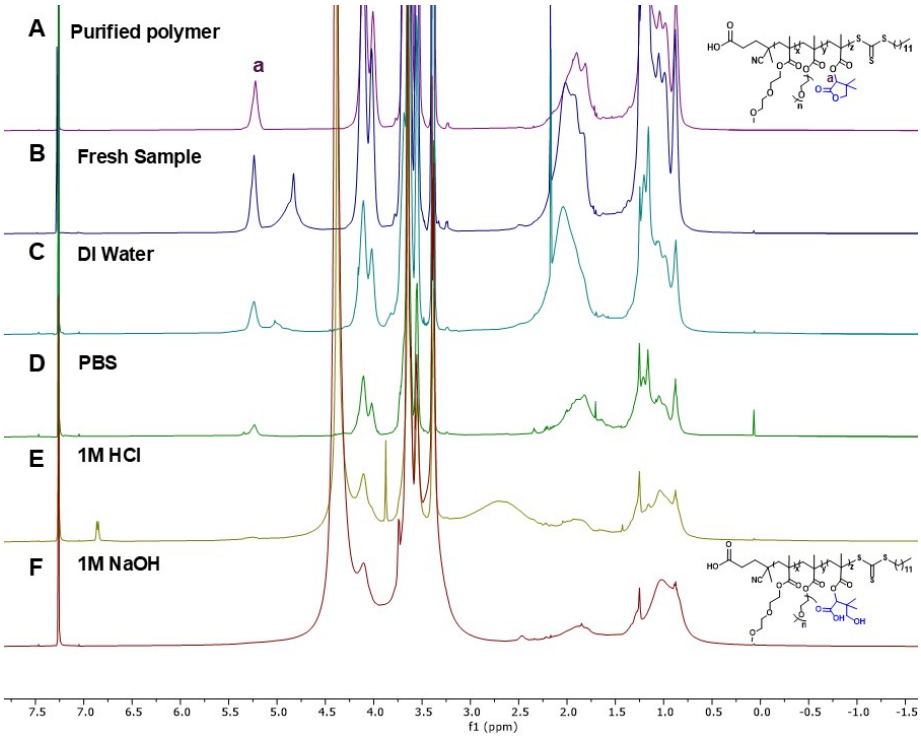

Figure S34. ^{1}H NMR spectra of P(DEGMA$_{60}$-*co*-OEGMA$_{10}$-*co*-LMA$_{30}$); A) purified polymer, B) fresh sample (the polymer was dissolved in DI water (1wt%) and lyophilized immediately, C) after 7 days in DI water at 50 °C, D) after 7 days in PBS at 50 °C, E) after 7 days in 1 M HCl at 50 °C, F) after being 7 days in 1 M NaOH at 50 °C

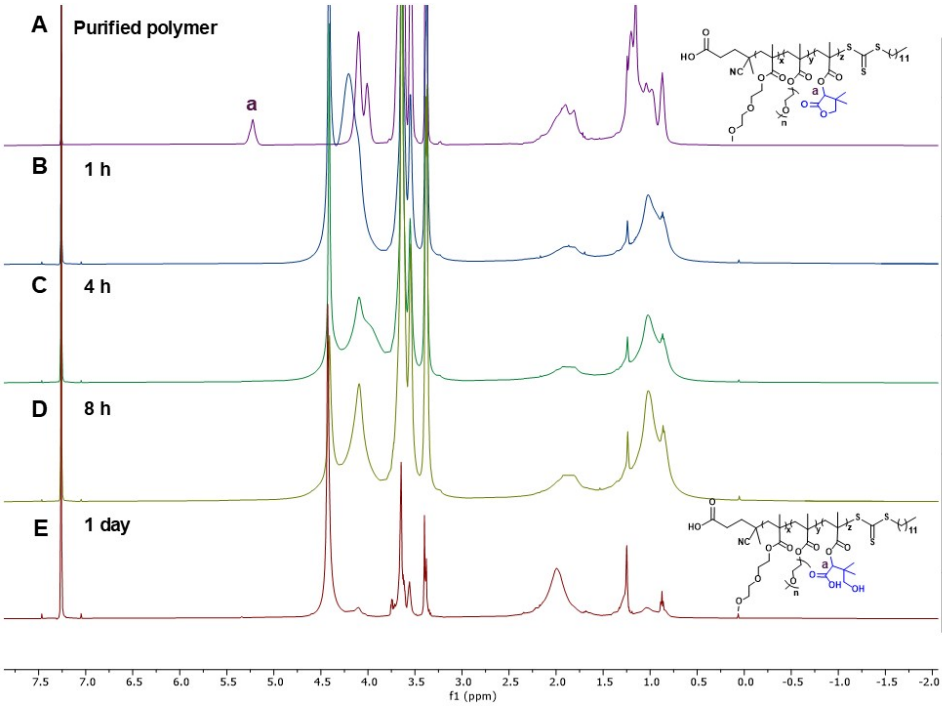

Figure S35.^{1}H NMR spectra of kinetic study of P(DEGMA$_{60}$-*co*-OEGMA$_{10}$-*co*-LMA$_{30}$); A) purified polymer, B) after being 1 h in 1 M NaOH at 50 °C, C) after being 4 h in 1 M NaOH at 50 °C, D) after being 8 h in 1 M NaOH at 50 °C, E) after being 1 day in 1 M NaOH at 50 °C

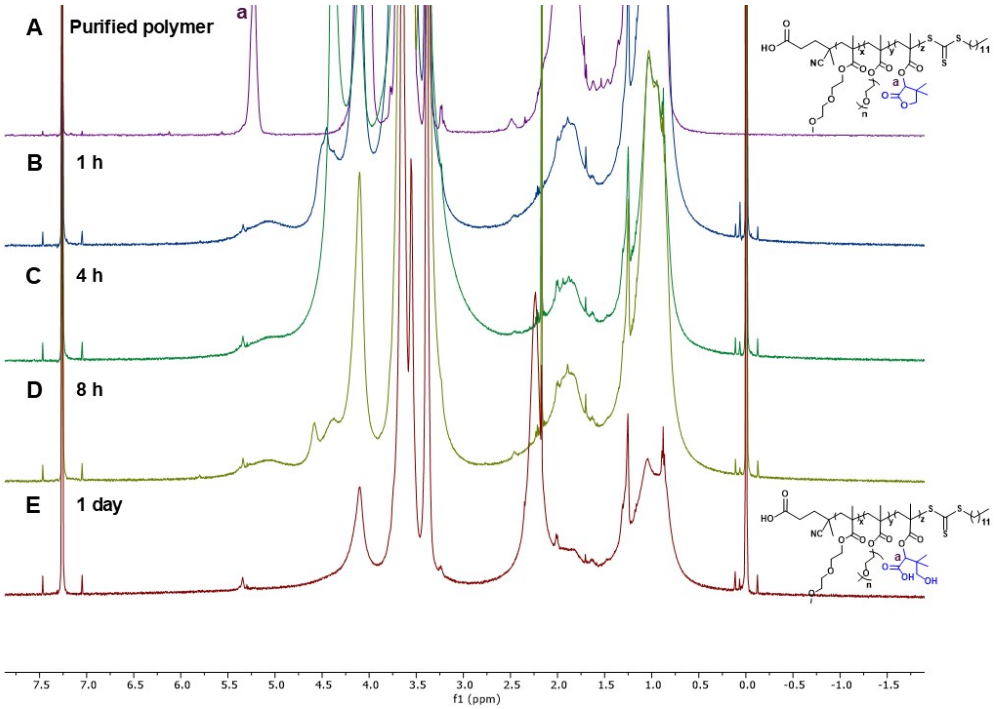

Figure S36. ^{1}H NMR spectra of kinetic study of P(DEGMA$_{60}$-*co*-OEGMA$_{10}$-*co*-LMA$_{30}$); A) purified polymer, B) after being 1 h in 0.5 M NaOH at 25 °C, C) after being 4 h in 0.5 M NaOH at 25 °C, D) after being 8 h in 0.5 M NaOH at 20 °C, E) after being 1 day in 0.5 M NaOH at 25 °C

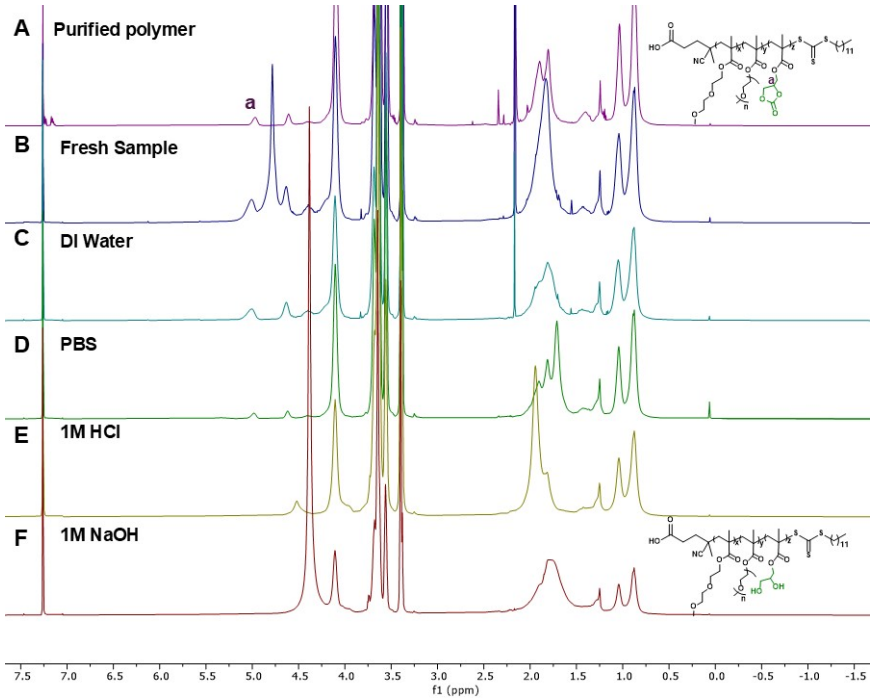

Figure S37. ^{1}H NMR spectra of P(DEGMA$_{80}$-*co*-OEGMA$_{10}$-*co*-C^{2}MA$_{10}$); A) purified polymer, B) fresh sample (the polymer was dissolved in DI water (1wt%) and lyophilized immediately, C) after 7 days in DI water at 50 °C, D) after 7 days in PBS at 50 °C, E) after 7 days in 1 M HCl at 50 °C, F) after being 7 days in 1 M NaOH at 50 °C

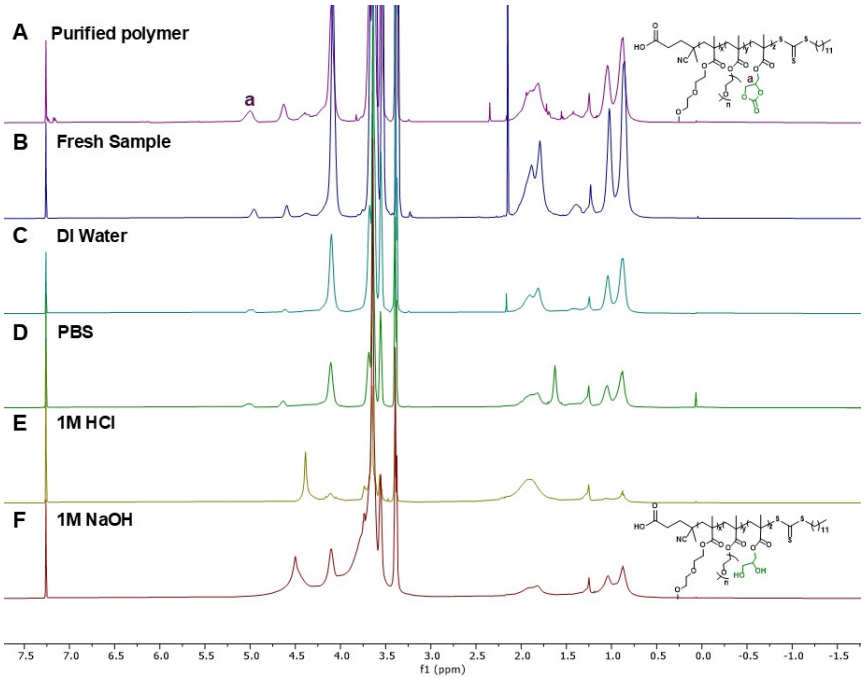

Figure S38. ^{1}H NMR spectra of P(DEGMA$_{60}$-*co*-OEGMA$_{10}$-*co*-C^{2}MA$_{30}$); A) purified polymer, B) fresh sample (the polymer was dissolved in DI water (1wt%) and lyophilized immediately, C) after 7 days in DI water at 50 °C, D) after 7 days in PBS at 50 °C, E) after 7 days in 1 M HCl at 50 °C, F) after being 7 days in 1 M NaOH at 50 °C

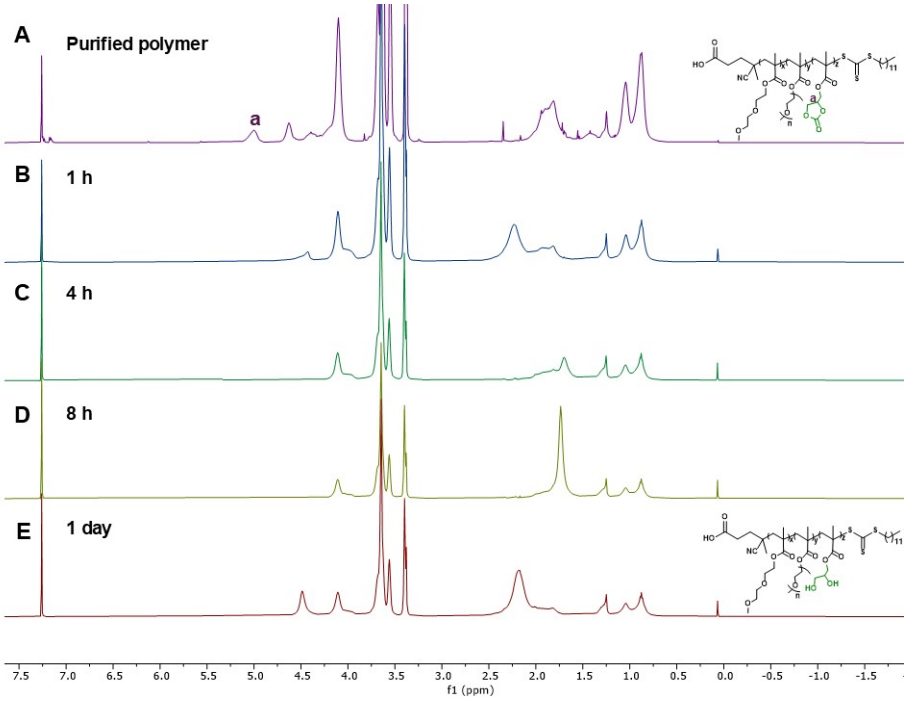

Figure S39. ^{1}H NMR spectra of kinetic study of P(DEGMA$_{60}$-*co*-OEGMA$_{10}$-*co*-C^{2}MA$_{30}$); ^{1}H NMR Spectra of kinetic study of P(DEGMA$_{60}$-*co*-OEGMA$_{10}$-*co*-LMA$_{30}$); A) purified polymer, B) after being 1 h in 1 M NaOH at 50 °C, C) after being 4 h in 1 M NaOH at 50 °C, D) after being 8 h in 1 M NaOH at 50 °C, E) after being 1 day in 1 M NaOH at 50 °C

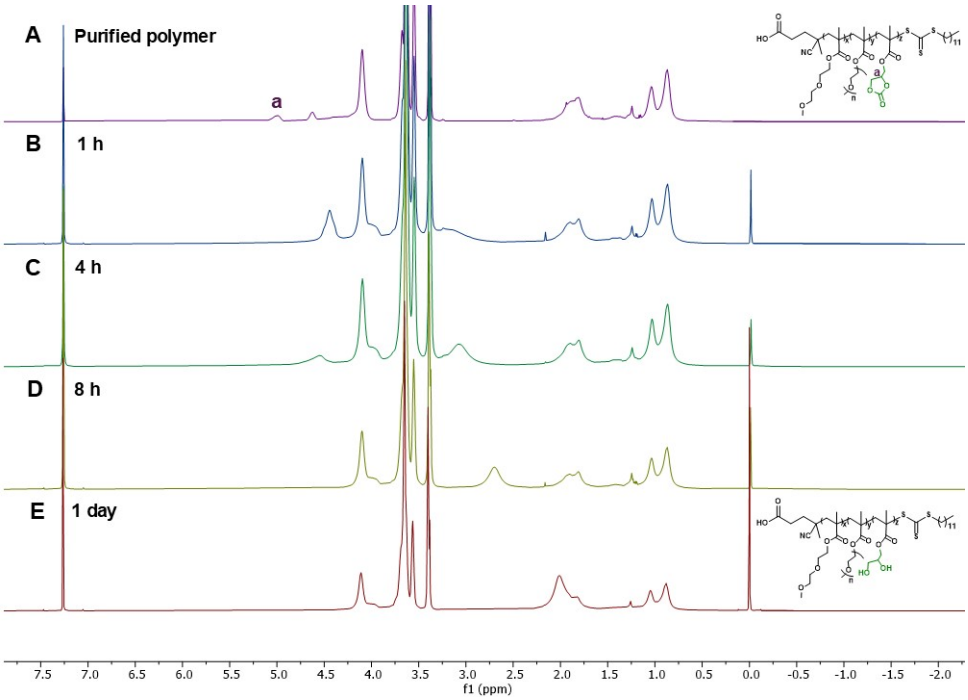

Figure S40. ^{1}H NMR spectra of kinetic study of P(DEGMA$_{60}$-*co*-OEGMA$_{10}$-*co*-C^{2}MA$_{30}$); A) purified polymer, B) after being 1 h in 0.5 M NaOH at 25 °C, C) after being 4 h in 0.5 M NaOH at 25 °C, D) after being 8 h in 0.5 M NaOH at 20 °C, E) after being 1 day in 0.5 M NaOH at 25 °C

12.3. FT-IR spectral analysis

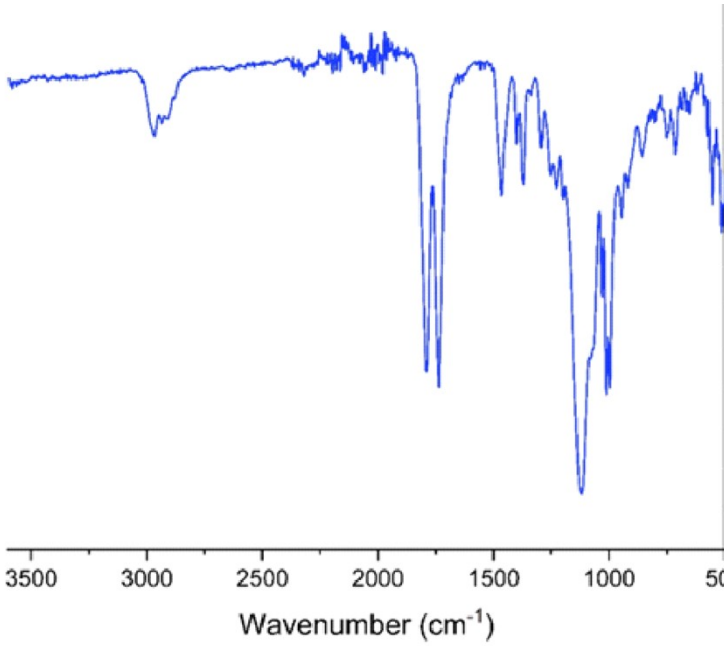

Figure S41. FT-IR spectrum of PLMA

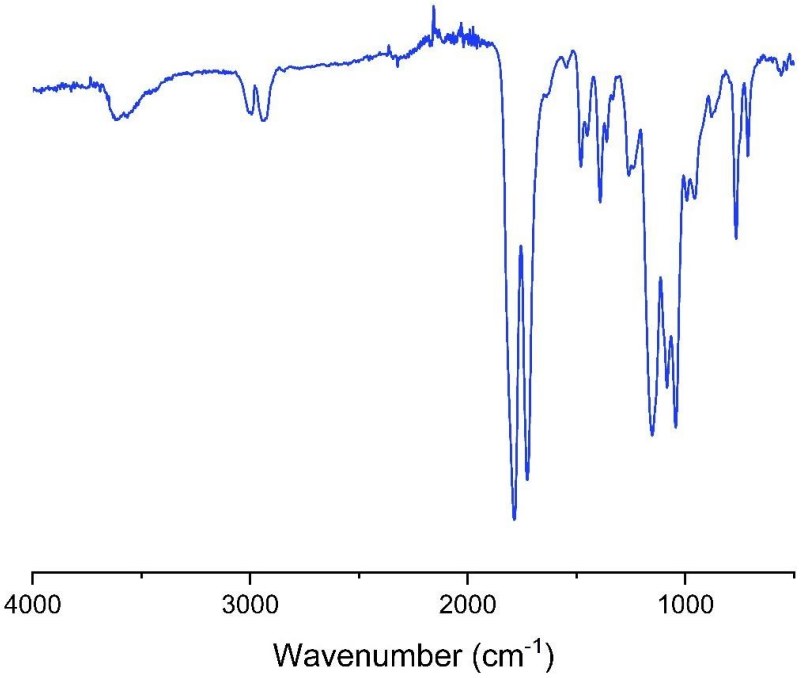

Figure S42. FT-IR spectrum of PC^2MA

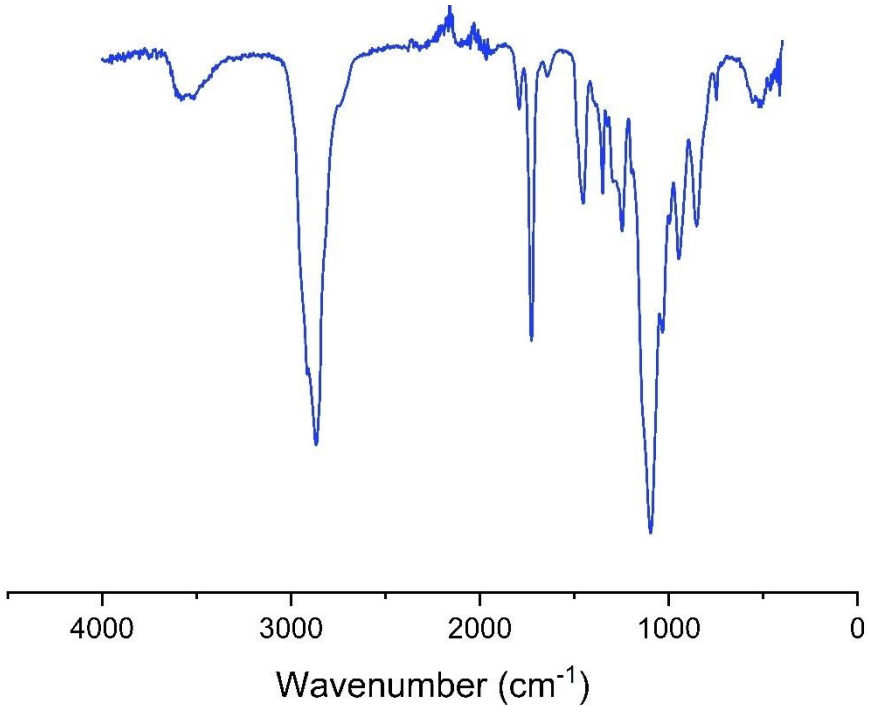

Figure S43. FT-IR spectrum of $P(OEGMA_{90}$-*co*-$LMA_{10})$

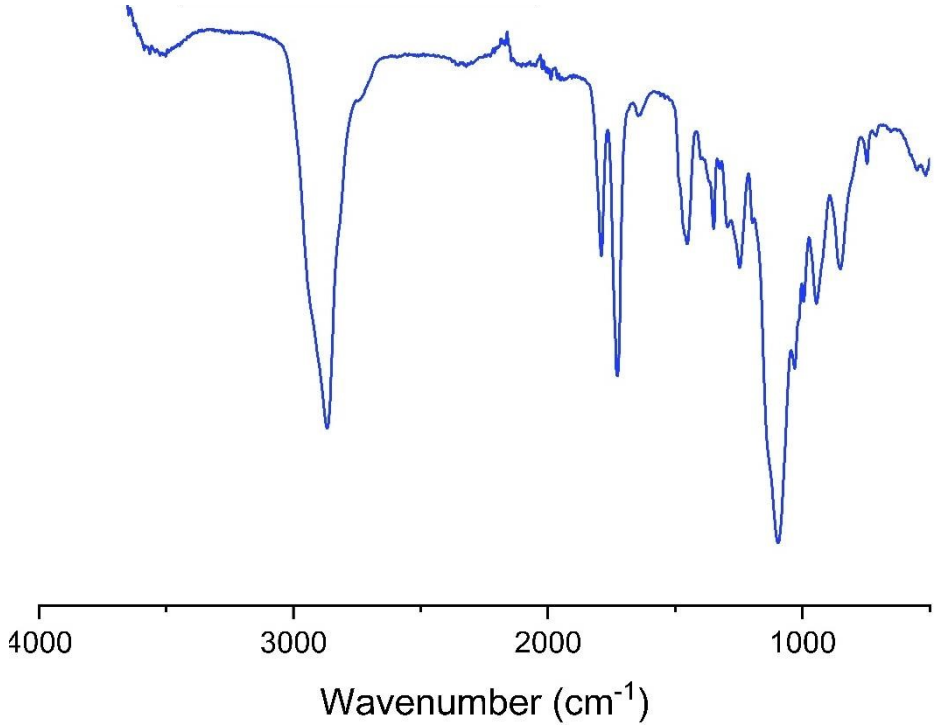

Figure S44. FT-IR spectrum of P(OEGMA$_{70}$-*co*-LMA$_{30}$)

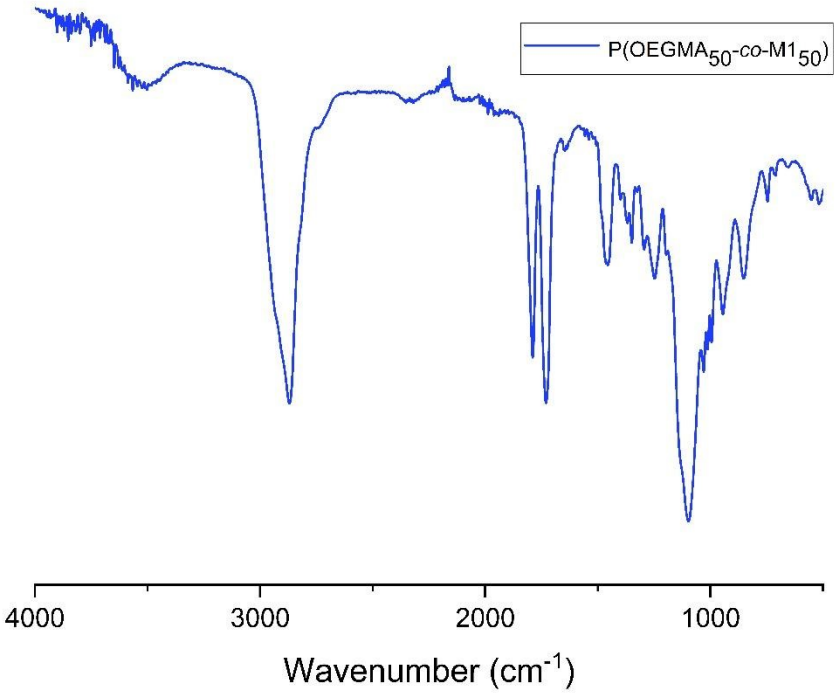

Figure S45. FT-IR spectrum of P(OEGMA$_{50}$-*co*-LMA$_{50}$)

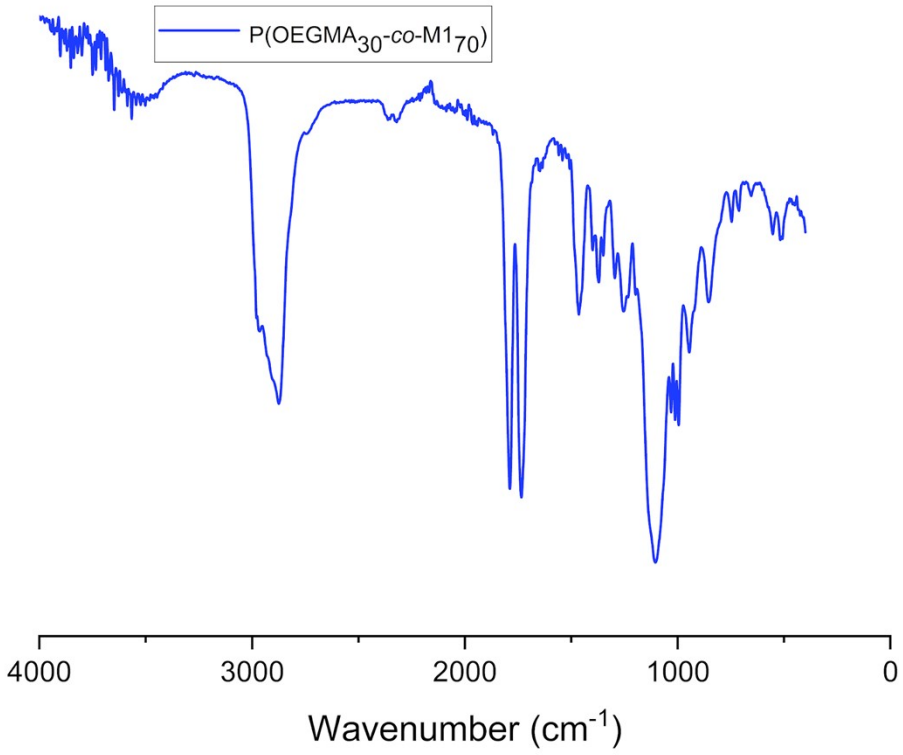

Figure S46. FT-IR spectrum of P(OEGMA$_{30}$-*co*-LMA$_{70}$)

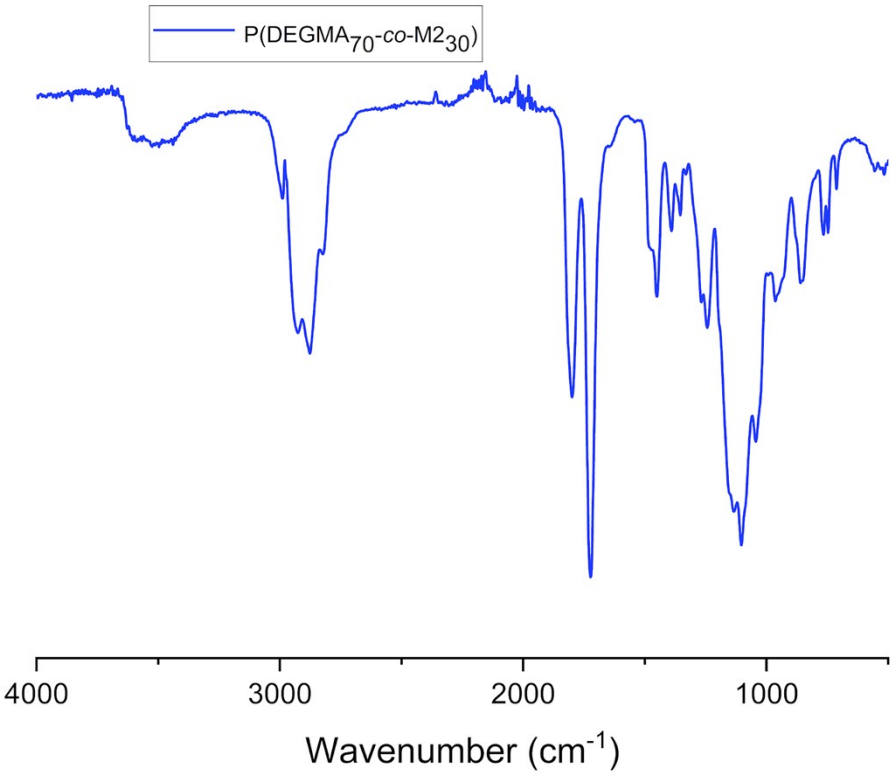

Figure S47. FT-IR spectrum of P(DEGMA$_{70}$-*co*-C^{2}MA$_{30}$)

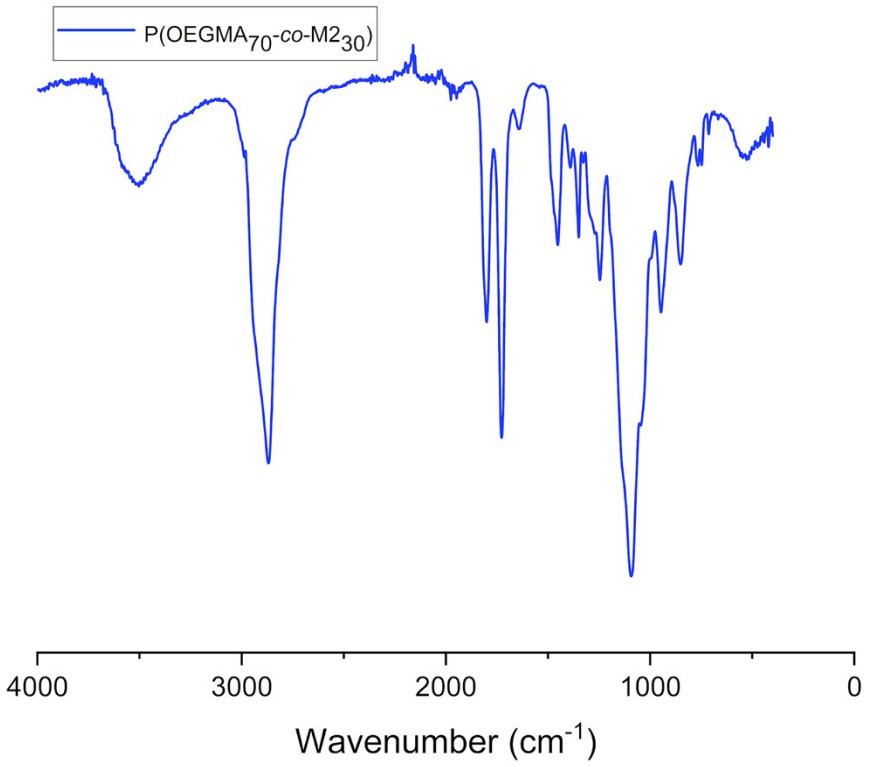

Figure S48. FT-IR spectrum of P(OEGMA$_{70}$-*co*-C^{2}MA$_{30}$)

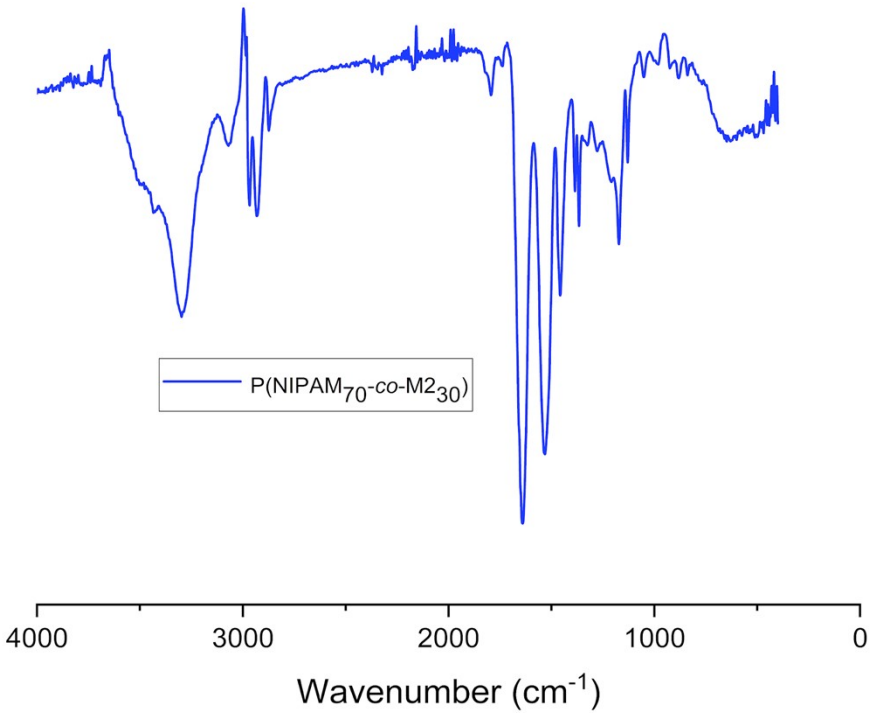

Figure S49. FT-IR spectrum of P(NIPAM$_{70}$-*co*-C^{2}MA$_{30}$)

12.4. Hydrolysis study using FT-IR spectral analysis

FT-IR analyses show a decrease in ester carbonyl absorption and the emergence of hydroxyl bands post-degradation.

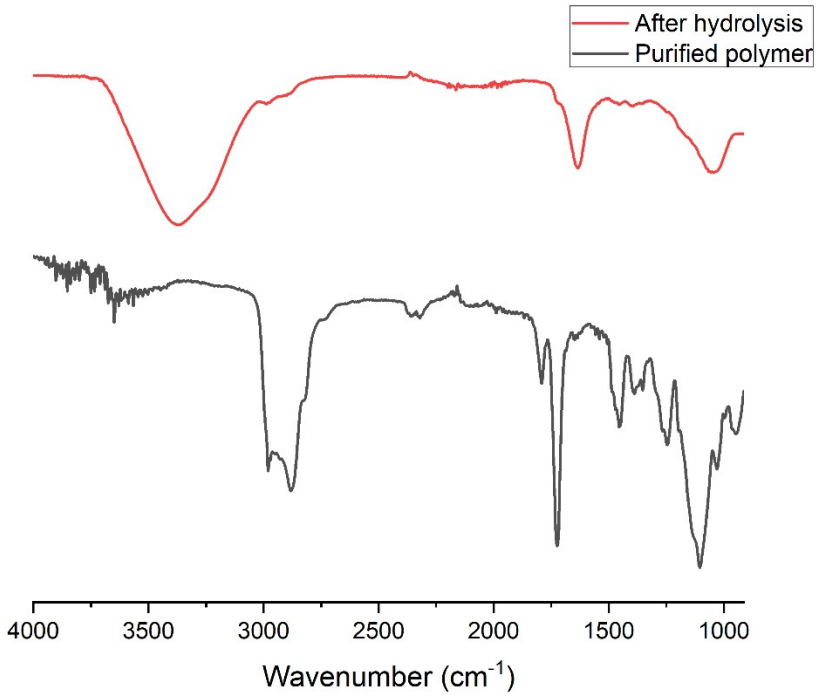

Figure S50. FT-IR Spectra of P(DEGMA$_{80}$-*co*-OEGMA$_{10}$-*co*-LMA$_{10}$) for purified polymer and after hydrolysis in 1M NaOH at 50 °C after 7 days

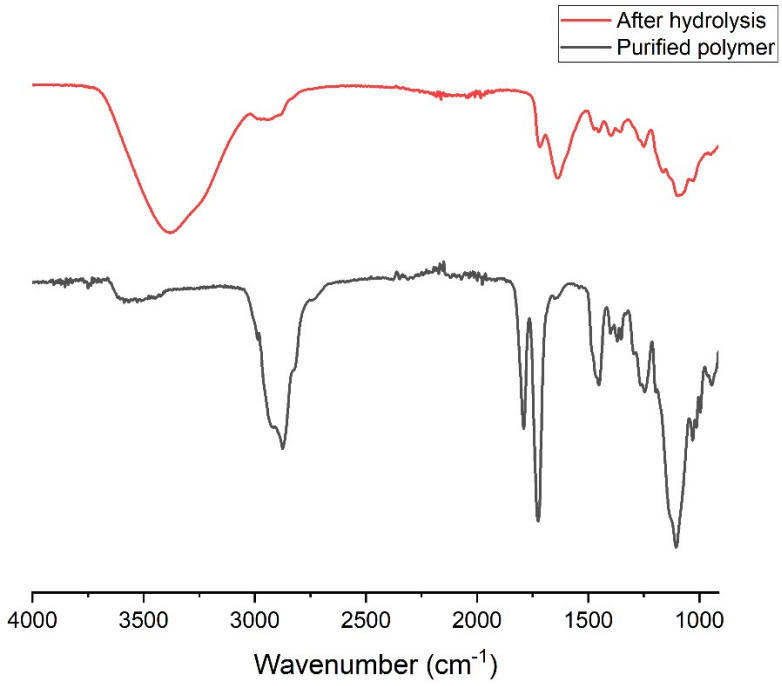

Figure S51. FT-IR Spectra of P(DEGMA$_{60}$-*co*-OEGMA$_{10}$-*co*-LMA$_{30}$) for purified polymer and after hydrolysis in 1M NaOH at 50 °C after 7 days

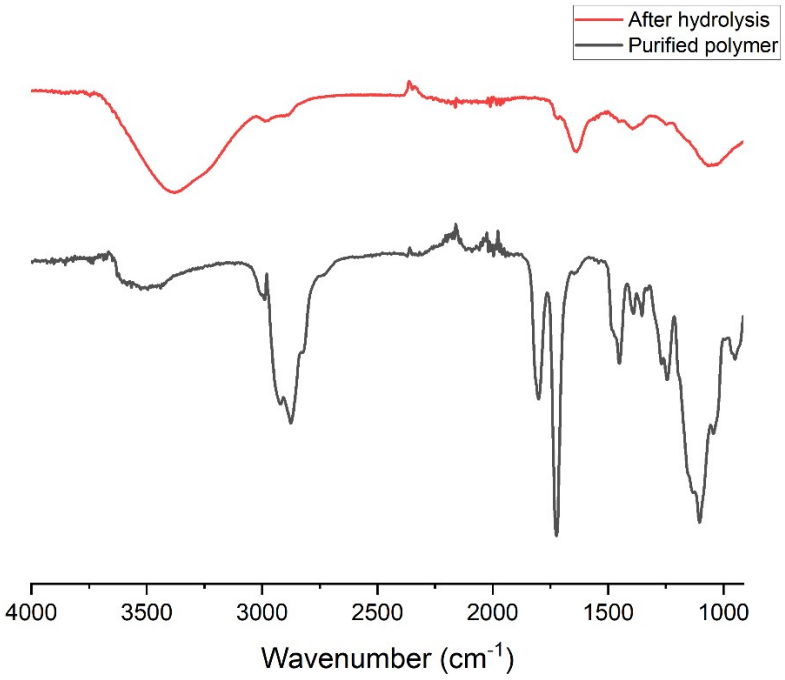

Figure S52. FT-IR Spectra of P(DEGMA$_{80}$-*co*-OEGMA$_{10}$-*co*-C^{2}MA$_{10}$) of purified polymer and after hydrolysis in 1M NaOH at 50 °C after 7 days

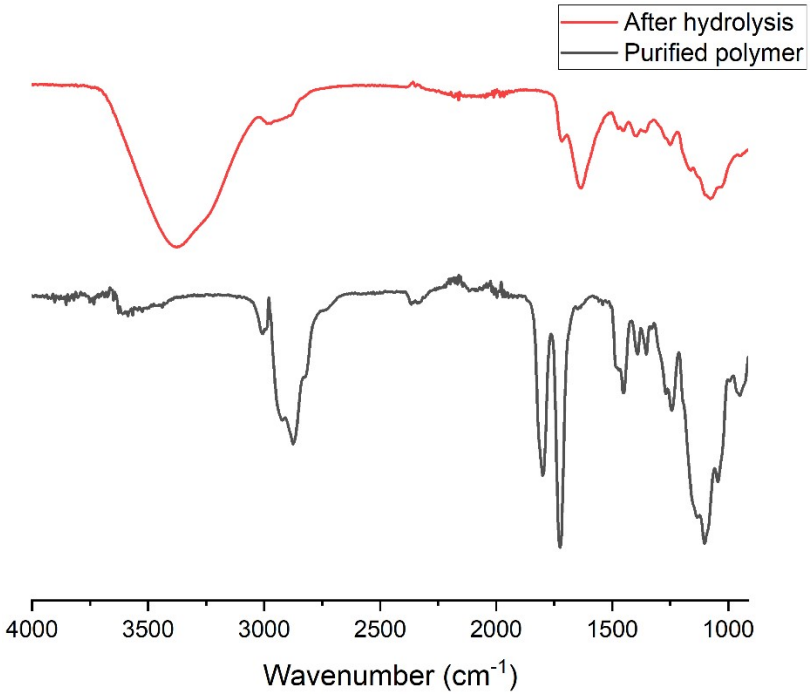

Figure S53. FT-IR Spectra of P(DEGMA$_{60}$-*co*-OEGMA$_{10}$-*co*-C^{2}MA$_{30}$) of purified polymer and after hydrolysis in 1M NaOH at 50 °C after 7 days

12.5. Thermal analysis

12.5A. TGA Curves

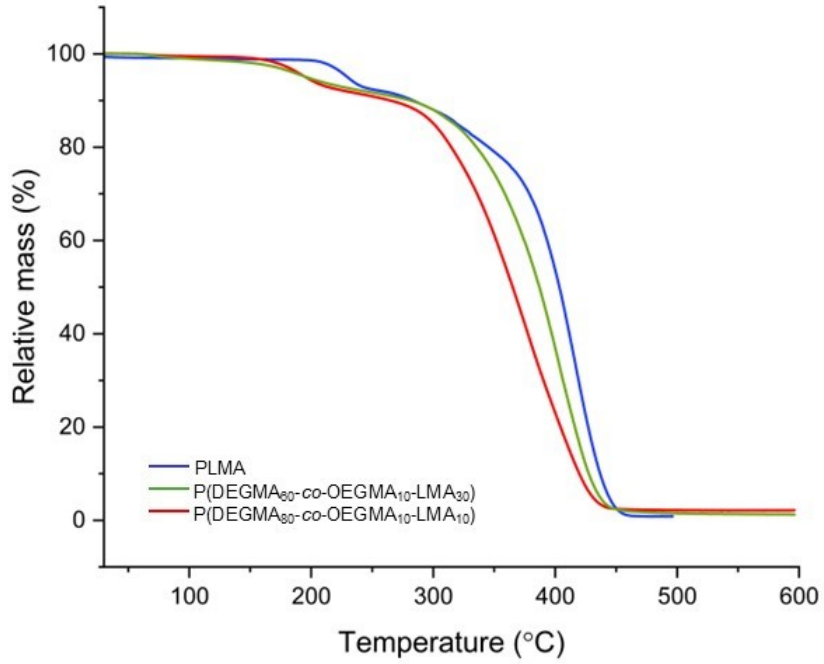

Figure S54. TGA curves of PLMA ($T_{d5\%}$ = 229 °C), P(DEGMA$_{80}$-*co*-OEGMA$_{10}$-*co*-LMA$_{10}$) ($T_{d5\%}$ = 196 °C), and P(DEGMA$_{60}$-co-OEGMA$_{10}$-co-LMA$_{30}$) ($T_{d5\%}$ = 195 °C)

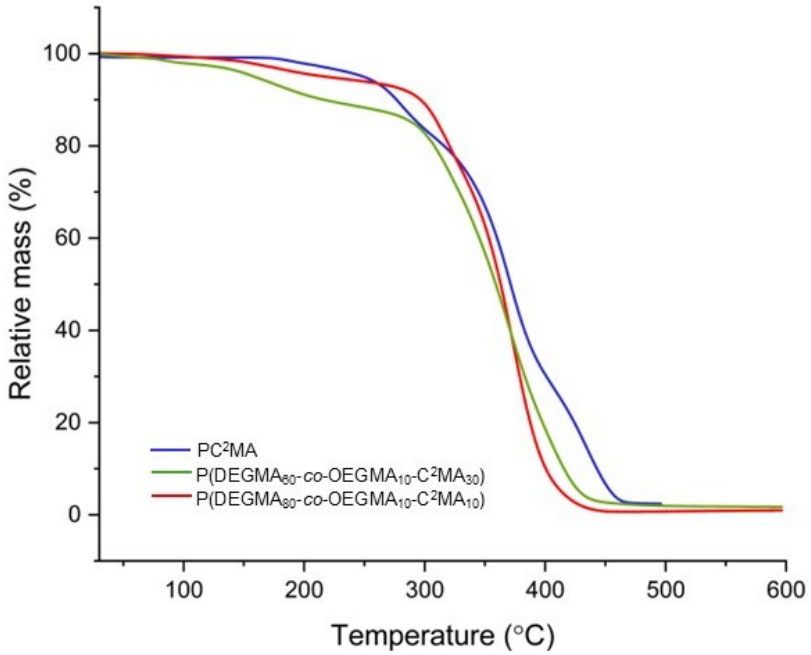

Figure S55. TGA curve of PC^{2}MA ($T_{d5\%}$ = 249 °C), P(DEGMA$_{80}$-*co*-OEGMA$_{10}$-*co*-C^{2}MA$_{10}$) ($T_{d5\%}$ = 160 °C), and P(DEGMA$_{60}$-*co*-OEGMA$_{10}$-*co*-C^{2}MA$_{30}$) ($T_{d5\%}$ = 205 °C)

12.5B. DSC Curves

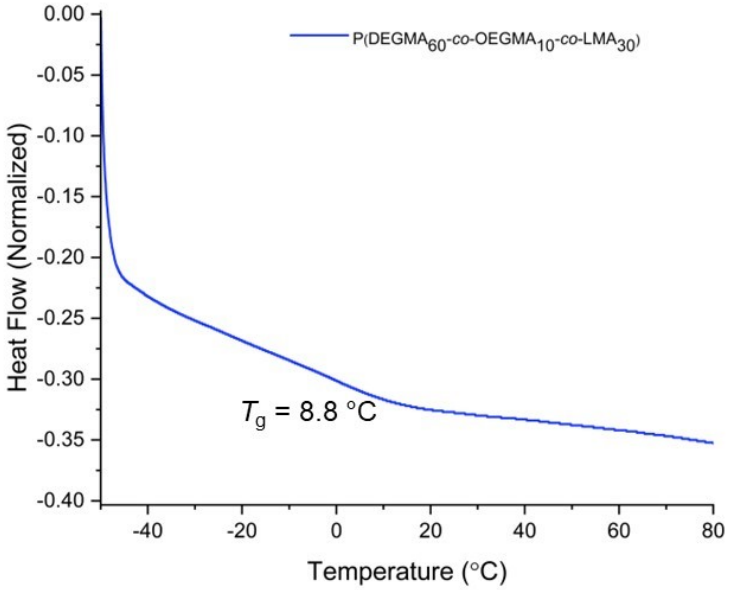

Figure S56. DSC curve of P(DEGMA$_{60}$-*co*-OEGMA$_{10}$-*co*-LMA$_{30}$)

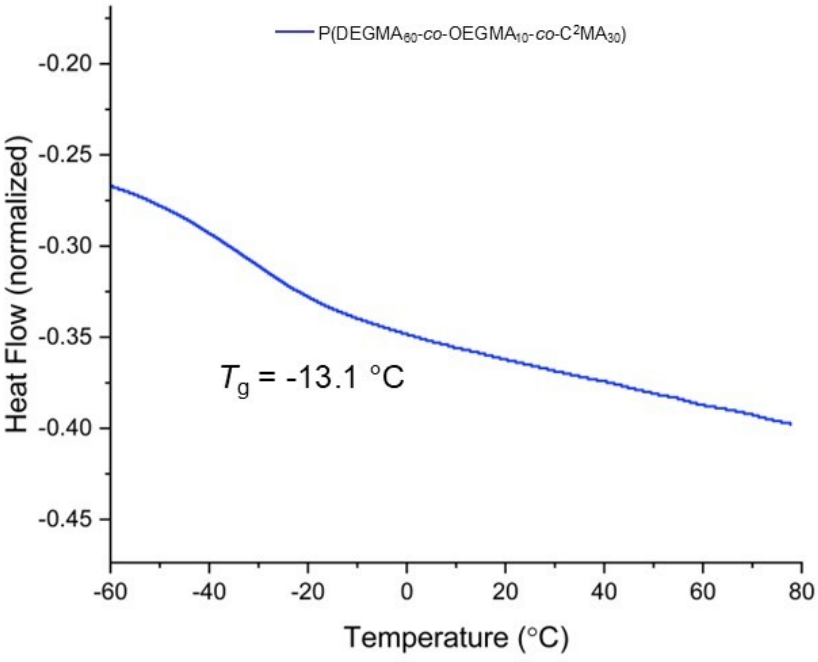

Figure S57. DSC curve of P(DEGMA$_{60}$-*co*-OEGMA$_{10}$-*co*-C2MA$_{30}$)

12.6. GPC results for terpolymers

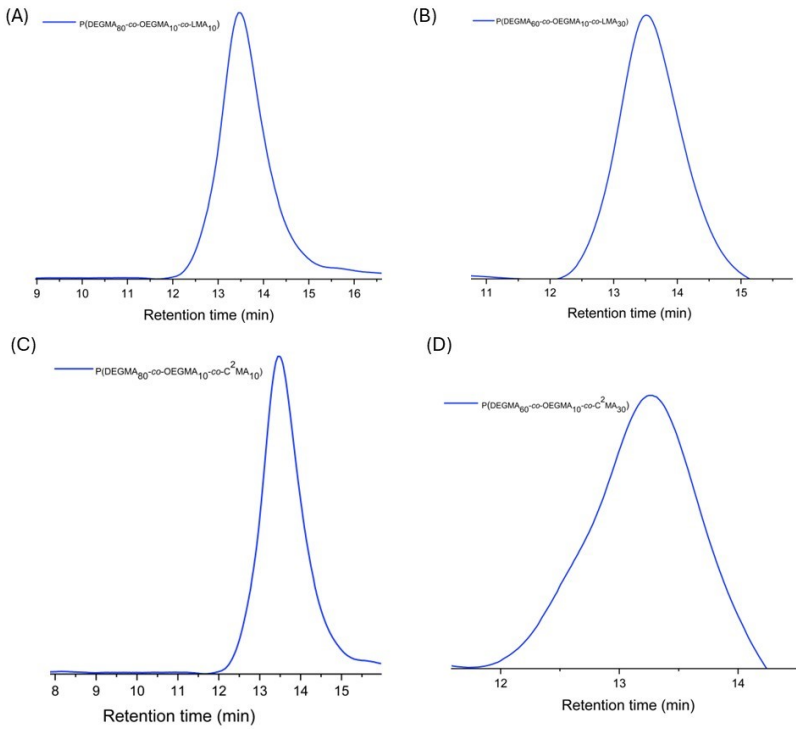

Figure S58. SEC traces of P(DEGMA$_{80}$-LMA-*co*-OEGMA$_{10}$-*co*-LMA$_{10}$) (A), P(DEGMA$_{60}$-*co*-OEGMA$_{10}$-*co*-LMA$_{30}$) (B), P(DEGMA$_{80}$-*co*-OEGMA$_{10}$-*co*-C^{2}MA$_{10}$) (C), P(DEGMA$_{60}$-*co*-OEGMA$_{10}$-*co*-C^{2}MA$_{30}$) (D)

Table S6. Terpolymers SEC results

Polymer	$\frac{dn}{dc}$	PDI	M_n (Da)	M_w (Da)	Theoretical M_w (Da)
P(DEGMA$_{80}$-*co*-LMA$_{10}$-*co*-OEGMA$_{10}$)	0.05	1.18	45,190	53,670	42,757
P(DEGMA$_{60}$-*co*-LMA$_{30}$-*co*-OEGMA$_{10}$)	0.1	1.27	20,490	26,700	43,145
P(DEGMA$_{80}$-*co*-M2$_{10}$-*co*-OEGMA$_{10}$)	0.1	1.25	20,410	22,670	41,646
P(DEGMA$_{60}$-*co*-M2$_{30}$-*co*-OEGMA$_{10}$)	0.1	1.28	42,200	53,990	41,568

12.7. Cloud point determination spectra of polymers using UV-vis spectroscopy

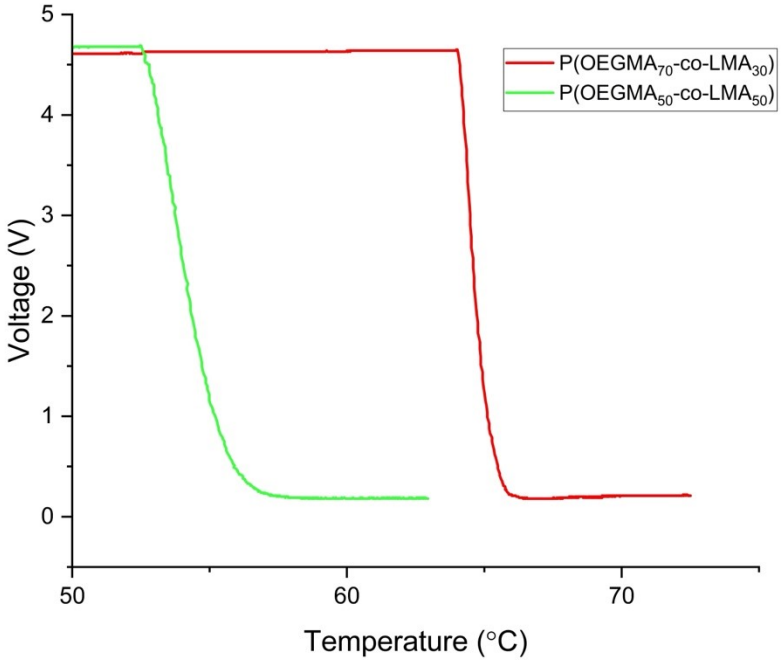

Figure S59. Cloud point temperature of copolymers from LMA monomer

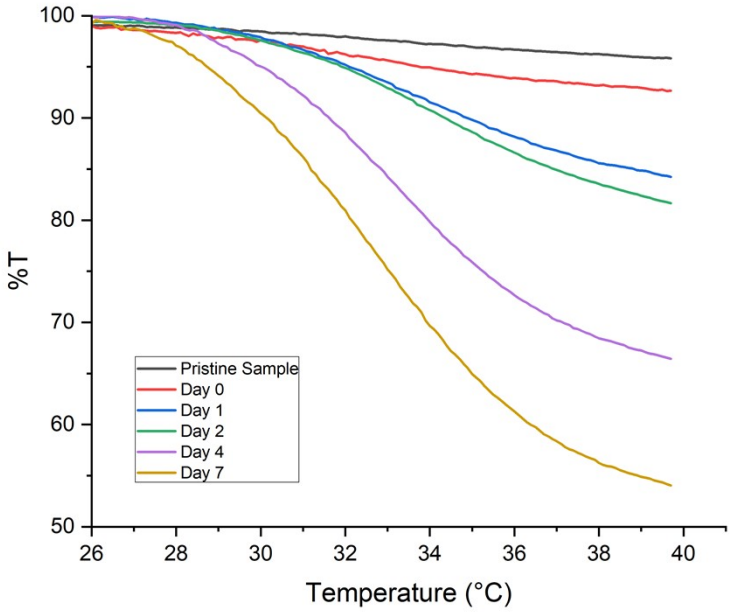

Figure S60. Cloud point measurements of P(DEGMA$_{60}$-*co*-OEGMA$_{10}$-*co*-LMA$_{30}$) in DI water (1 wt%)

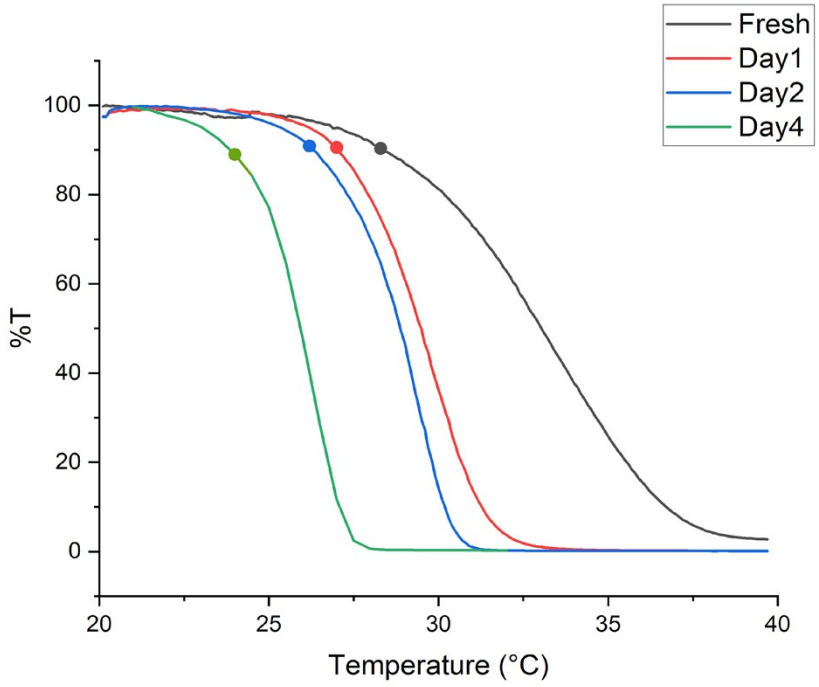

Figure S61. Cloud point measurements of P(DEGMA$_{60}$-*co*-OEGMA$_{10}$-*co*-LMA$_{30}$) in DI water (5 wt%)

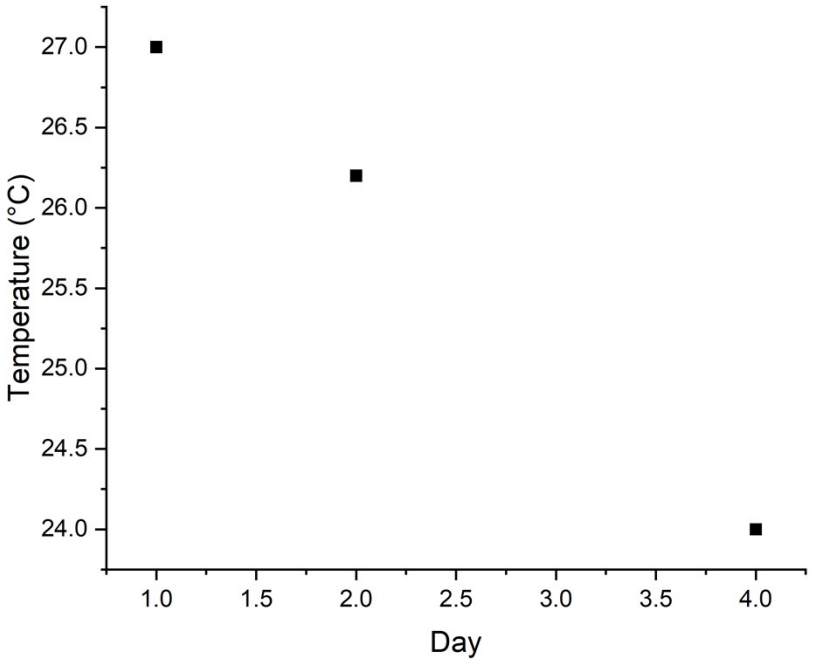

Figure S62. Hydrolysis study of P(DEGMA$_{60}$-*co*-OEGMA$_{10}$-*co*-LMA$_{30}$) in DI water over time (1 wt%)

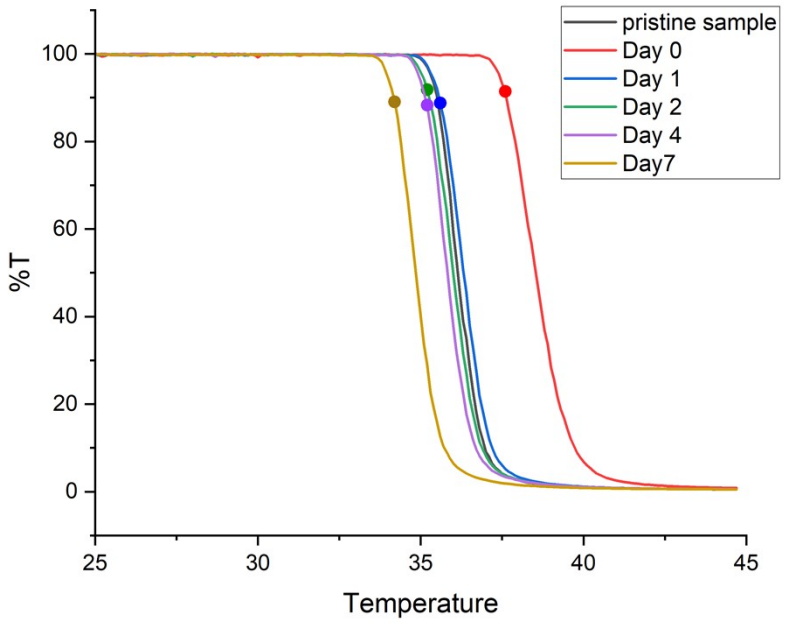

Figure S63. Cloud point measurements of P(DEGMA$_{80}$-*co*-OEGMA$_{10}$-*co*-C^{2}MA$_{10}$) in DI water

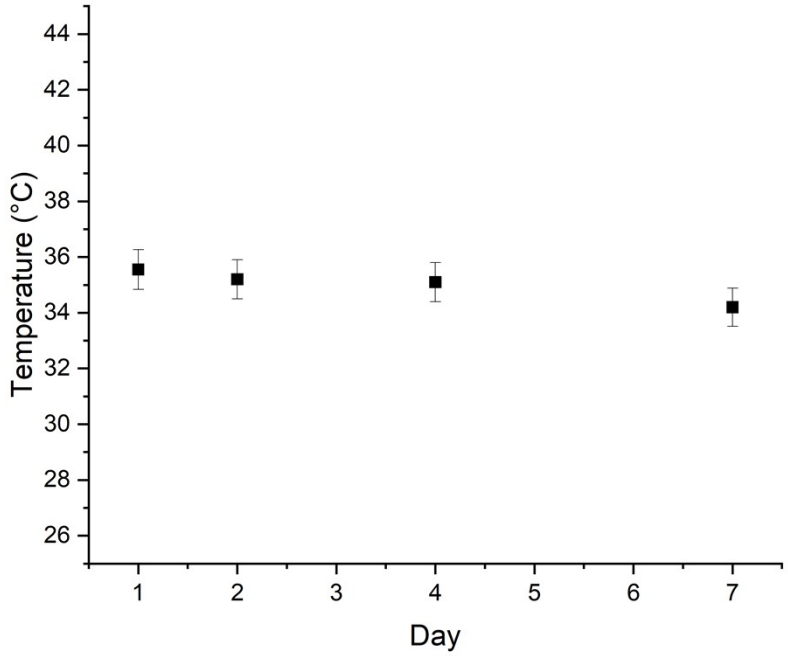

Figure S64. Hydrolysis study of P(DEGMA$_{80}$-*co*-OEGMA$_{10}$-*co*-C^{2}MA$_{10}$) in DI water over time (1 wt%)

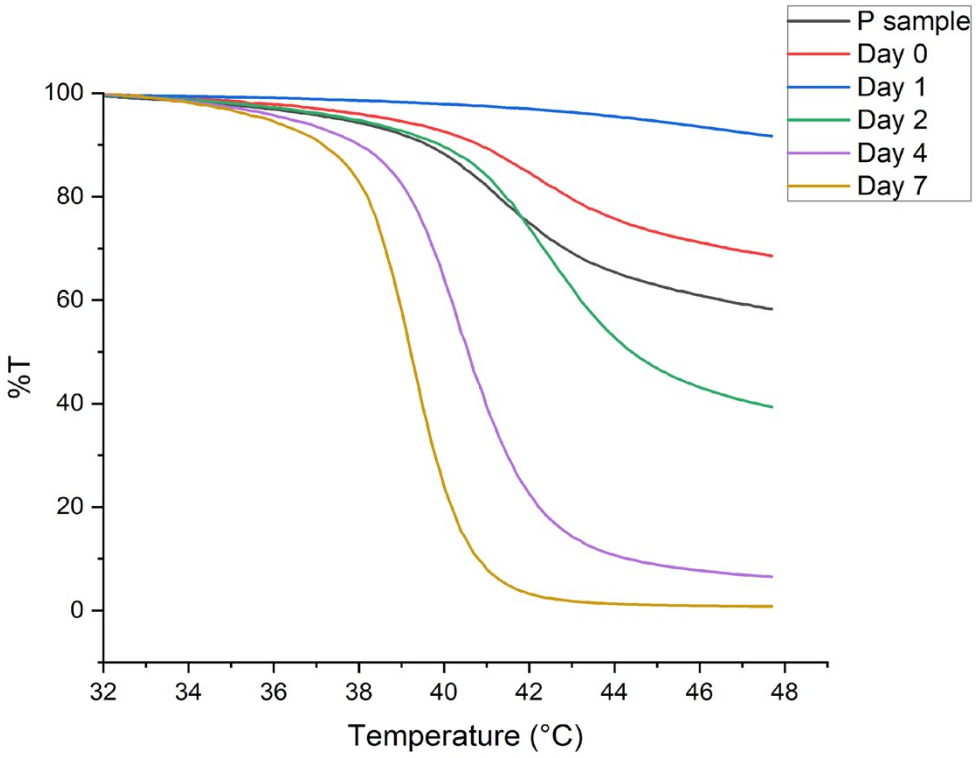

Figure S65. Cloud point measurements of P(DEGMA$_{60}$-*co*-OEGMA$_{10}$-*co*-C^{2}MA$_{30}$) in DI water (1 wt%)

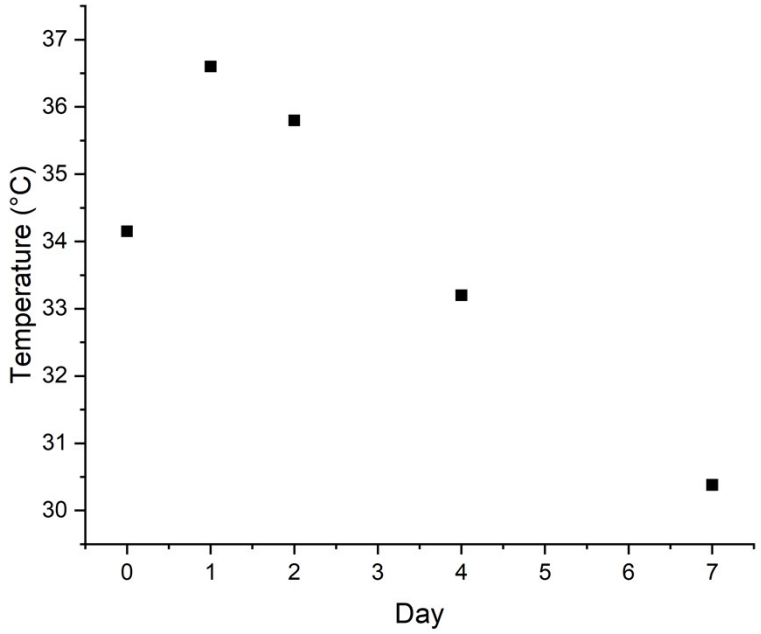

Figure S66. Hydrolysis study of P(DEGMA$_{60}$-*co*-OEGMA$_{10}$-*co*-C^{2}MA$_{30}$) in DI water over time (1 wt%)

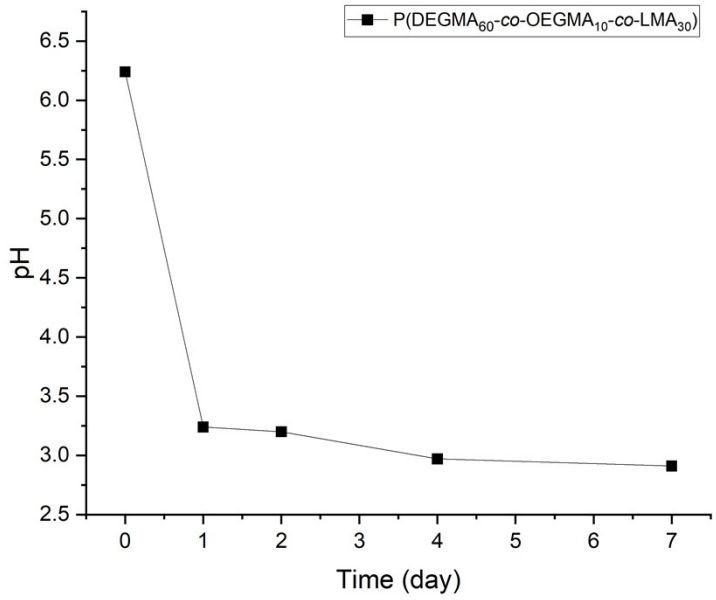

Figure S67. pH changes over time during hydrolysis study

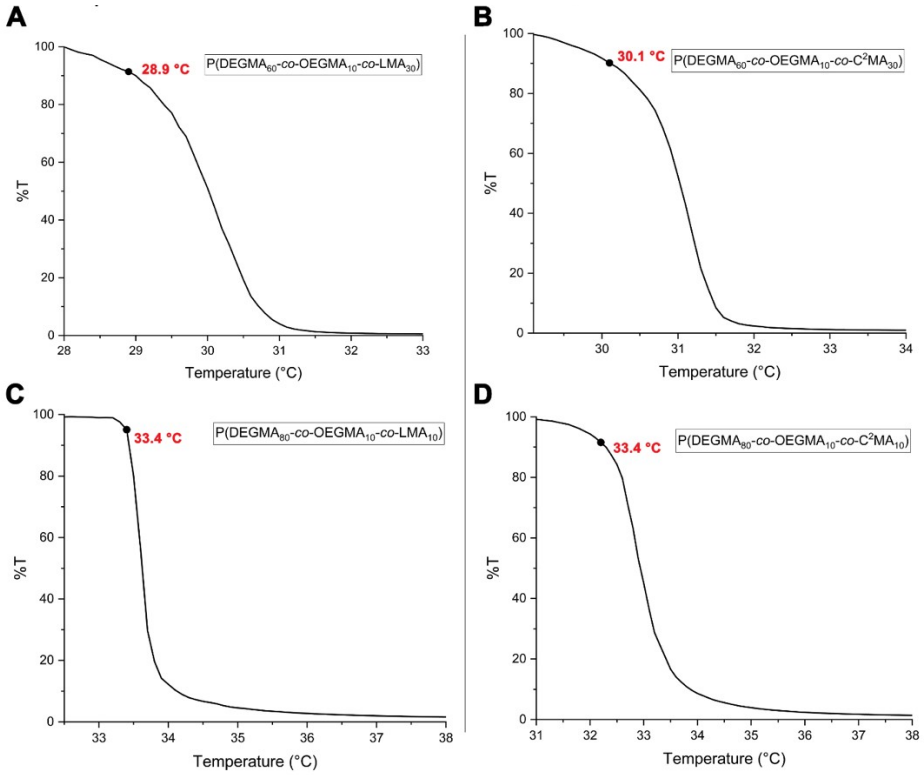

Figure S68. Cloud point temperatures of terpolymers (A) L10, (B) C10, (C) L30, and (D) C30, highlighting the influence of monomer composition on their thermoresponsive behavior

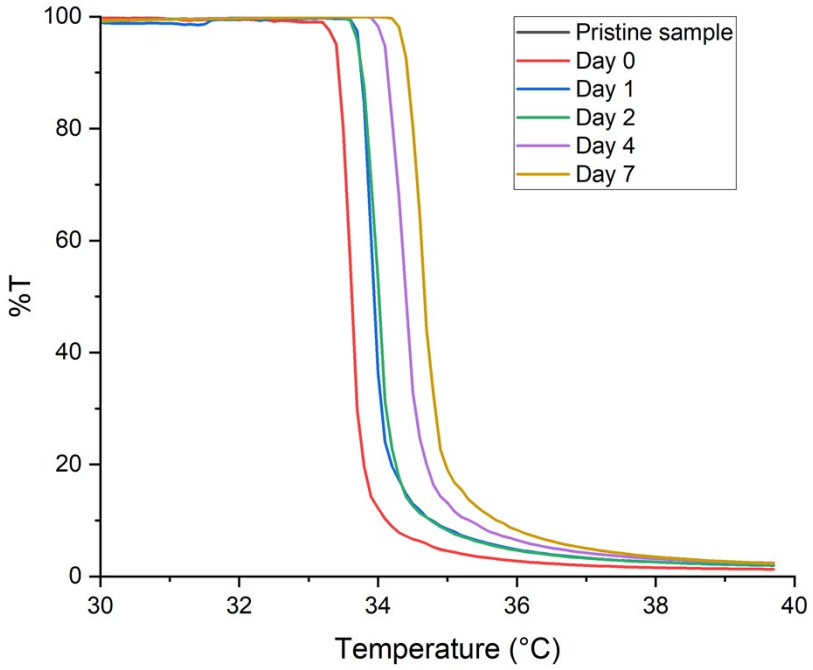

Figure S69. Cloud point measurements of P(DEGMA$_{80}$-*co*-OEGMA$_{10}$-*co*-LMA$_{10}$) in PBS (1 wt%)

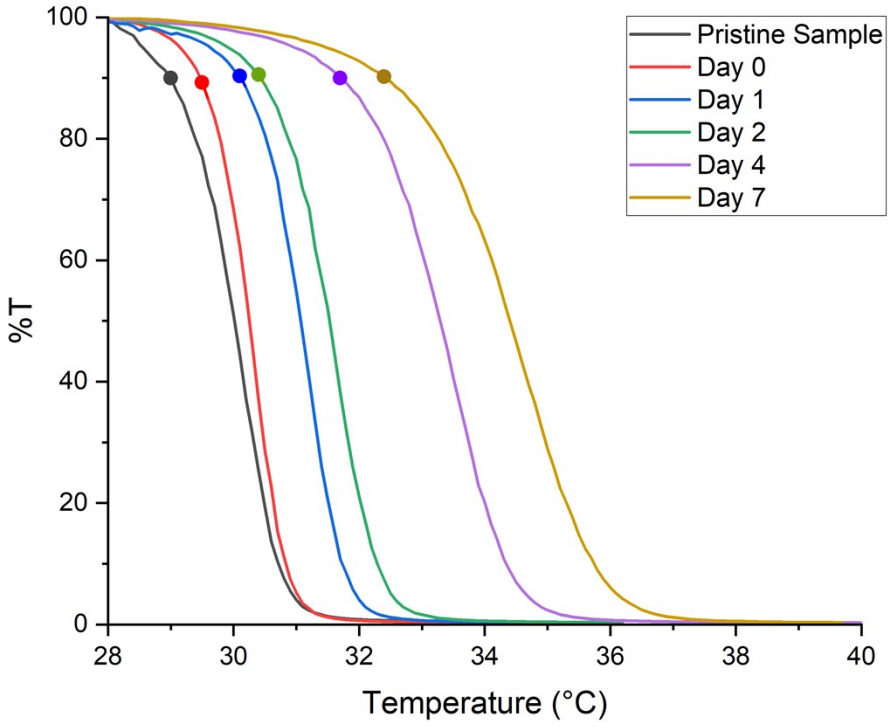

Figure S70. Cloud point measurements of P(DEGMA$_{60}$-*co*-OEGMA$_{10}$-*co*-LMA$_{30}$) in PBS (1 wt%)

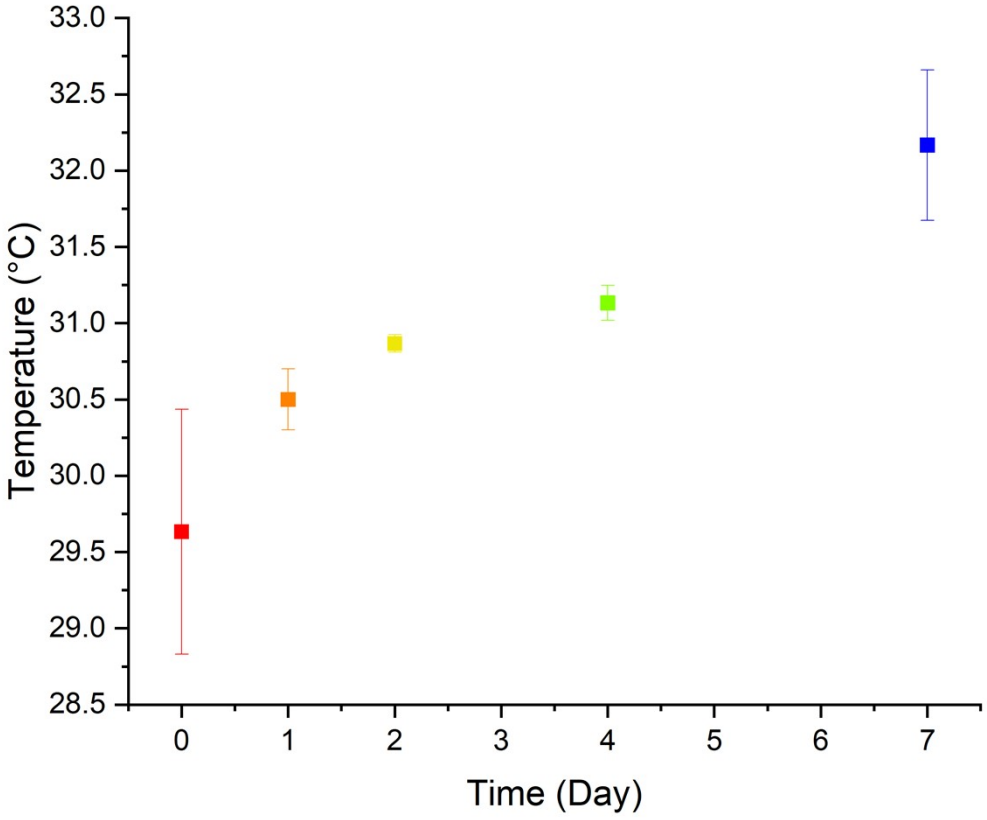

Figure S71. T_{cp} increasing over time; P(DEGMA$_{60}$-*co*-OEGMA$_{10}$-*co*-LMA$_{30}$) in PBS (1 wt%)

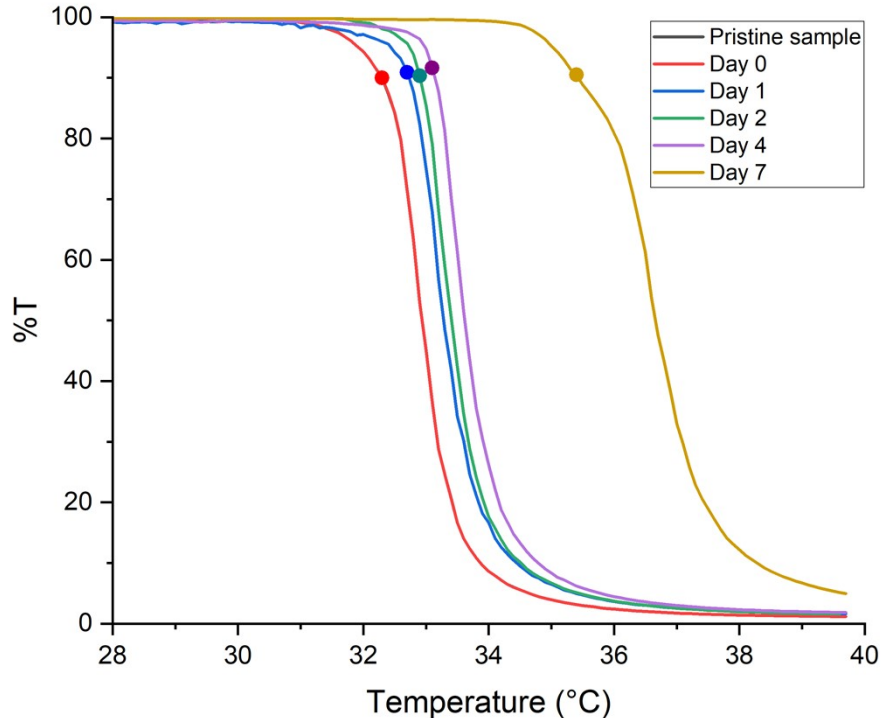

Figure S72. Cloud point measurements of P(DEGMA$_{80}$-*co*-OEGMA$_{10}$-*co*-C^{2}MA$_{10}$) in PBS (1 wt%)

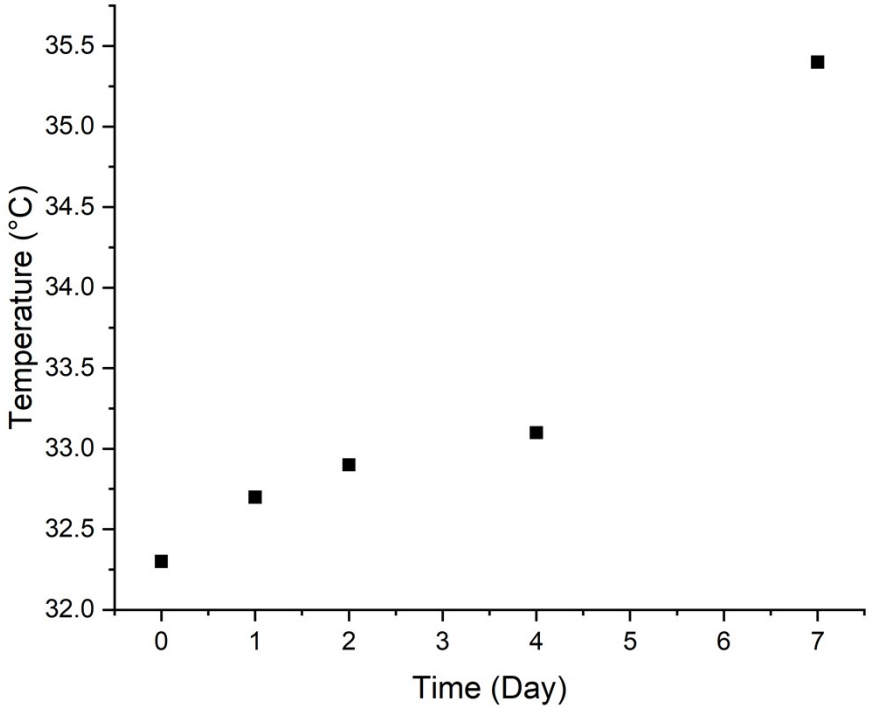

Figure S73. T_{cp} increasing over time; P(DEGMA$_{80}$-*co*-OEGMA$_{10}$-*co*-C^{2}MA$_{10}$) in PBS (1 wt%)

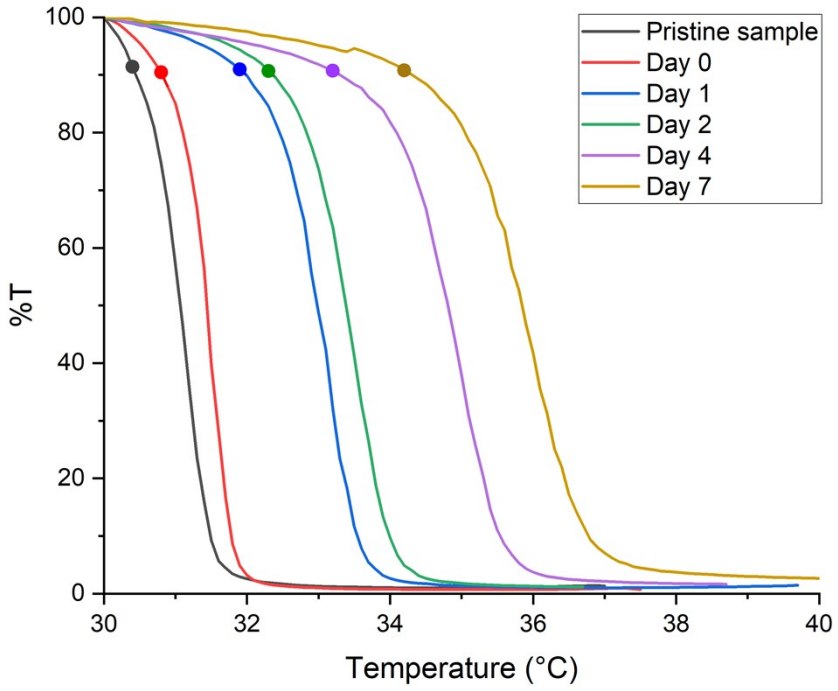

Figure S74. Cloud point measurements of P(DEGMA$_{60}$-*co*-OEGMA$_{10}$-*co*-C^{2}MA$_{30}$) in PBS (1 wt%)

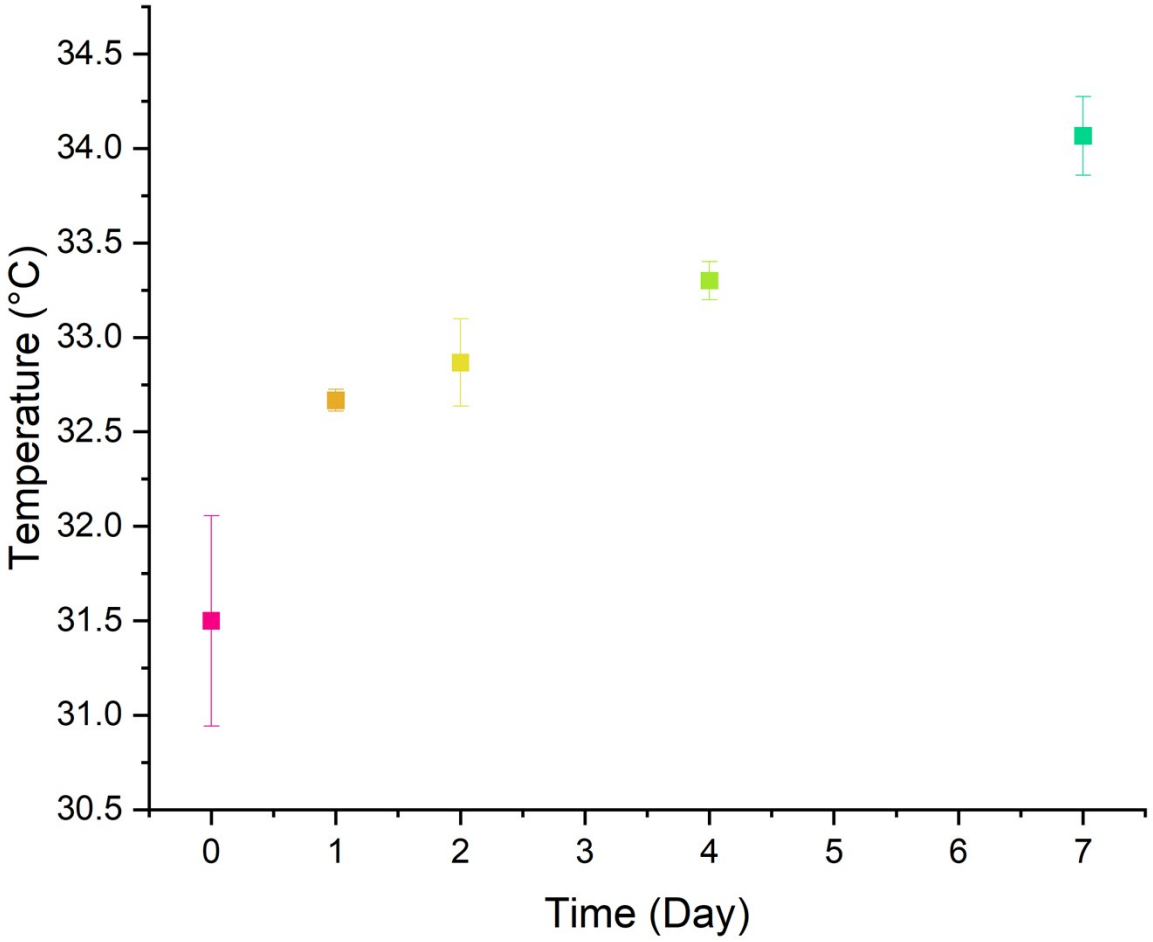

Figure S75. T_{cp} increasing over time; P(DEGMA$_{60}$-*co*-OEGMA$_{10}$-*co*-LMA$_{30}$) in PBS (1 wt%).

12.8. Radiofrequency (RF)-assisted heating plots

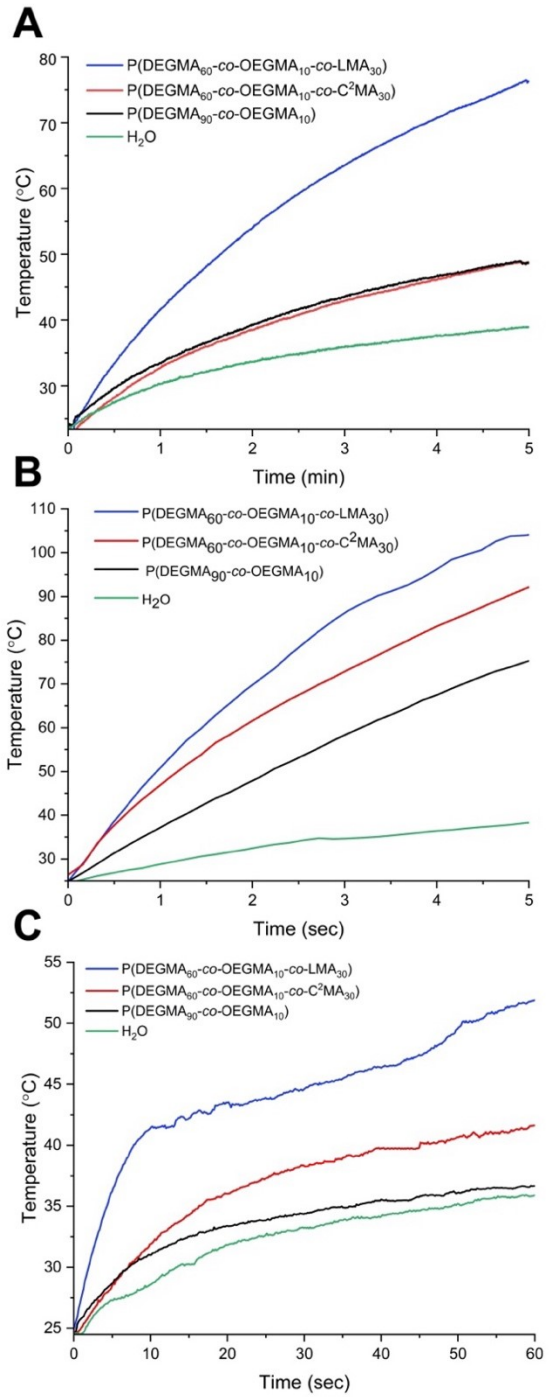

Figure S76. (A) Temperature changes over time upon dielectric heating on non-contact applicator at 300 MHz and input power of 50 Watt; and Temperature change over time upon dielectric heating on direct contact applicator at 300 MHz and input power of 20 Watt (B) and 5 Watt (C)

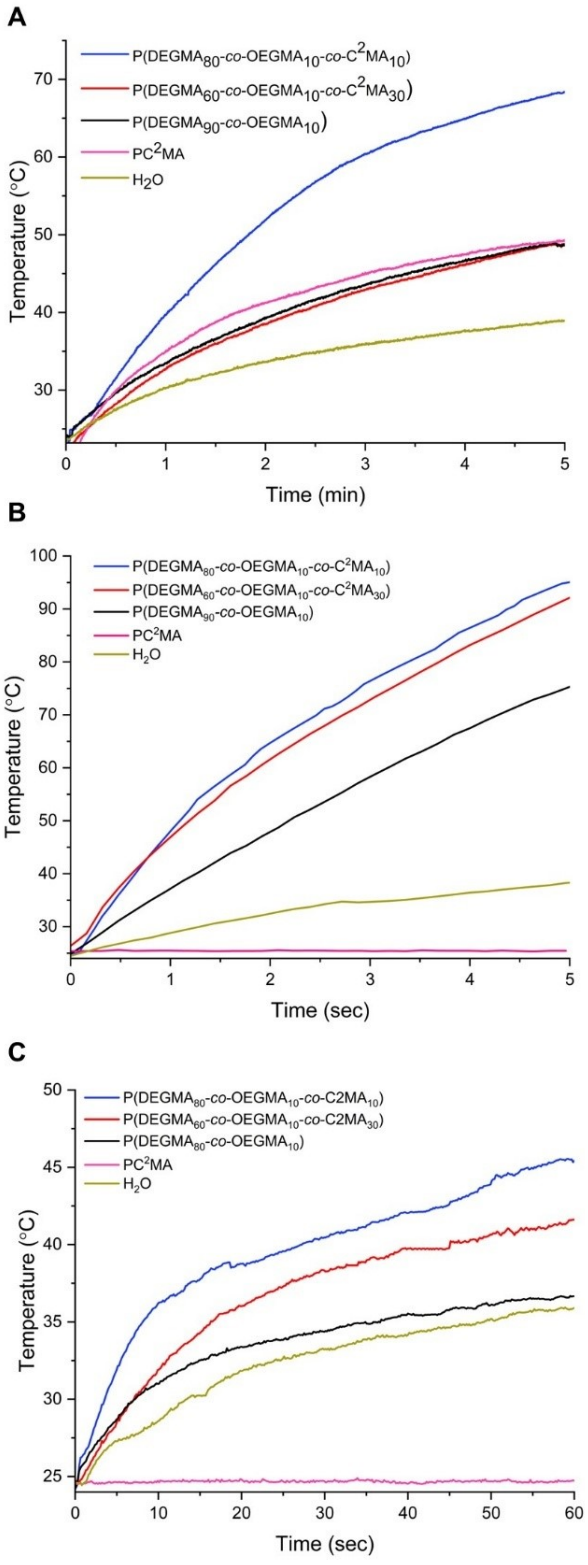

Figure S77. (A) Temperature change over time upon dielectric heating on non-contact applicator at 300 MHz and input power of 50 Watt; and Temperature change over time upon dielectric heating on direct contact applicator at 300 MHz and input power of 20 Watt (B) and 5 Watt (C)

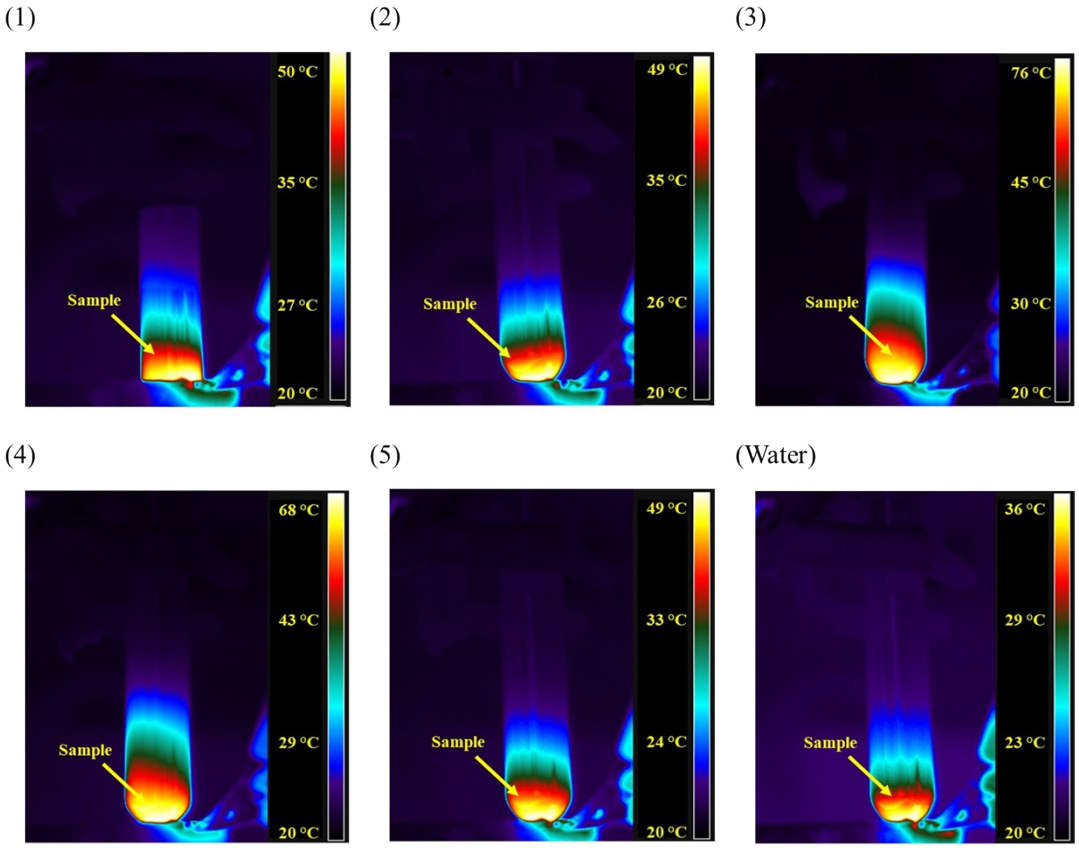

Figure S78. (a) Thermal images captured by FLIR camera at 5 minutes mark during RF-assisted heating on non-contact applicator at 300 MHz and input power of 50 Watt

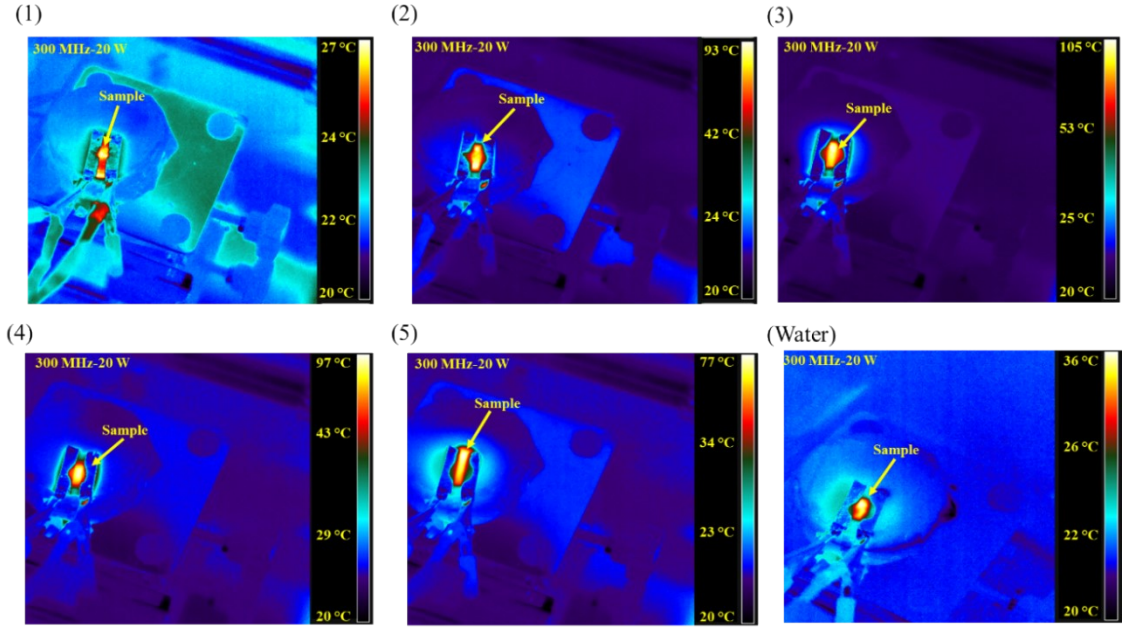

Figure S79. Thermal images captured by FLIR camera at 5 seconds mark during RF-assisted heating on direct contact applicator at 300 MHz and input power of 20 Watts

12.9. Rheology of terpolymers

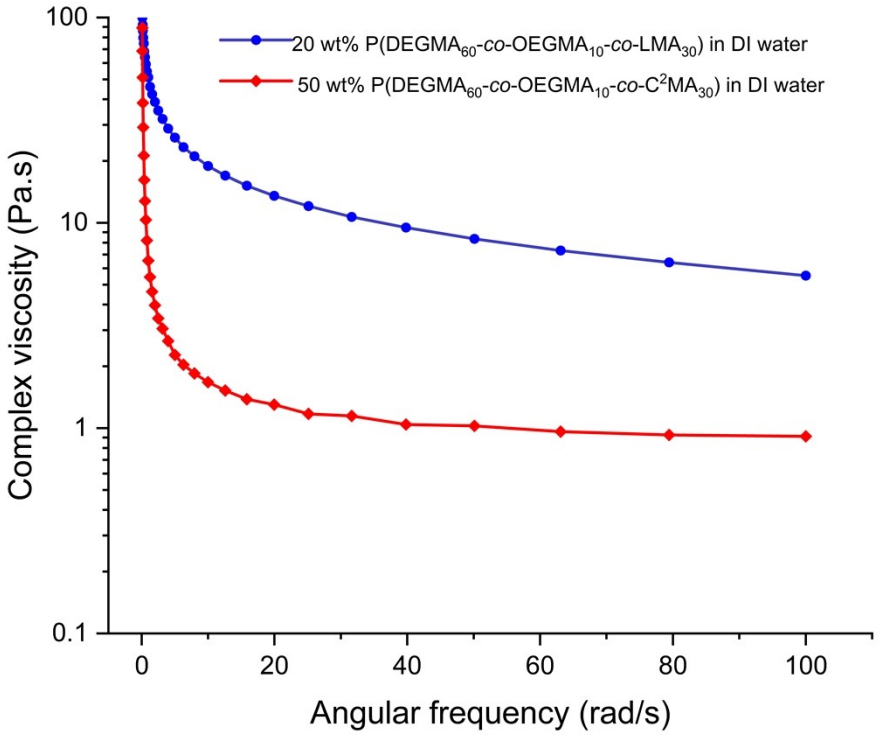

Figure S80. Complex viscosity of 20 wt% L30 and 50 wt% C30 in DI water

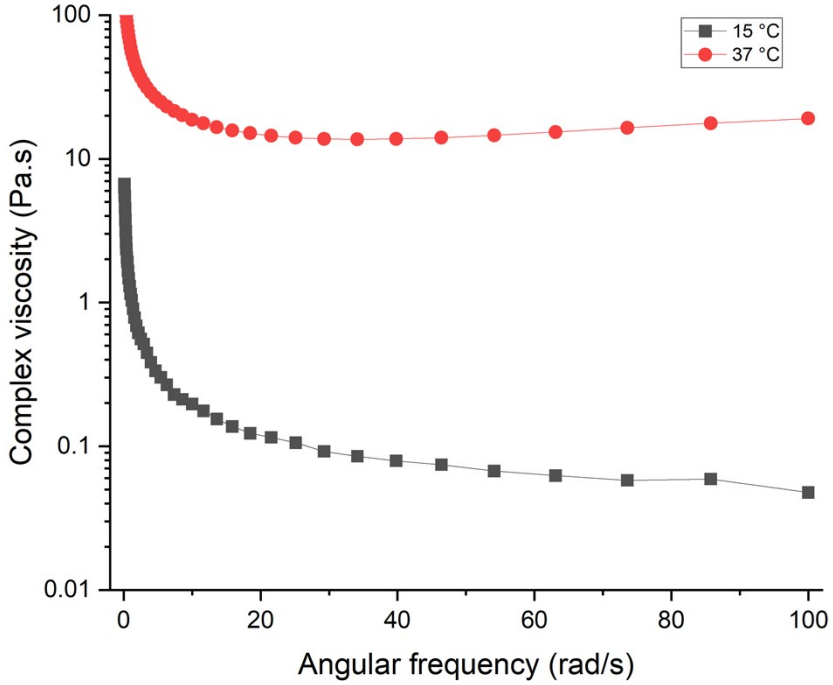

Figure S81. Complex viscosity of 10wt% L30 in PBS at 15 °C and 37 °C

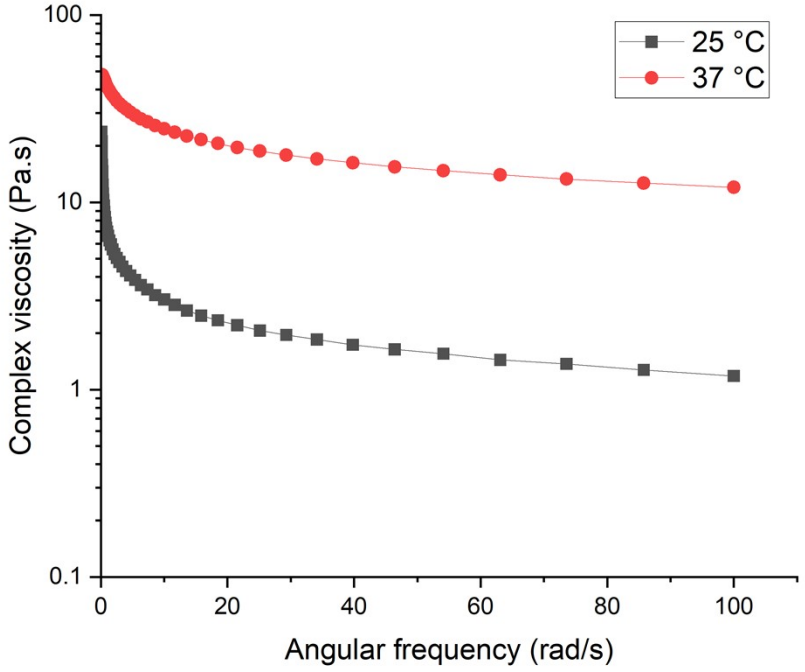

Figure S82. Complex viscosity of 10wt% C30 in PBS at 25 °C and 37 °C

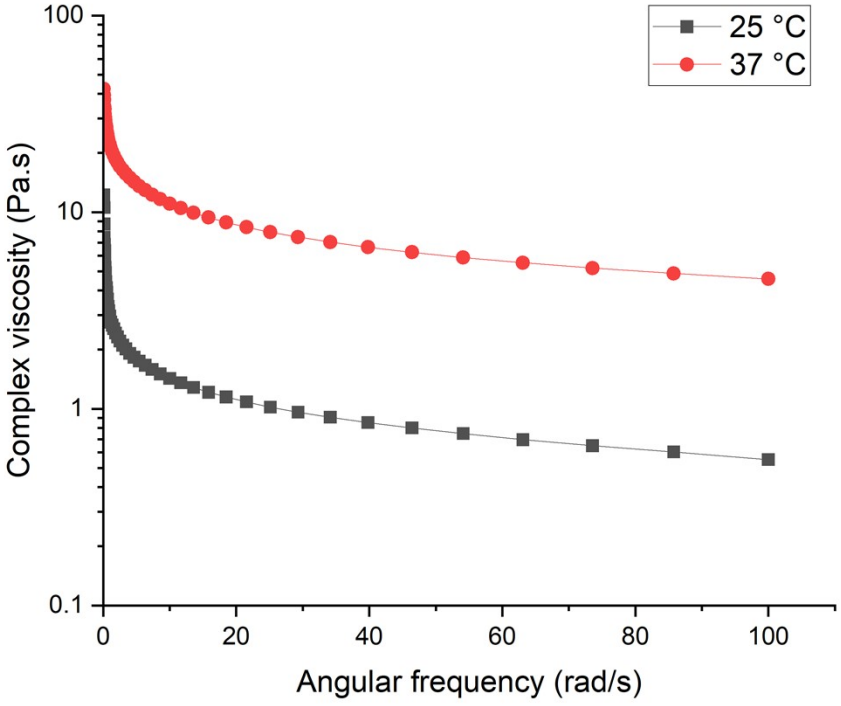

Figure S83. Complex viscosity of 25wt% C30 in PBS at 25 °C and 37 °C

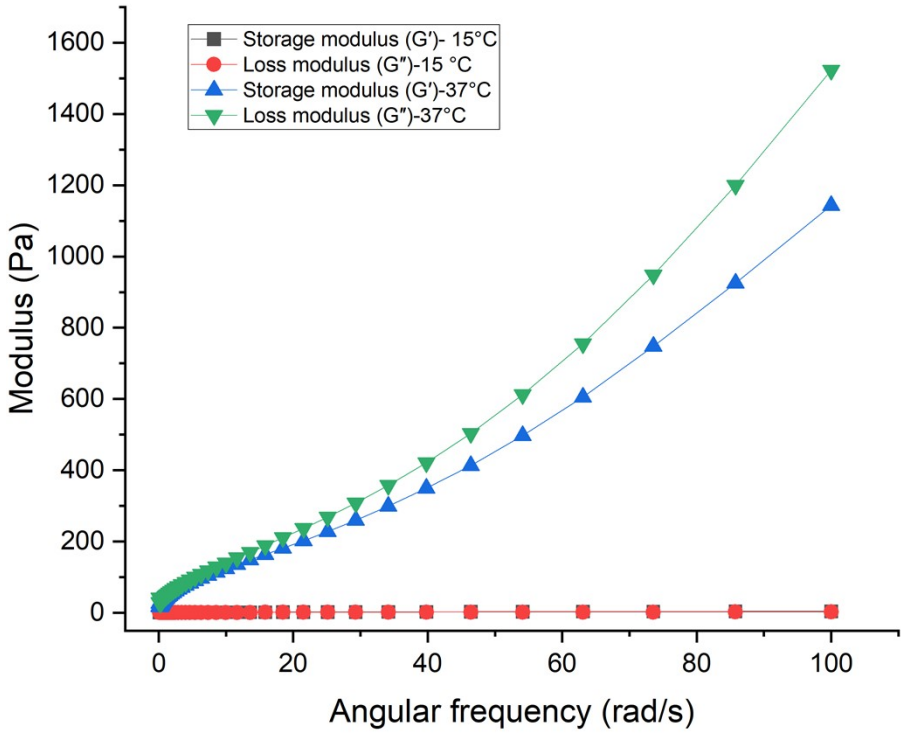

Figure S84. Storage (G′) and loss (G″) moduli of 10 wt% L30 in PBS obtained from a frequency sweep measurement

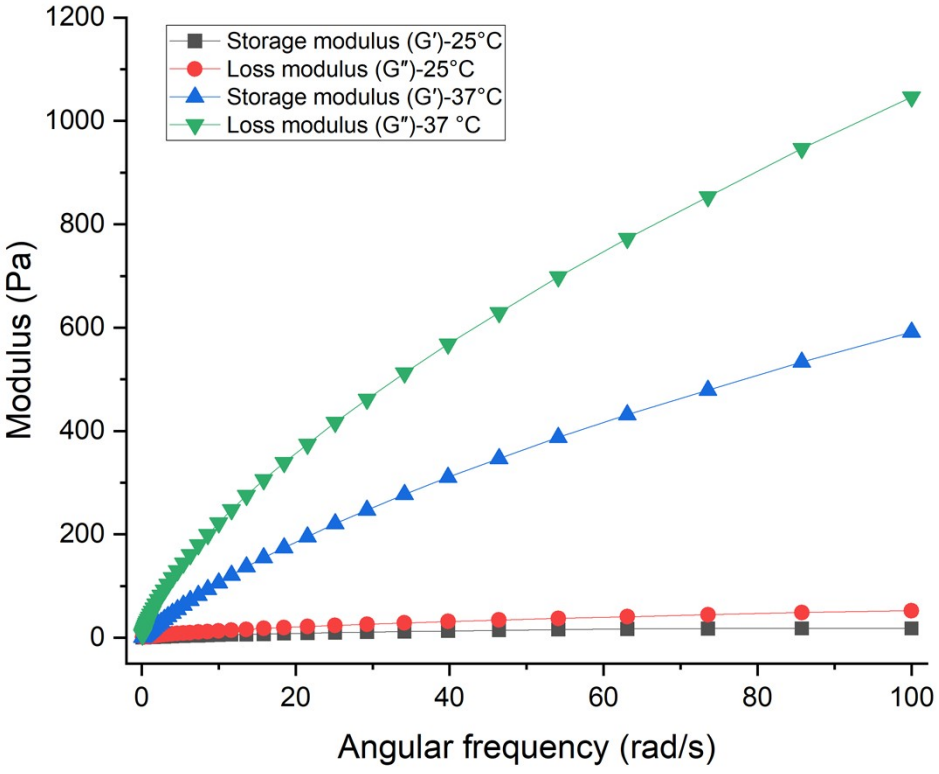

Figure S85. Storage (G′) and loss (G″) moduli of 10 wt% C30 in PBS obtained from a frequency sweep measurement

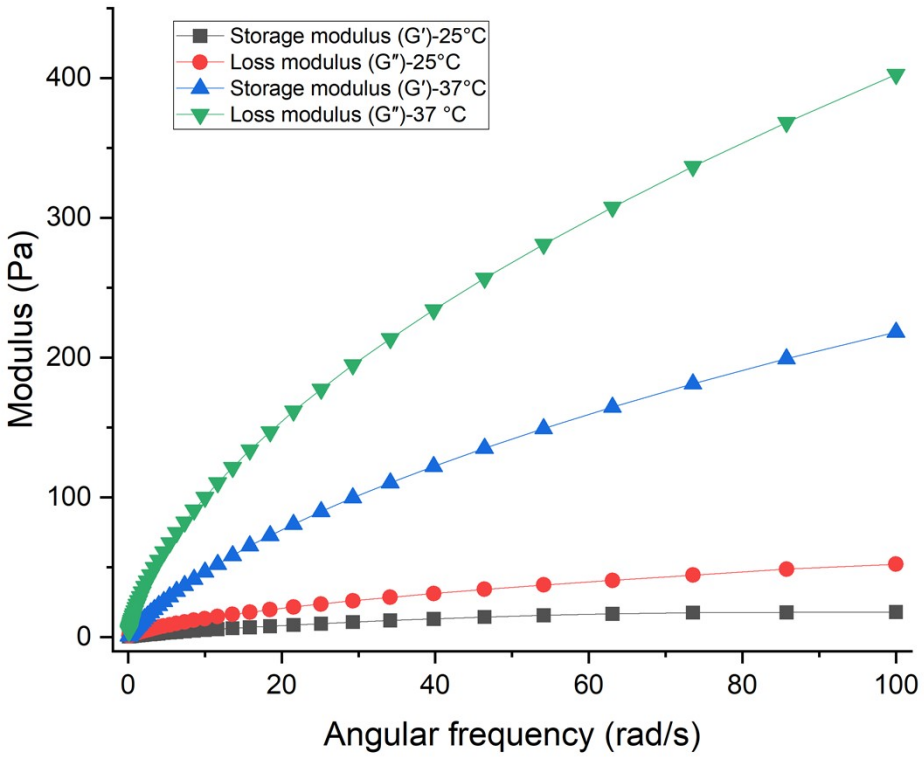

Figure S86. Storage (G′) and loss (G″) moduli of 25 wt% C30 in PBS obtained from a frequency sweep measurement

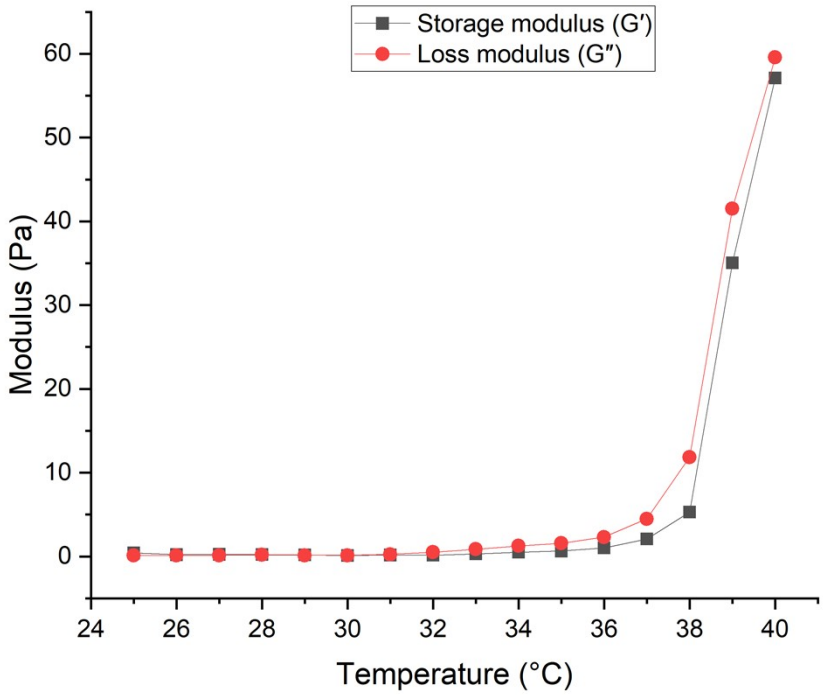

Figure S87. Storage (G′) and loss (G″) moduli of 10 wt% C30 in PBS obtained from a temperature sweep (25–40 °C) at an angular frequency of ω = 1 rad s^{-1}

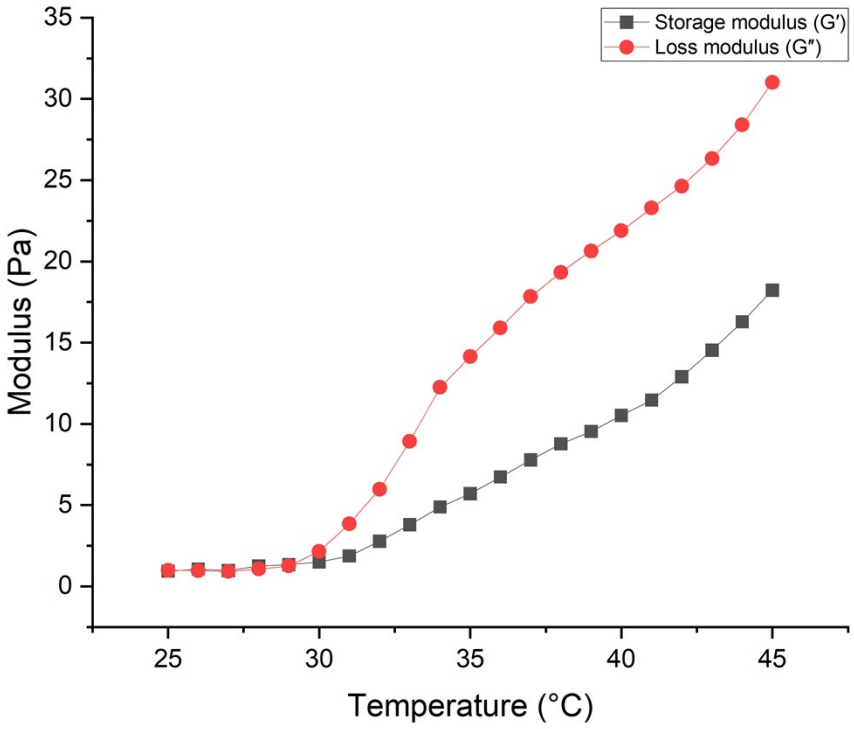

Figure S88. Storage (G′) and loss (G″) moduli of 25 wt% C30 in PBS obtained from a temperature sweep (25–45 °C) at an angular frequency of ω = 1 rad s^{-1}

12.10. Controlled injectability experiments using 10 wt% P(DEGMA$_{60}$-co-OEGMA$_{10}$-co-LMA$_{30}$) and P(DEGMA$_{60}$-co-OEGMA$_{10}$-co-C^{2}MA$_{30}$)

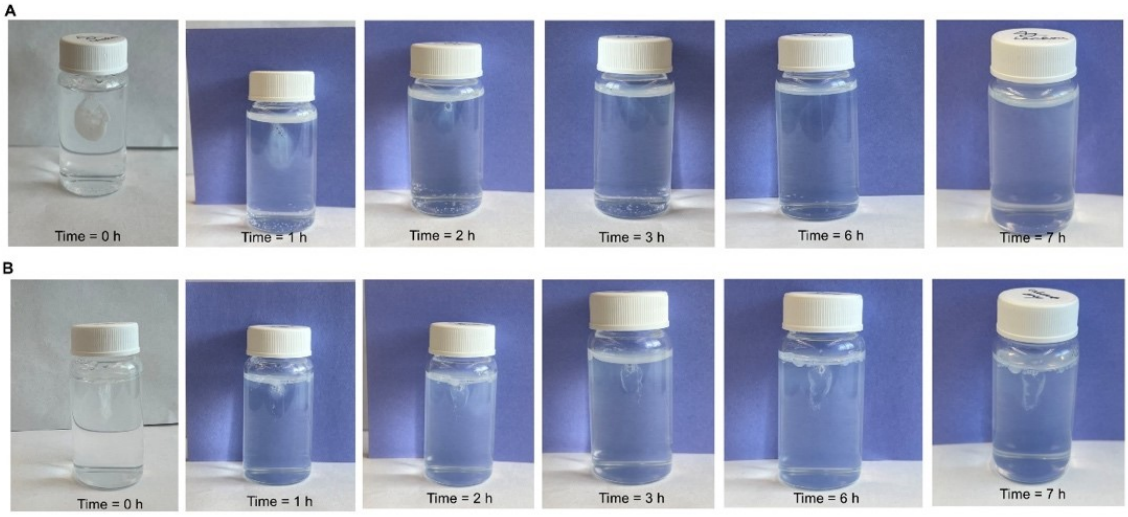

Figure S89. Injectability test of terpolymers: **(A)** 10 wt% P(DEGMA$_{60}$-*co*-OEGMA$_{10}$-*co*-LMA$_{30}$) at 37 °C with different time intervals and (**B**) 10 wt% P(DEGMA$_{60}$-*co*-OEGMA$_{10}$-*co*-C^{2}MA$_{30}$) at 37 °C with different time intervals

12.11. DFT Calculations

All density functional theory (DFT) calculations were performed using Gaussian 16 (Rev. C.02).[1] The PBE0 hybrid functional and the def2-TZVPD basis set was used, D3BJ dispersion correction was included to account for weak interactions. Polarizable continuum model was employed to account for implicit water solvation, while one water molecule is also introduced to further recover the solvation effect. Geometry optimizations were carried out to locate transition states and stationary points. Frequency analysis confirmed the absence of imaginary frequencies for all stationary points and the presence of a single imaginary frequency corresponding to the reaction coordinate for each transition state. Thermodynamic properties were calculated at 298 K and 1 atm.

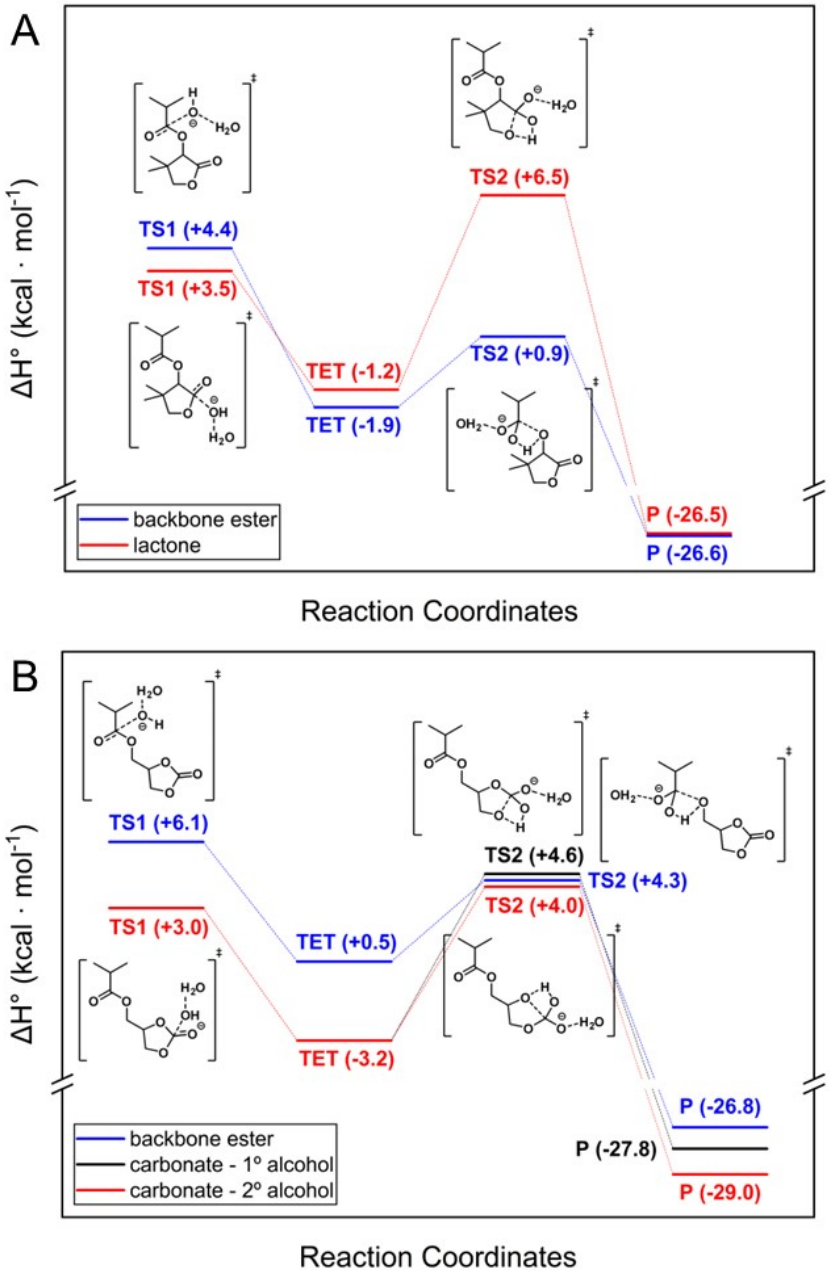

Figure S90. Enthalpy calculated for the alkaline hydrolysis of (A) saturated LMA and (B) saturated C2MA at 298 K

Cartesian Coordinates in Angstrom and 3D structures of Transition States and Stationary Points

Saturated LMA – backbone ester hydrolysis transition state 1 (TS1)

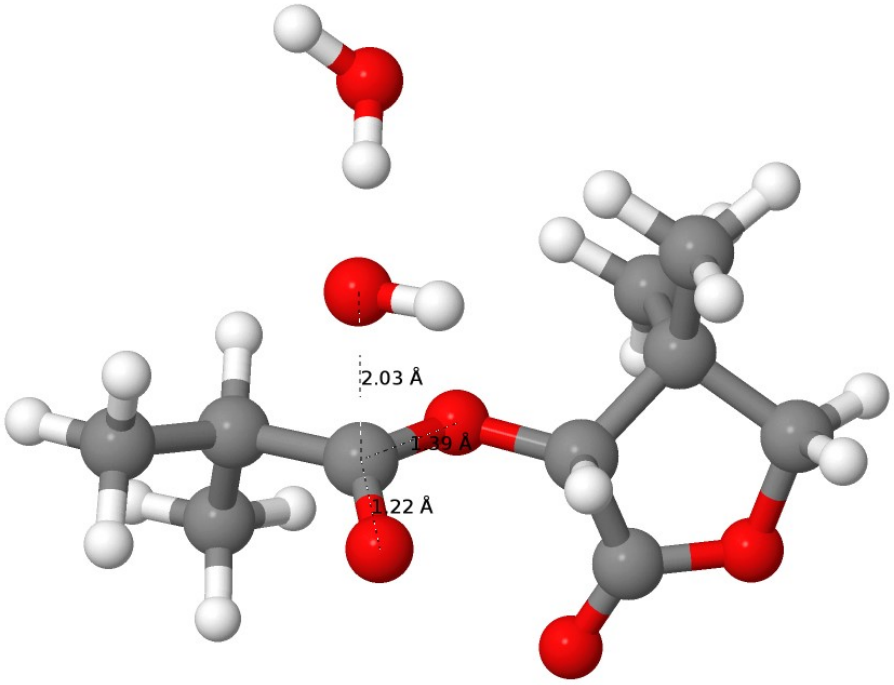

O	-1.12337229	3.71926422	1.92703875
H	-1.26661731	2.71720277	2.13679799
H	-1.79308574	4.18046029	2.43705988
H	-2.83757455	1.67837133	0.30217623
H	-3.92078825	0.72742491	2.32687911
O	-1.62959988	-1.13139287	1.37014115
H	-5.06755101	0.80936955	0.97080842
C	-4.15257423	0.33663872	1.33712985
C	-3.00770844	0.60244182	0.37921887
C	-1.71330387	-0.01706471	0.87170561
H	-4.25950950	0.49031720	-1.37850908
C	-3.32695459	0.05483913	-1.01106387
H	-4.34013344	-0.73678505	1.42405724
H	-2.53692849	0.28447487	-1.72741565
O	-0.66718653	0.47936249	0.09705939
H	0.56342436	-0.74187161	1.18216823
C	0.57679572	-0.11372541	0.28115629
O	0.26575778	-1.69445914	-1.57484976
H	-3.45525572	-1.03094339	-0.97876114
C	0.97017556	-1.03492516	-0.86089098
H	2.88884850	2.06828276	1.72774500
H	2.05835956	0.69827883	2.48161828
C	1.75656766	0.86221296	0.34247329
C	1.97258355	1.47174941	1.71400455
O	2.30370650	-1.02588578	-0.98526308
C	2.87625278	-0.10840848	-0.03018641
H	3.21834780	-0.68402159	0.83400273
H	0.74547894	2.57019570	-0.51455001

H	1.13854259	2.12585348	1.97396900
C	1.61771944	1.94843890	-0.71821064
H	1.50502497	1.52737144	-1.72106619
H	3.72898018	0.37308946	-0.50721956
H	2.50537622	2.58500651	-0.71642280
O	-1.51025100	1.25886487	2.43726132
H	-0.73444728	0.86602158	2.84607799

Saturated LMA – backbone ester hydrolysis tetrahedral intermediate (TET)

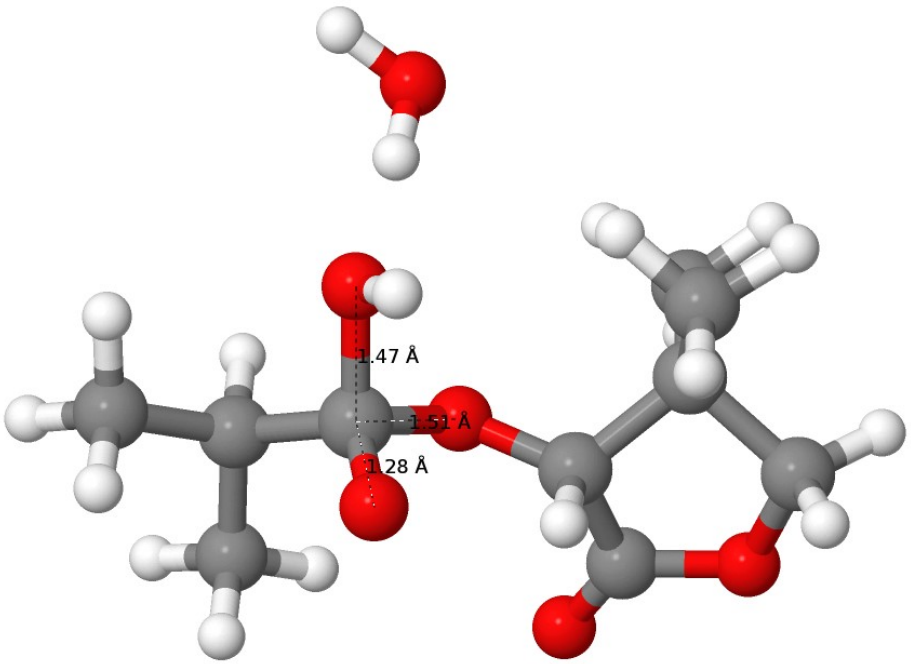

O	-0.97697217	3.97476449	1.32939719
H	-1.15096847	3.03539951	1.56391011
H	-1.69205494	4.46502466	1.74282850
H	-3.02314558	1.53632747	-0.01133532
H	-4.07235386	1.19188642	2.21386811
O	-1.44901405	-0.82731607	1.64903268
H	-5.14492583	0.61862945	0.92700918
C	-4.18409818	0.45033576	1.42179230
C	-3.04682038	0.52645330	0.41587025
C	-1.68290597	0.30367304	1.09955551
H	-4.20847347	-0.27340893	-1.22209962
C	-3.26397792	-0.47264245	-0.70757074
H	-4.21648582	-0.54019964	1.88438152
H	-2.45269038	-0.43346566	-1.43495443
O	-0.70656239	0.66714562	0.00586734
H	0.40301745	-0.83171187	0.77619100
C	0.49586477	0.00666149	0.06018918
O	0.17445287	-1.03619446	-2.14229265
H	-3.31051464	-1.48934636	-0.30658711
C	0.88160791	-0.62456626	-1.26040068
H	2.92121429	1.49547130	2.10231950

H	1.90116222	0.08720472	2.44456016
C	1.75488048	0.82362838	0.41121710
C	1.95057264	1.03343279	1.89982774
O	2.22025006	-0.69519927	-1.34624092
C	2.81143174	-0.11137830	-0.16758555
H	3.05993350	-0.91973412	0.52628726
H	0.91456119	2.76925096	-0.00081021
H	1.17815717	1.69725776	2.29243839
C	1.75667514	2.15710487	-0.32524084
H	1.67928274	2.02148123	-1.40786665
H	3.72634403	0.39504282	-0.47508675
H	2.68270514	2.70022366	-0.11880014
O	-1.53909924	1.40925450	2.05843727
H	-1.04194003	1.00552921	2.77805131

Saturated LMA – backbone ester hydrolysis transition state 2 (TS2)

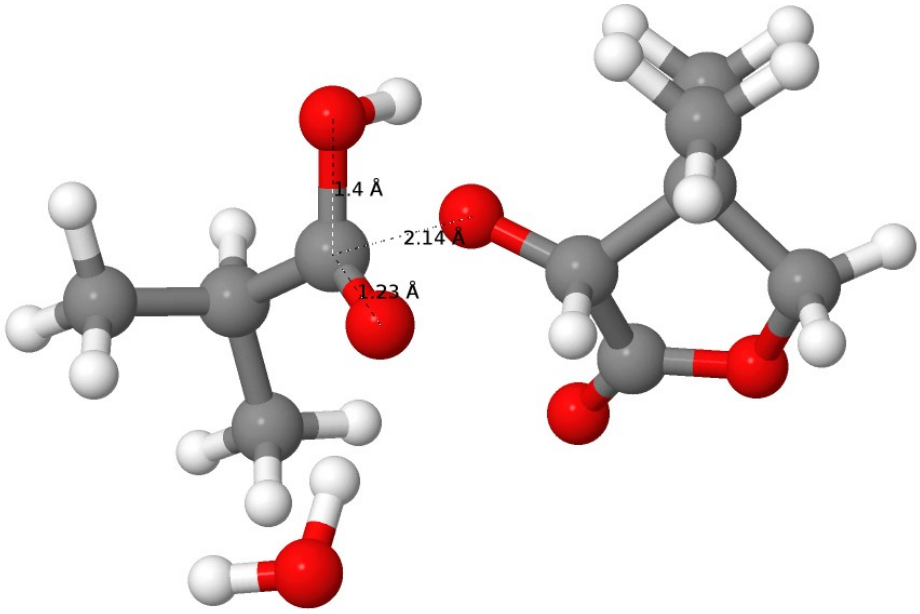

O	-2.74507522	-2.50517844	2.87822857
H	-2.32422217	-1.64748791	2.61437678
H	-3.68574834	-2.39223454	2.68502856
H	-2.97581092	1.40731744	-0.33303913
H	-4.47452013	1.70013887	1.65865399
O	-1.59181825	-0.15486261	2.15519966
H	-5.24740139	0.68980675	0.41183534
C	-4.41258072	0.73911913	1.12717623
C	-3.07512180	0.58071881	0.38690729
C	-1.94795746	0.74431279	1.39275012
H	-3.81074683	-0.81189876	-1.09921381
C	-2.99942845	-0.74678727	-0.35779767
H	-4.54919842	-0.07079115	1.86163056
H	-2.03458111	-0.83844657	-0.87489199
O	-0.42057169	1.04522603	-0.06991479

H	0.35047201	-0.51560488	1.00793006
C	0.60846381	0.21045213	0.18261872
O	0.37333200	-1.11822631	-1.90761707
H	-3.10756817	-1.59441243	0.33560418
C	1.02853757	-0.70891874	-0.97123001
H	3.02345695	1.62990665	2.33210606
H	1.76058452	0.42997557	2.72577645
C	1.98858978	0.81811117	0.59589284
C	2.02454667	1.25936749	2.05189190
O	2.33067248	-1.05941681	-0.82811945
C	2.88521309	-0.39431635	0.33836381
H	2.86032939	-1.10434832	1.18147152
H	1.60494378	2.77595757	-0.25140740
H	1.30414094	2.07464048	2.21848180
C	2.35553557	1.97683702	-0.33243895
H	2.39443547	1.65954800	-1.38645064
H	3.92934784	-0.14456553	0.10545860
H	3.33954249	2.39110972	-0.06354932
O	-1.67759127	2.06937936	1.74584357
H	-0.97367203	2.23635166	1.06021362

Saturated LMA – backbone ester hydrolysis product (P)

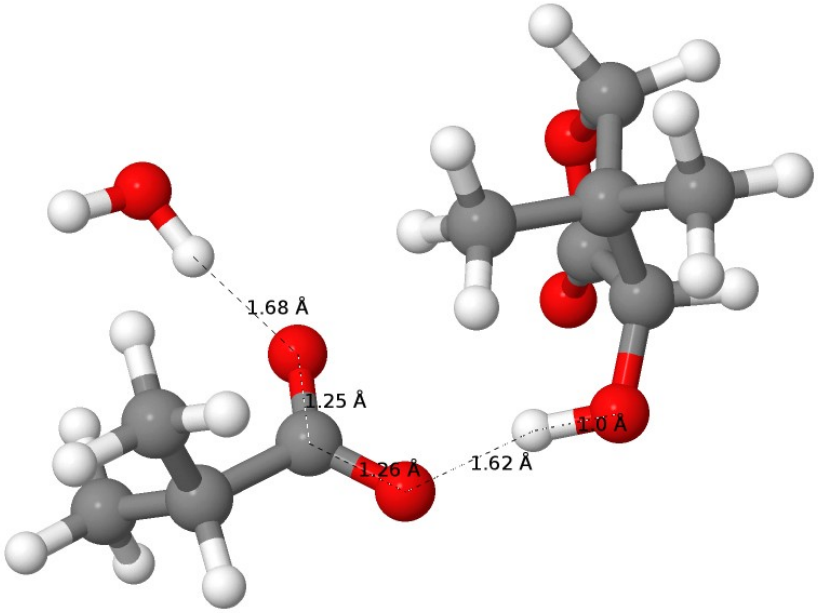

H	-3.21968119	1.35003045	3.21137640
O	-2.39592930	1.76966164	2.95331865
H	-2.23507437	1.48395508	2.01846225
H	-3.56056203	-1.06558890	-1.06417562
H	-4.64058399	1.16087980	-0.77898257
O	-1.72282963	1.13277897	0.45807646
H	-5.46580622	-0.06836528	0.18862513
C	-4.52621760	0.47726210	0.06620407

C	-3.37416404	-0.49050024	-0.15301144
C	-2.04036519	0.23259859	-0.35415843
H	-2.43220280	-2.18325479	0.84053049
C	-3.23954325	-1.46672359	1.01184780
H	-4.36564036	1.07988092	0.96277087
H	-3.02482337	-0.93312720	1.94152691
O	1.24378138	-0.11128744	-1.73553475
H	3.11541900	0.42083345	-1.25245350
C	2.12288122	0.35494496	-0.77994419
O	1.32745362	2.67940449	-0.84856508
H	-4.16694345	-2.02836213	1.15147768
C	1.85128731	1.76449161	-0.27241811
H	3.38933453	-2.14114543	1.31170237
H	4.19246231	-1.33713231	-0.04691875
C	2.29767992	-0.44767875	0.52396513
C	3.22184988	-1.63881833	0.35521236
O	2.32665093	1.88576428	0.97296239
C	2.92041985	0.63995331	1.39646301
H	4.00105176	0.71321169	1.24635936
H	0.47045890	-1.59665121	0.41946415
H	2.77895951	-2.36602750	-0.32937814
C	0.95360230	-0.88398091	1.09011292
H	0.26885843	-0.04270981	1.22041941
H	2.71013082	0.52206830	2.45881923
H	1.10020150	-1.37043824	2.05753337
O	-1.32698424	-0.14981195	-1.31671152
H	0.28837783	-0.03096562	-1.44649831

Saturated LMA – lactone hydrolysis transition state 1 (TS1)

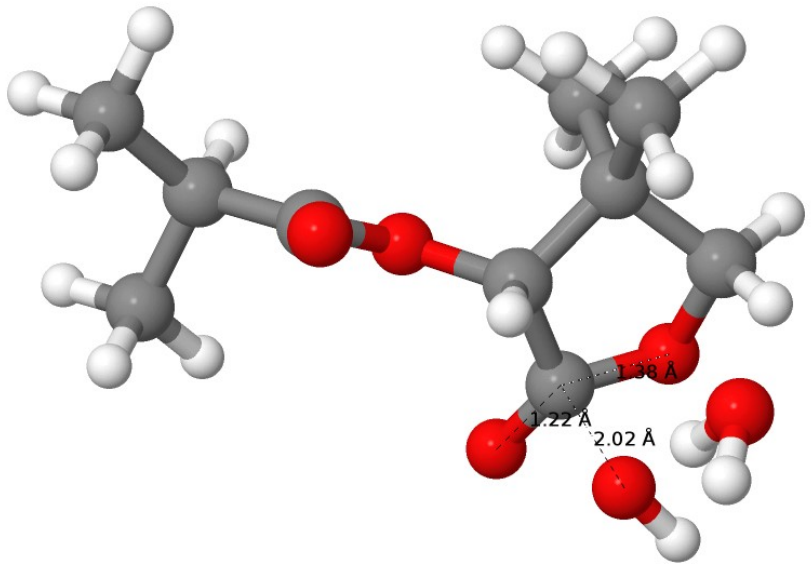

H	-2.56218875	1.35535885	-0.80252376
H	-3.31222042	2.19566351	1.43504568
O	-1.47315563	-0.07786147	1.82375412
H	-4.68493332	1.67154281	0.44921861

C	-3.78582361	1.33072565	0.96644036
C	-2.85285670	0.65054100	-0.01823226
C	-1.57993747	0.19566175	0.65263643
H	-4.41772121	-0.24102909	-1.20752838
C	-3.51386496	-0.55774619	-0.68351939
H	-4.08685411	0.63986312	1.75634995
H	-2.84652637	-1.03188463	-1.40474054
O	-0.58516946	0.10410430	-0.23289254
H	0.55712233	-0.84668445	1.18103293
C	0.68076178	-0.37852837	0.21129374
O	0.50622258	-2.06210204	-1.56831745
H	-3.79908542	-1.30063671	0.06578994
C	1.19831868	-1.40626839	-0.81016873
H	2.83090337	1.97288369	1.63702910
H	2.19505697	0.47713157	2.34760100
C	1.75965934	0.71506895	0.24363607
C	1.98574950	1.27831040	1.63542298
O	2.45093735	-1.00378805	-1.21362668
C	2.96424922	-0.09280950	-0.24985447
H	3.42343139	-0.65279318	0.56938626
H	0.55207733	2.37736316	-0.46468356
H	1.10471679	1.82648552	1.97855133
C	1.45504160	1.83358344	-0.74688448
H	1.31461515	1.44877497	-1.75949613
H	3.71332385	0.52968587	-0.74087302
H	2.28785814	2.54088492	-0.76193724
O	1.80707499	-2.66672902	0.64449253
H	2.42775647	-3.19574109	0.13503511
O	2.85323468	-2.06292779	2.91000115
H	2.44865410	-2.31314935	2.00344928
H	2.65330179	-2.80546417	3.48472204

Saturated LMA – lactone hydrolysis tetrahedral intermediate (TET)

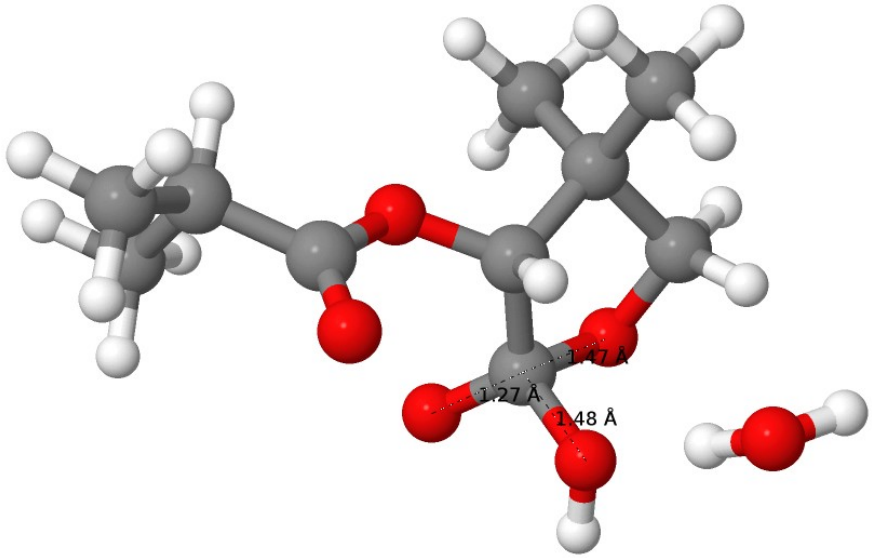

H	-2.55523237	1.71989254	-0.05866300
H	-3.66955148	1.17368095	2.11775910
O	-1.64861098	-0.83552768	1.58517813
H	-4.83807136	1.25037928	0.79081349
C	-3.98109675	0.70015925	1.18475797
C	-2.85991950	0.69233004	0.16181462
C	-1.63618520	-0.01675128	0.69610212
H	-4.18025342	0.55069786	-1.53773280
C	-3.29864659	0.03766381	-1.14792434
H	-4.30435288	-0.31711048	1.41435004
H	-2.51286620	0.08476506	-1.90264946
O	-0.53720002	0.38314202	0.06334109
H	0.66384908	-0.44472024	1.49512458
C	0.70874660	-0.19291157	0.43620811
O	0.19265577	-1.93251372	-1.24356227
H	-3.56130377	-1.01104006	-0.98634624
C	1.02581693	-1.50090615	-0.38603394
H	3.07696063	2.25797029	1.16942944
H	2.42471710	1.00723429	2.24052806
C	1.85316540	0.78445020	0.16195434
C	2.20220116	1.63286801	1.37201588
O	2.33595854	-1.20121666	-0.97641797
C	2.95390215	-0.21964235	-0.18647776
H	3.37834493	-0.65309679	0.73253071
H	0.73604993	2.34513745	-0.85726312
H	1.37373183	2.29664516	1.63398601
C	1.57352461	1.67187158	-1.04614175
H	1.33845673	1.07593682	-1.92977409
H	3.76764386	0.23787834	-0.75515393
H	2.45657198	2.27826924	-1.26480429
O	1.31888551	-2.49577324	0.67643775
H	1.37101792	-3.33045886	0.19761123
O	2.53598559	-2.25854973	3.11256726
H	2.15182526	-2.33496753	2.21250441
H	3.46316899	-2.05243588	2.97105063

Saturated LMA – lactone hydrolysis transition state 2 (TS2)

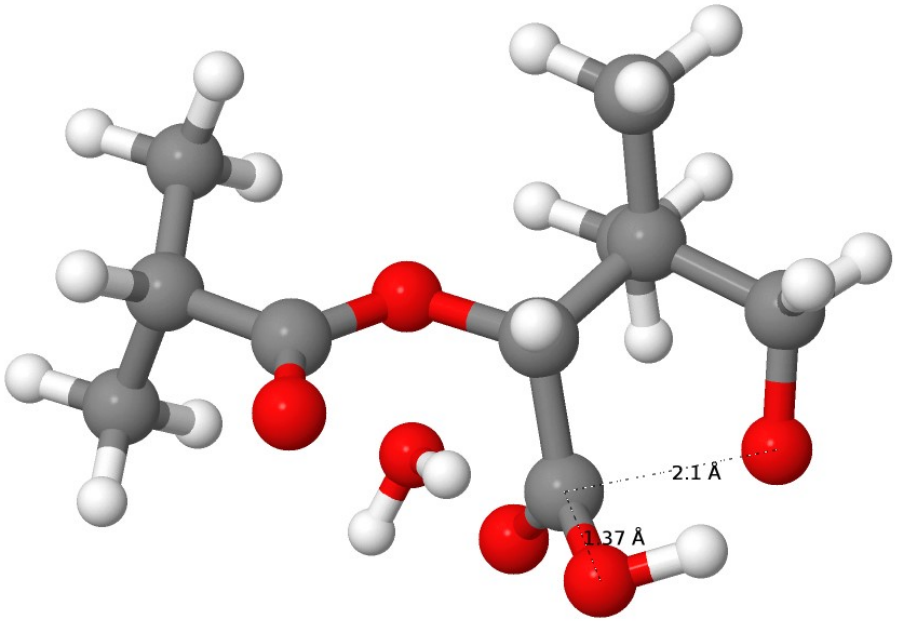

H	-3.19474473	0.12692022	1.61790092
H	-3.28898512	-1.87186093	0.16204809
O	-1.08088574	-1.23024280	1.95983466
H	-4.25469015	-0.55477992	-0.51976457
C	-3.23914340	-0.87281345	-0.27488413
C	-2.60736882	0.12716289	0.69527402
C	-1.25107195	-0.39960265	1.09722877
H	-3.59904518	1.86756262	-0.07896861
C	-2.57795054	1.52938086	0.11036585
H	-2.66192598	-0.92498624	-1.20132288
H	-2.10430180	2.24040835	0.79017246
O	-0.26314301	0.12215247	0.37705461
H	1.20491646	-0.38046088	1.72749253
C	1.06935834	-0.32652673	0.64489893
O	0.64658072	-2.11291600	-0.91188673
H	-2.03247050	1.54857768	-0.83470441
C	1.26571295	-1.74311792	0.07473229
H	2.73843583	2.69332005	0.48064810
H	2.16944115	1.82070602	1.91186797
C	2.03854687	0.69792558	0.05973005
C	1.98081464	1.99551321	0.84865307
O	3.29653306	-1.29577748	-0.23644584
C	3.39679783	-0.00046730	0.20835324
H	3.69135697	0.06398294	1.27807070
H	0.74762565	1.36334746	-1.56113103
H	1.00594894	2.47963319	0.74957740
C	1.75257711	0.96381331	-1.41313795
H	1.85149390	0.05026564	-1.99951143
H	4.14893126	0.59361480	-0.34667326
H	2.46943622	1.69688948	-1.79293297

O	1.73482705	-2.68391152	0.95357439
H	2.68190658	-2.40500603	0.96295100
O	-0.74578810	-1.02784205	-3.02216333
H	-0.25097177	-1.32294868	-2.22970250
H	-1.21393472	-1.81191618	-3.31989943

Saturated LMA – lactone hydrolysis product (P)

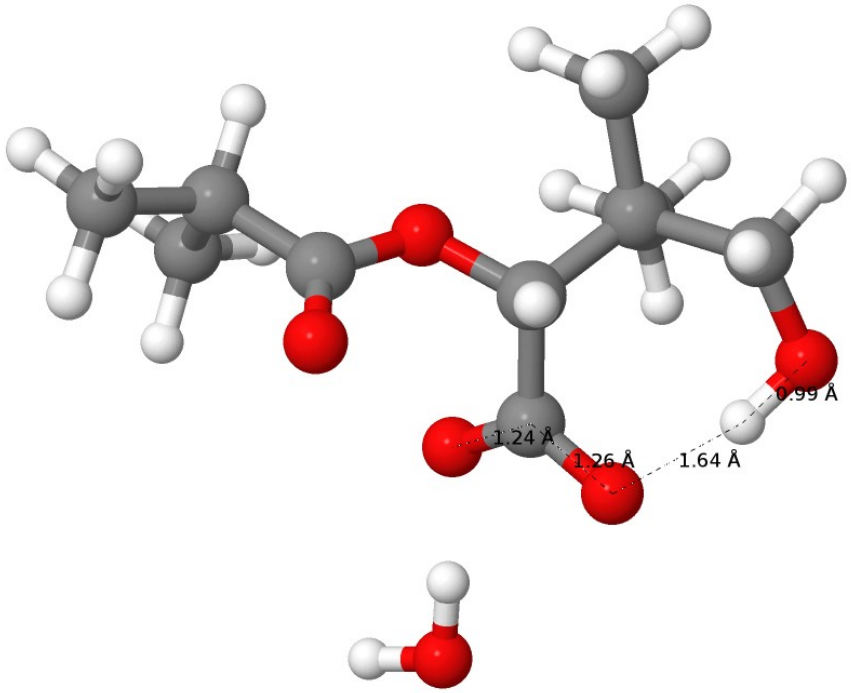

O	-0.36110865	-4.39288966	-1.79251284
H	-1.22330086	-4.42428057	-2.21418416
H	-0.29797544	-3.48153615	-1.40895417
H	-2.58475496	1.92476873	0.27036444
H	-3.80336983	1.19947873	2.33594069
O	-1.74003471	-0.69864693	1.79289596
H	-4.90662845	1.40694595	0.96770344
C	-4.07343005	0.81443175	1.35099130
C	-2.90573132	0.88419724	0.38511561
C	-1.70930842	0.12695291	0.91060105
H	-4.13160476	0.91552218	-1.38885250
C	-3.28182525	0.35249701	-0.99771317
H	-4.41539688	-0.21532397	1.47358250
H	-2.45317311	0.44505798	-1.70008090
O	-0.59659245	0.48915710	0.27799909
H	0.63593107	-0.29567456	1.72124735
C	0.61243283	-0.18533639	0.63349416
O	-0.25344772	-1.89596300	-0.80239558
H	-3.57014943	-0.70026455	-0.94109104
C	0.62026549	-1.60984518	0.03651041
H	2.35601075	2.78732403	0.48005054
H	1.37002985	2.14454573	1.80209925

C	1.78381545	0.72357133	0.20408733
C	1.50966627	2.13792079	0.71697886
O	3.66960754	-0.90782820	0.42529522
C	3.09466571	0.28725848	0.88297805
H	2.91667197	0.24858114	1.96955248
H	1.01607843	1.07196186	-1.79098239
H	0.61676794	2.56140861	0.25848897
C	1.94034447	0.74316872	-1.31096989
H	2.19714799	-0.24429208	-1.69863476
H	3.82904822	1.07964863	0.70767498
H	2.73691541	1.43463051	-1.59798455
O	1.51566097	-2.37773955	0.46570164
H	2.95664197	-1.58838862	0.48934267

Saturated C^2MA – backbone ester hydrolysis transition state 1 (TS1)

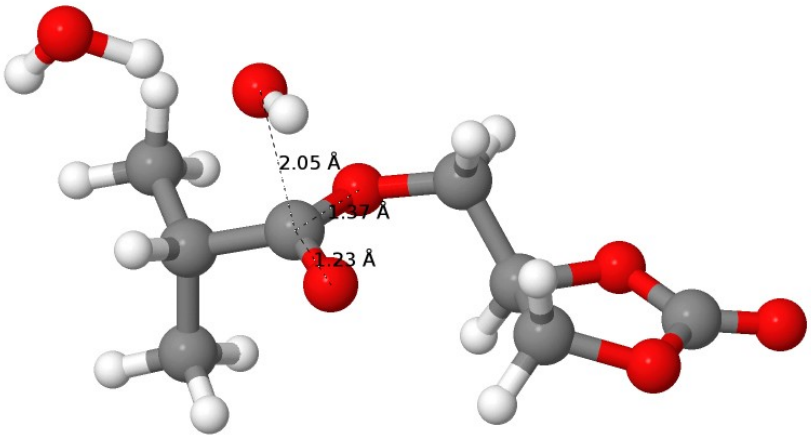

C	-3.50875501	-0.86815864	-0.63508636
C	-4.37900153	-0.19287345	-1.67876260
H	-3.80922390	0.01246007	-2.58795175
H	-4.77736326	0.74911625	-1.30364298
H	-5.21436403	-0.84480553	-1.94861582
C	-2.40549499	0.00786488	-0.07403356
O	-1.71018075	-0.33962700	0.87921354
O	-1.86811646	0.80123124	-1.05236037
C	-0.73784697	1.54347392	-0.65898603
C	0.52004700	0.69608894	-0.52768065
H	-0.94527187	2.08102297	0.26992189
H	-0.57026349	2.26652123	-1.45824817
C	0.97628515	0.33428518	0.88097024
O	1.63980125	1.45992035	-1.02611971
H	0.42368609	-0.18809054	-1.16173018
O	2.38759103	0.61252725	0.86457120
H	0.83192830	-0.71274205	1.12391934
H	0.51016044	0.95973037	1.64147554
C	2.69399023	1.31899305	-0.22076711
O	3.77958034	1.77245675	-0.44951755
O	-3.62225665	1.42469364	0.77271098
H	-3.17859539	1.35621636	1.62184392

O	-6.09299329	0.96299678	1.22754907
H	-6.34583220	0.24258860	0.64591929
H	-5.09178506	1.12359594	1.03787489
H	-4.12084539	-1.13801572	0.22852167
C	-2.87501890	-2.14196473	-1.19322818
H	-2.27584459	-2.65122627	-0.43644241
H	-3.65163744	-2.82925550	-1.53752597
H	-2.22906240	-1.91291860	-2.04575950

Saturated C^2MA – backbone ester hydrolysis tetrahedral intermediate (TET)

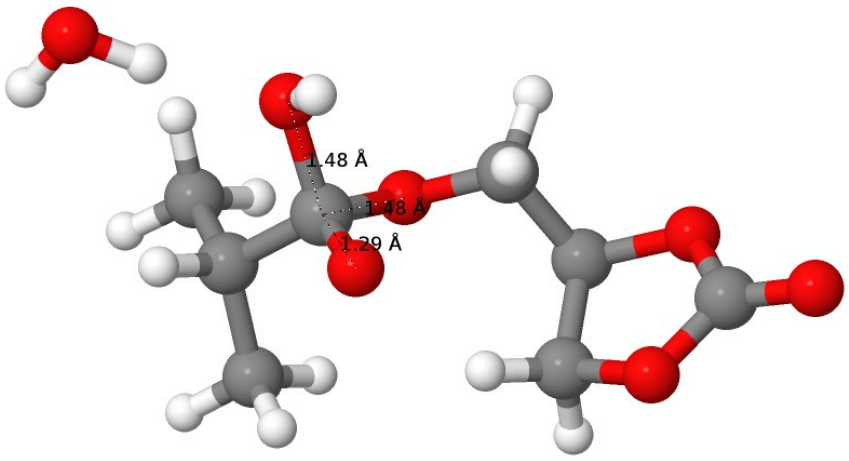

C	-2.76358440	-0.30748910	-0.42741137
C	-3.38498751	0.29589710	-1.67838020
H	-2.68213682	0.25599915	-2.51353382
H	-3.67106364	1.33879113	-1.53138818
H	-4.28103694	-0.26196639	-1.96676453
C	-1.58675291	0.50309169	0.15411132
O	-1.03707177	0.04497266	1.22299667
O	-0.66644268	0.65281878	-0.98990611
C	0.60111623	1.13657869	-0.66725384
C	1.61902173	0.07827407	-1.04957068
H	0.68335180	1.33499714	0.40720801
H	0.81297530	2.06251010	-1.21559340
C	1.53239667	-1.16556997	-0.17689581
O	2.95103503	0.55938239	-0.78632028
H	1.55407202	-0.15079202	-2.11287567
O	2.60746864	-0.97424216	0.76077726
H	1.71995559	-2.09134060	-0.72185506
H	0.58874549	-1.19654735	0.36973192
C	3.42572757	-0.02068368	0.31868686
O	4.46008826	0.28008728	0.84534641
O	-2.09702118	1.87710820	0.38994250
H	-1.68254401	2.08340259	1.23581876
O	-4.73747663	2.47951118	0.87013473
H	-3.81470212	2.20677784	0.67035210
H	-5.28449179	1.76404542	0.53658266
C	-2.34913207	-1.74816080	-0.67638672

H	-3.51257019	-0.30113792	0.37401293
H	-1.60590439	-1.80005247	-1.47664850
H	-3.21037634	-2.35144546	-0.97731887
H	-1.91313896	-2.19034750	0.22050089

Saturated C^2MA – backbone ester hydrolysis transition state 2 (TS2)

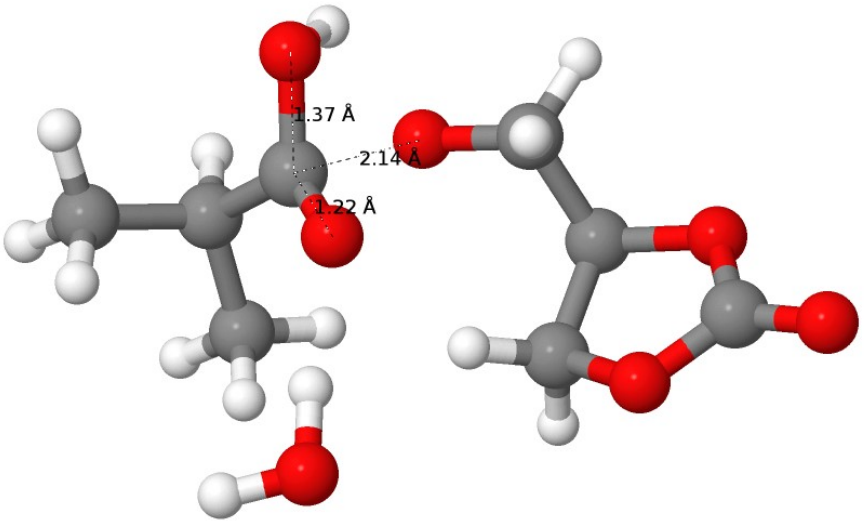

O	0.20123064	-2.57178371	3.01962566
H	-0.21127626	-1.75730196	2.66124074
H	-0.52848487	-3.08200003	3.37944997
H	-2.17467175	1.83305883	0.74610384
C	-2.79077873	-0.69139729	0.90765460
C	-3.74192009	-1.04035113	2.05395449
H	-4.15273197	-0.14401994	2.52292422
H	-3.22460415	-1.62316168	2.82119611
H	-4.57393206	-1.64135901	1.67984374
C	-1.71645394	0.22109510	1.46096557
O	-0.75789790	-0.18960360	2.10326361
O	-1.13222497	0.85335641	-0.49934120
C	0.14371632	1.33061394	-0.46577726
C	1.09205003	0.38111875	-1.18792500
H	0.53328905	1.44633825	0.57095859
H	0.25818577	2.32549159	-0.93979789
C	1.29435632	-0.93674516	-0.45401655
O	2.43444470	0.92179806	-1.22077643
H	0.77164284	0.24010530	-2.22013409
O	2.56400924	-0.75951327	0.19771862
H	1.37210220	-1.80124293	-1.11499463
H	0.53257461	-1.09787040	0.30455794
C	3.19737034	0.28614070	-0.33538696
O	4.31829578	0.60813845	-0.05056564
O	-2.11903816	1.51625582	1.66940688
H	-3.34225218	-0.11650244	0.16040548
C	-2.23137891	-1.94227625	0.25975332
H	-3.04702448	-2.57706200	-0.09577483

H	-1.59782156	-1.67914410	-0.58695016
H	-1.64044585	-2.52457631	0.97086726

Saturated C^2MA – backbone ester hydrolysis product (P)

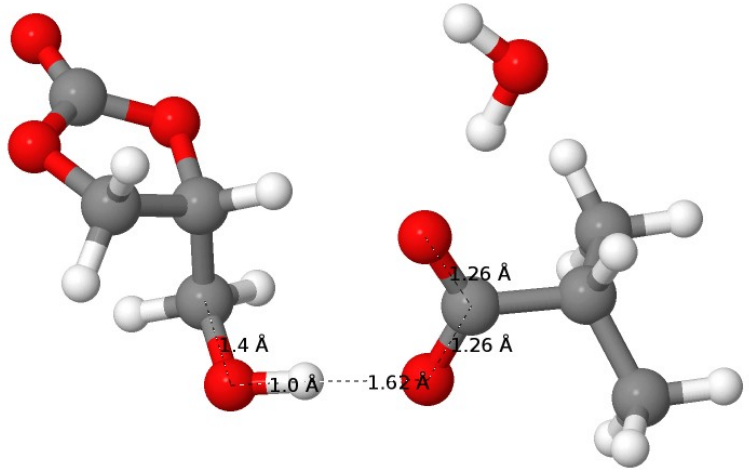

O	2.16085926	3.71574949	-0.23042933
H	2.01011620	2.78402248	0.07804816
H	1.30023884	4.13800142	-0.17492968
C	3.97559577	0.67908254	0.12412992
C	4.03487205	0.48760057	-1.39009312
H	5.01187459	0.78915053	-1.77658988
H	3.27126890	1.08157747	-1.89728920
H	3.88054878	-0.56359281	-1.64971068
C	2.56956809	0.31571961	0.60374015
O	1.70270636	1.22590624	0.60903963
O	-0.09142580	-1.74107346	1.28410894
C	-0.76450416	-1.59768382	0.06822918
C	-1.19749349	-0.15402207	-0.13096089
H	-1.64906274	-2.24558739	0.07798743
H	-0.14526147	-1.89794066	-0.78728679
C	-2.26099719	0.30347721	0.85572425
O	-1.87768267	-0.02480672	-1.39554514
H	-0.32435971	0.49885654	-0.13355767
O	-3.47931941	0.17162869	0.10810477
H	-2.15210562	1.34715763	1.15278633
H	-2.31654521	-0.33266990	1.73690308
C	-3.19276787	0.06594766	-1.19198199
O	-4.01510624	0.05612708	-2.06323055
O	2.35078816	-0.87829637	0.92716753
H	0.82757529	-1.35684602	1.17580721
H	4.11657596	1.74321511	0.33670641
C	5.06502589	-0.11763918	0.82002895
H	4.95621411	-1.18398894	0.61236864
H	5.03109976	0.01807825	1.90374262
H	6.05078358	0.20060880	0.46958170

Saturated C^2MA – carbonate hydrolysis transition state 1 (TS1)

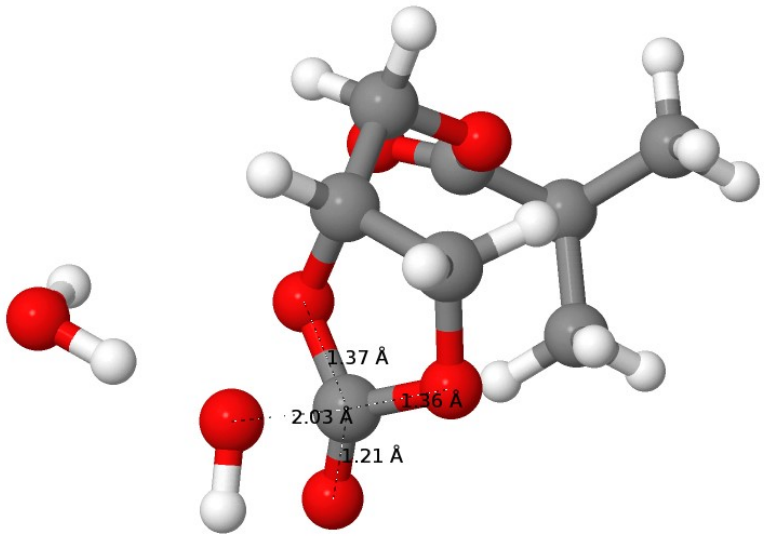

C	-2.87588421	0.22731136	-0.16887346
C	-2.35180152	-1.05310939	-0.81798656
H	-1.56876215	-0.82555139	-1.54435190
H	-3.16692948	-1.56064173	-1.33772775
H	-1.94056414	-1.73972565	-0.07514317
C	-1.76176854	0.86922016	0.61893450
O	-1.66514886	0.83872830	1.82146878
O	-0.87326158	1.46230291	-0.18605646
C	0.32941285	1.97431472	0.38260252
C	1.49444056	1.09635778	0.00170898
H	0.23012928	2.03463306	1.46580456
H	0.47477995	2.97581680	-0.02552131
C	1.62848808	0.80555770	-1.50261849
O	1.32631378	-0.18934229	0.57534841
H	2.40987908	1.54661948	0.39493482
O	1.48001261	-0.59861063	-1.60026662
H	2.60911609	1.09942314	-1.87707707
H	0.84310439	1.27602331	-2.09450039
C	1.64069444	-1.13885078	-0.35852342
O	1.48217019	-2.32138156	-0.14775546
O	3.64683140	-0.82606084	-0.24818218
H	3.90047040	-1.73855526	-0.40605044
O	3.99687785	-0.22325656	2.21555453
H	3.09643586	-0.12567808	2.53498420
H	3.87218279	-0.48931136	1.23204321
H	-3.63495265	-0.03670283	0.57095658
C	-3.47938937	1.17063284	-1.20059042
H	-4.32724545	0.68433047	-1.68745463
H	-3.83671846	2.09448581	-0.74054531
H	-2.74805185	1.42971118	-1.96803037

Saturated C[2]MA – carbonate hydrolysis tetrahedral intermediate (TET)

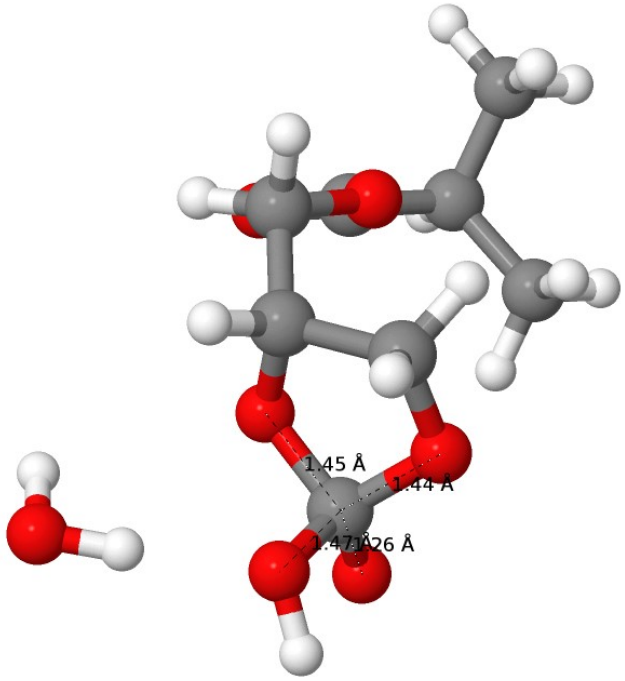

C	-2.79580412	0.11004237	-0.15733016
C	-2.31442400	-1.01939742	-1.05991420
H	-1.74420215	-0.62641217	-1.90337803
H	-3.17462169	-1.56537735	-1.45295885
H	-1.68057193	-1.72504155	-0.51864335
C	-1.64363650	0.81301327	0.51841114
O	-1.54066170	0.96153475	1.71276347
O	-0.76542179	1.27797607	-0.37191030
C	0.41759294	1.92360016	0.09914076
C	1.63055833	1.06058050	-0.15294647
H	0.31514480	2.14289696	1.16148845
H	0.50751234	2.85850340	-0.45766440
C	1.78477191	0.56584574	-1.60768755
O	1.55189276	-0.11886819	0.60533672
H	2.50741503	1.65376498	0.14053326
O	1.66562929	-0.82889213	-1.52215701
H	2.75897258	0.86056863	-2.01278650
H	0.99949407	0.94984241	-2.26212308
C	2.04391946	-1.22466208	-0.18783533
O	1.65133967	-2.36673394	0.15793627
O	3.50706183	-1.05477858	-0.12228966
H	3.83841082	-1.95530949	-0.19630156
O	4.17282580	0.13984304	2.28550845
H	3.31530613	0.43004027	2.60836911
H	3.95166627	-0.29921451	1.43729423
H	-3.39061052	-0.30774215	0.65801680
C	-3.64784915	1.11614671	-0.92677848
H	-3.07863394	1.55685690	-1.74781077

H	-4.00135784	1.92191989	-0.27968830
H	-4.52001870	0.61206352	-1.34824465

Saturated C^2MA – carbonate hydrolysis transition state 2 – primary alcohol dissociation

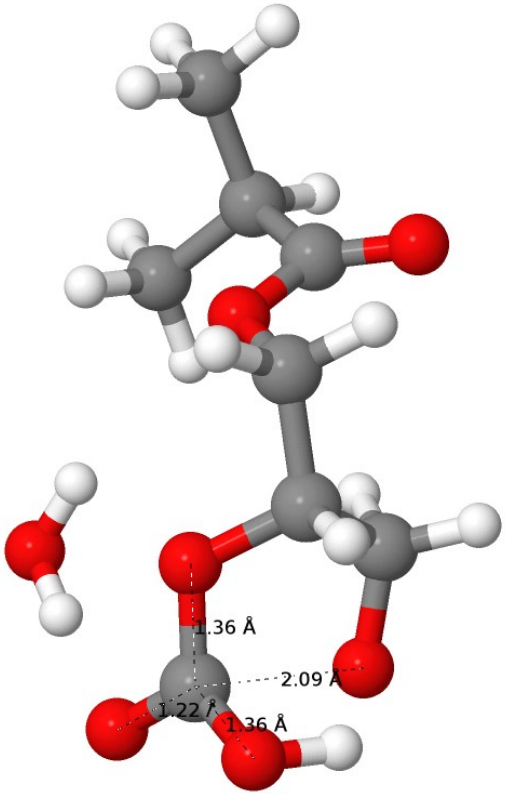

H	-0.77269814	-2.40822504	1.67264718
O	-0.64167787	-3.33179376	1.90576572
H	0.32626485	-3.45364413	1.79328393
C	-2.63187253	0.49320708	-0.06330913
C	-2.86202668	-0.85569062	0.59778279
H	-2.36861933	-1.66270172	0.05203656
H	-3.93189020	-1.07219441	0.62333726
H	-2.49757818	-0.85343168	1.62711157
C	-1.17611045	0.83301761	-0.26731494
O	-0.75696537	1.45611526	-1.21343522
O	-0.40930294	0.41504119	0.74318961
C	0.97945026	0.76348007	0.71900109
C	1.85994554	-0.38969712	0.32198194
H	1.21739179	1.08887320	1.73214441
H	1.13555660	1.58948949	0.02531702
C	1.55582246	-1.08754453	-1.00751510
O	1.75001440	-1.41084128	1.30637902
H	2.89052103	-0.01188464	0.30900878
O	2.22003841	-2.28475481	-1.00104218
H	1.86068912	-0.40986049	-1.82428388
H	0.46025319	-1.21422699	-1.09589696
C	2.47537081	-2.53144505	1.05603968

O	2.06777102	-3.58815716	1.51558585
O	3.80324948	-2.34236222	0.81310806
H	3.75602188	-2.14499876	-0.15229214
H	-3.06371094	0.48615741	-1.06715638
C	-3.28231107	1.62485127	0.73394461
H	-3.14407917	2.59008265	0.24332360
H	-4.35400291	1.43877699	0.82734996
H	-2.85840507	1.68187221	1.73943727

Saturated C^2MA – carbonate hydrolysis product – primary alcohol formed

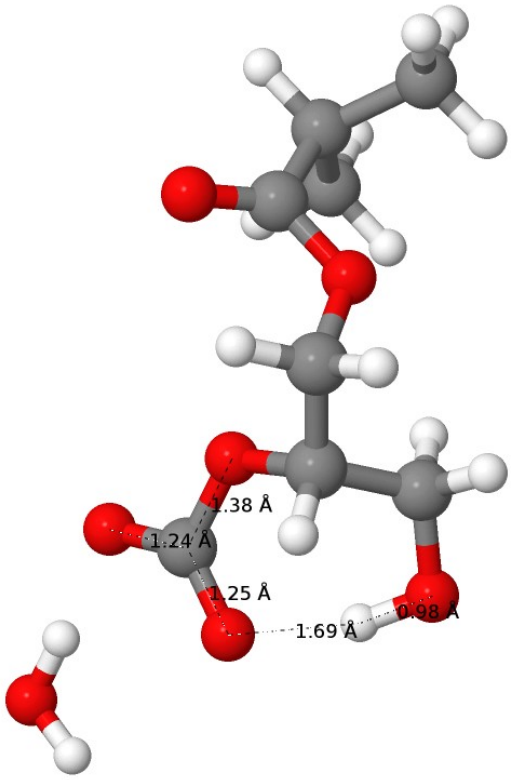

C	-3.08903812	0.32663745	-0.40341502
C	-2.70981456	-0.94535950	-1.15802651
H	-1.90511302	-0.74758646	-1.86911540
H	-3.57450183	-1.31351500	-1.71389405
H	-2.38170316	-1.73383559	-0.47733815
C	-1.93279140	0.77540101	0.45559163
O	-1.92003061	0.73915455	1.66229707
O	-0.91267969	1.20896202	-0.28978529
C	0.31113888	1.56680800	0.35635260
C	1.41558481	0.62349553	-0.05887742
H	0.17400181	1.54094042	1.43612686
H	0.55147237	2.58312159	0.04102678
C	1.59378986	0.56771898	-1.56748012
O	1.08909213	-0.64801873	0.49981210
H	2.34424703	0.99072850	0.39260375
O	2.83067217	0.01528368	-1.95636885

H	1.53405632	1.58831240	-1.96142563
H	0.75739398	-0.00008495	-1.99572930
C	2.09879114	-1.55455890	0.73918809
O	1.72339251	-2.54965600	1.38278412
O	3.24063443	-1.30460046	0.30264245
H	3.13189718	-0.53262016	-1.19529844
O	3.74728841	-4.26729831	1.81057443
H	3.01756043	-3.62011755	1.64086033
H	4.51499103	-3.86402820	1.39772893
H	-3.89378496	0.09702588	0.29848868
C	-3.54789313	1.42490236	-1.35488802
H	-2.76697318	1.66375285	-2.07901593
H	-3.81045158	2.33882270	-0.81757317
H	-4.43044922	1.08845189	-1.90288652

Saturated C[2]MA – carbonate hydrolysis transition state 2 – secondary alcohol dissociation

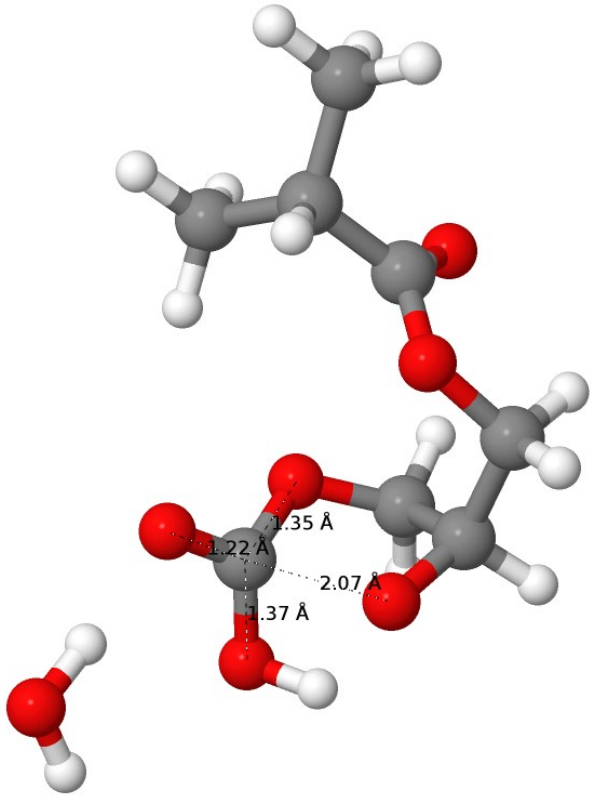

C	-2.05911534	-0.95531715	0.29961521
C	-3.35732003	-1.01895981	1.09148913
H	-3.19330965	-1.39260359	2.10480812
H	-4.06333068	-1.68622275	0.59279950
H	-3.81217180	-0.02872020	1.16126799
C	-1.07456993	-0.03501865	0.98031531
O	-1.33710861	1.08951225	1.34187530
O	0.11544149	-0.60852494	1.13023725
C	1.17488839	0.15093059	1.73246921
C	2.13447935	0.75453709	0.71123892

H	1.72078150	-0.56980211	2.34298187
H	0.74547577	0.92329430	2.37345875
C	1.48026721	1.82094295	-0.18479448
O	2.69923647	-0.16883816	-0.12145064
H	2.87810921	1.28885572	1.33727876
O	0.88954118	1.11792590	-1.26540295
H	2.23971078	2.51451057	-0.55908276
H	0.68032641	2.37946455	0.29883607
C	1.72020616	0.25742328	-1.89632171
O	1.22572214	-0.70503736	-2.46658872
O	2.90714136	0.78088824	-2.33720646
H	3.44490372	0.69263033	-1.52165454
O	2.93480520	-2.02028598	-4.12928187
H	2.33690212	-1.52508082	-3.52424210
H	3.73294227	-1.48656430	-4.15595368
H	-1.60514970	-1.94800905	0.25955184
C	-2.29471242	-0.46265623	-1.12628295
H	-1.36213665	-0.42529358	-1.69182145
H	-2.98912168	-1.13375468	-1.63650303
H	-2.73395425	0.53793758	-1.11431589

Saturated C^2MA – carbonate hydrolysis product – secondary alcohol formed

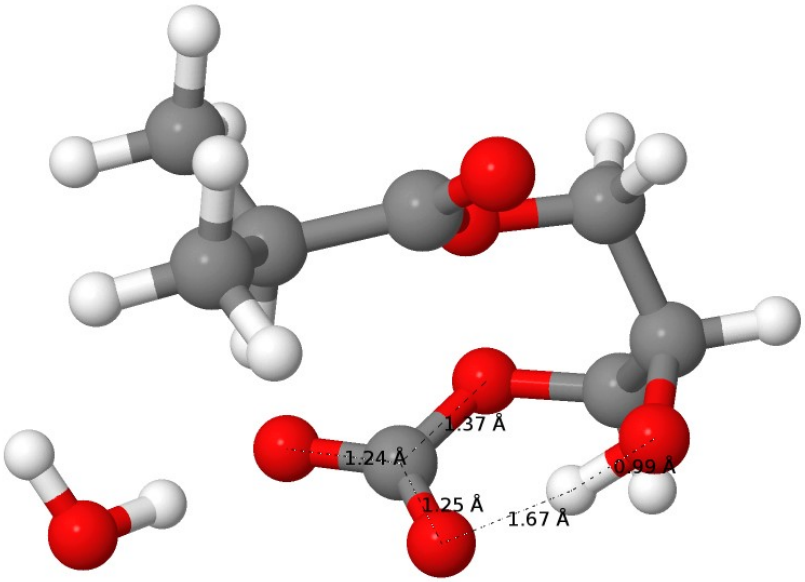

O	-0.23685020	-4.10516849	-0.57704038
H	-0.97022150	-4.00417937	-1.18856836
H	0.42951818	-3.43086176	-0.86400816
C	-1.95054439	-0.63260448	-0.44513167
C	-2.36582687	-0.70944651	-1.91411470
H	-3.13016028	0.03897710	-2.14043945
H	-2.78689121	-1.69424974	-2.12640288
H	-1.51588860	-0.54896604	-2.57801271
C	-1.32021875	0.70930288	-0.15866314
O	-1.80103626	1.57331969	0.53414540

O	-0.15479492	0.82250177	-0.79982899
C	0.65564355	1.97274597	-0.56243792
C	1.86397484	1.60140521	0.28734673
H	0.06152009	2.72937526	-0.05145580
H	0.96666065	2.35034837	-1.53840581
C	2.90591181	0.76882348	-0.45243234
O	1.46160390	1.01425907	1.50148685
H	2.36545275	2.54887848	0.52655875
O	2.41564994	-0.29885687	-1.25115205
H	3.63410069	0.39610137	0.27429940
H	3.42677896	1.41644850	-1.16021214
C	1.89579192	-1.40932914	-0.63154495
O	1.54950701	-2.29941390	-1.42994122
O	1.82709078	-1.42691975	0.61404239
H	1.52604260	0.04241148	1.33976012
H	-1.16282422	-1.37538300	-0.27998862
C	-3.11467424	-0.91008324	0.48617571
H	-3.91843975	-0.18639743	0.33433326
H	-2.81033893	-0.86138809	1.53305872
H	-3.51313752	-1.90786083	0.29130397

12.12. Dye Release Test

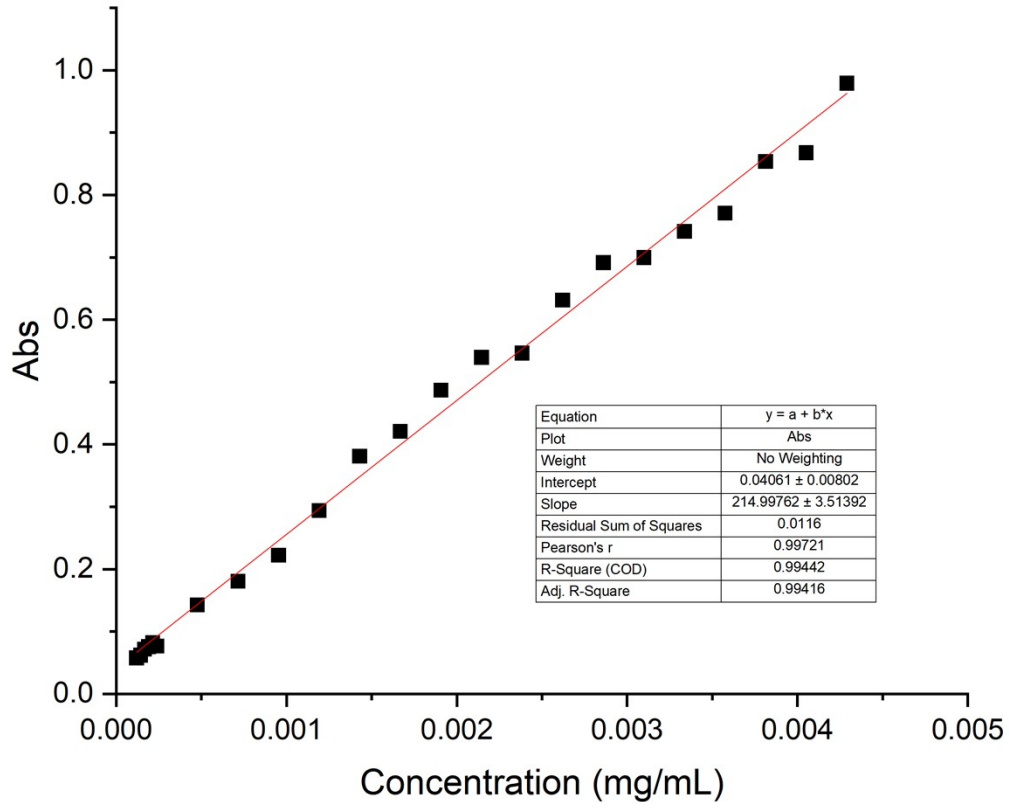

Figure S91. Calibration plot for rhodamine B generated by using UV-Vis spectroscopy

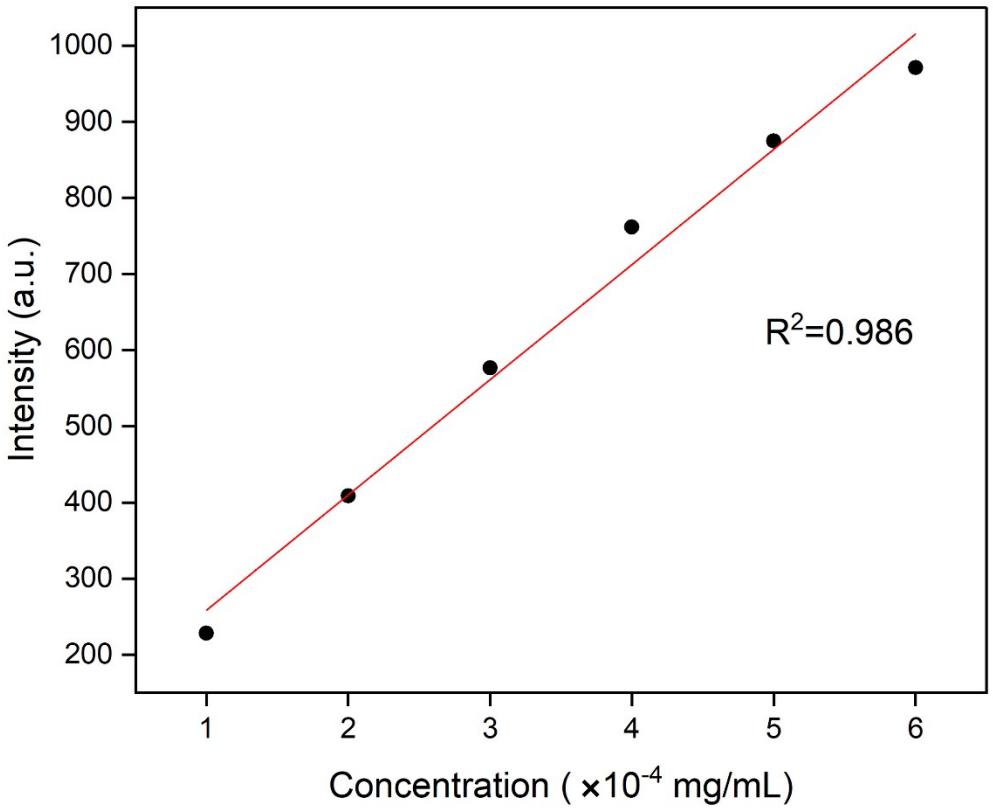

Figure S92. Calibration plot for rhodamine B generated by using fluorescence spectroscopy

Calibration curves. A series of dye standards spanning a range of concentrations was analyzed by UV–Vis absorbance and fluorescence spectroscopy to construct calibration curves. Linear regression analysis yielded the following calibration equations:

UV–Vis:

$$A = 214.99\,C + 0.040,$$

where A is absorbance and C is dye concentration (mg/mL).

Fluorescence:

$$I = 151.33542\,C + 107.30031,$$

where I is fluorescence intensity (a.u.) and C is dye concentration reported in units of 10^{-4} mg/mL.

Sample preparation. Three independent batches were prepared for each polymer formulation (30% L5MA content and 30% C2MA content), and three independent batches were prepared as dye-only controls. Polymer samples were prepared by mixing 950 µL of a 10 wt% polymer solution in PBS with 50 µL of dye stock solution (1 mg/mL), giving a total sample volume of 1.00 mL. Dye-only controls were prepared by mixing 950 µL PBS with 50 µL dye stock solution (1 mg/mL).

Dialysis release experiment. Each 1.00 mL sample was transferred to a dialysis tube (length=5-6 cm) and pre-equilibrated at 37 °C for 15 min. In parallel, individual release baths were prepared by adding 60 mL PBS to separate jars (one jar per sample) and equilibrating at 37 °C. After pre-equilibration, each dialysis tube was immersed in its corresponding PBS bath to initiate release.

Sampling and analysis. At predetermined time points, 1.0 mL aliquots were withdrawn from the external bath and analyzed by UV–Vis and fluorescence spectroscopy. Immediately after sampling, 1.0 mL of fresh PBS pre-warmed to 37 °C was added back to the bath to maintain constant volume.

Data processing. Dye concentrations were calculated from the UV–Vis and fluorescence calibration equations. Cumulative released mass and cumulative percent release (relative to the initial dye loading) were calculated.

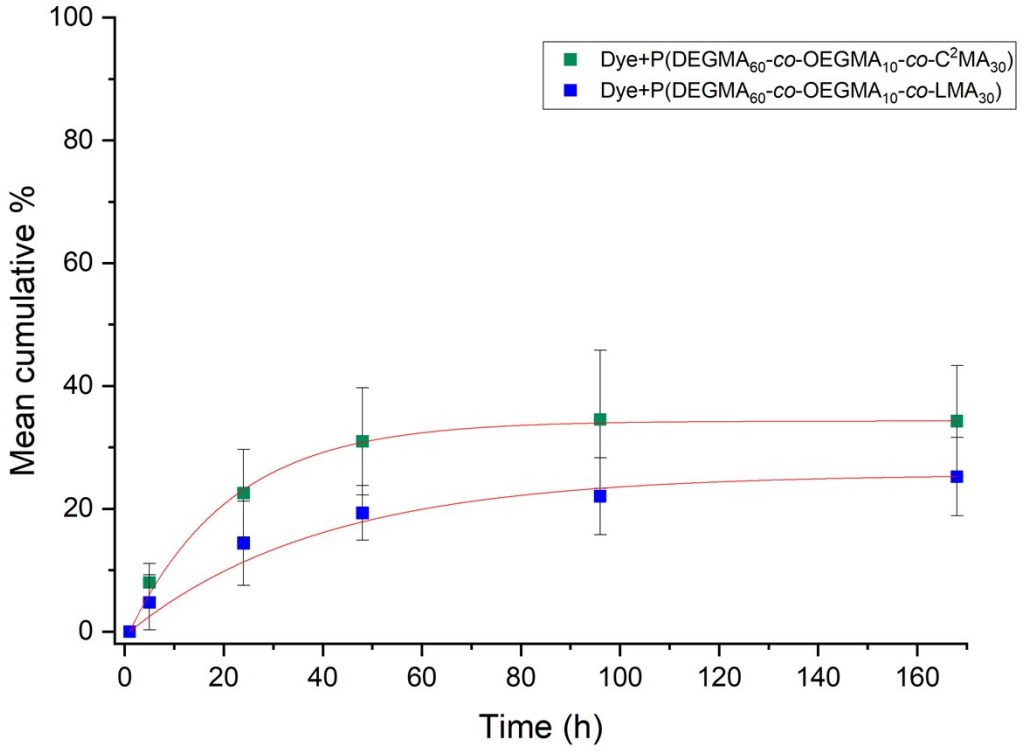

Figure S93. Mean cumulative percentage release of rhodamine B over time for polymer formulations and dye-only control samples, as determined by fluorescence spectroscopy

References.

(1) *Gaussian 16 Rev. C.01*; Wallingford, CT, 2016.